Investigating a novel CTRP8-DLK1 interaction and its impact on glioma stemness

by

Leanne Arreza

A Thesis submitted to the Faculty of Graduate Studies of

The University of Manitoba

in partial fulfilment of the requirements of the degree of

MASTER OF SCIENCE

Department of Human Anatomy and Cell Science

University of Manitoba

Winnipeg

ABSTRACT

Background: The C1Q-tumor necrosis factor related protein (CTRP) family has functions in metabolism, immunity, and cancer. Among the CTRP family, CTRP8 remains the least well characterized in terms of function and receptors. In the brain tumor glioblastoma (GBM), CTRP8 impacts migration and treatment resistance through its receptor RXFP1. We investigate a new interaction between CTRP8 and the EGF-like protein Delta-like homolog 1 (DLK1). DLK1 is a well-known regulator of differentiation and is considered a marker of stemness in several cancers. In GBM, elevated DLK1 expression promotes migration, stemness and has been correlated with poor prognosis. There is interest in further understanding complex mechanisms of DLK1 in a cancer context.

Methodology: A yeast-two hybrid (Y2H) screen and co-immunoprecipitation (co-IP) were used to characterize CTRP8-DLK1 interaction domains. The U251 cell line was used to assess stemness using tumor sphere formation and glioma stem cell (GSC) marker expression. In the same U251 model we investigate mechanisms responsive to CTRP8-DLK1 that regulate GSCs.

Results: The Y2H identified DLK1 as a CTRP8 interaction partner. In co-IP CTRP8 binds full-size DLK1 and a truncated, soluble form of DLK1. DLK1 enhanced sphere formation and GSC marker expression in U251. The pro-stemness effect of DLK1 was counteracted by CTRP8, resulting in an overall reduction in stemness. Reduced stemness in cells expressing a cleavage-resistant DLK1 form revealed potential functions of DLK1 cleavage products as factors regulating the GSC population. In U251 cells expressing DLK1, CTRP8 treatment increased DLK1 intracellular domain (ICD) release and nuclear translocation. DLK1 ICD may act as a transcriptional co-factor revealing a new function for DLK1 ICD.

Conclusions: This is the first study describing CTRP8 as a DLK1 ligand. Our findings reveal DLK1 as a promoter of glioma stemness, and CTRP8 as an antagonist. The CTRP8-DLK1 interaction may be part of a novel regulatory system impacting the glioma stem cell niche that can be of clinical relevance.

ACKNOWLEDGEMENTS

First I would like to thank my advisor, Dr. Thomas Klonisch, for his guidance and encouragement throughout the MSc program. It has helped me grow as a scientist and I am very grateful. I would like to extend my gratitude to the members of my committee, Dr. Susan Logue and Dr. Prashen Chelikani, for their valuable feedback and excellent support during my studentship applications.

Next I would like to thank members of the Hombach and Klonisch lab, past and present, for their contributions. A special thank you to Dr. Sabine Hombach-Klonisch, Dr. Aleksandra Glogowska, Dr. Thatchawan Thanasupawat, Danyyl Ippolitov, Farhana Begum and Dana Henderson for sharing their knowledge and kind assistance over the years.

I would like to acknowledge financial support from Natural Science and Engineering Research Council (NSERC), Canadian Institutes of Health Research (CIHR) Canada Graduate Scholarship-Master's (CGS-M) and the University of Manitoba.

Finally, thank you to my friends and family for their constant support. Thank you for being reassuring and celebrating successes over the years.

TABLE OF CONTENTS

LIST OF TABLES

LIST OF FIGURES

LIST OF ABBREVIATIONS

A disintegrin and metalloprotease (ADAM)

Brain tumor initiating cell (BTIC)

C1q-tumor necrosis factor related protein (CTRP)

CBF1/Su(H)/LAG1 (CSL)

Co-immunoprecipitation (co-IP)

Complement component 1q (C1q)

Complement related factor (CRF)

Complementary DNA (cDNA)

Cysteine rich FGF receptor (CRF)

Delta and OSM-11 like (DOS)

Delta-like homolog 1 (DLK1)

Delta-like homolog 2 (DLK2)

Delta-like ligand (DLL)

Delta-Serrate-LAG2 (DSL)

Dulbecco's Modified Eagle Medium/Nutrient Mixture F12 (DMEM/F12)

Epidermal growth factor (EGF)

Fetal antigen 1 (FA1)

Fetal bovine serum (FBS)

Fibroblast growth factor (FGF)

Focal adhesion kinase (FAK)

Glioblastoma (GBM)

Glioblastoma stem cell (GSC)

Hypoxia-inducible factor (HIF)

Insulin-like growth factor 1(IGF1)

Intracellular domain (ICD)

Jagged ligand (JAG)

Matrix metalloprotease 9 (MMP9)

Mitogen-activated protein kinase kinase (MAPK)

Neural stem cell (NSC)

Neurogenic locus notch homolog protein (NOTCH)

Normal goat serum (NGS)

NOTCH intracellular domain (NICD)

Nuclear co-repressor 1 (NCOR1)

Nuclear factor of activated T-cells (NFAT)

Phosphate buffered saline (PBS)

Pre-adipocyte factor 1 (Pref1)

Quantitative real-time polymerase chain reaction (qPCR)

Relaxin family peptide receptor 1 (RXFP1)

Sodium dodecyl-sulfate polyacrylamide gel electrophoresis (SDS-PAGE)

Tris buffered saline (TBS)

Tumor necrosis-alpha converting enzyme (TACE)

Yeast-two hybrid (Y2H)

1 INTRODUCTION

1.1 C1q-TNF related protein family

The complement component 1q (C1q)-tumor necrosis factor related protein (CTRP) family is composed of adiponectin and the CTRPs (CTRP1-15). The CTRPs are adiponectin paralogs that exhibit structural and functional similarities to adiponectin (Kishore et al. 2004; Wong et al. 2004). The CTRPs share a similar protein structure composed of a C-terminal globular complement component 1q (C1q)-like domain, variable region, collagen domain and N-terminal signal peptide (Figure ***1.1***). CTRPs can organize into homotrimers, but can also form heterotrimeric complexes with other CTRPs (Wong et al. 2004; Kishore et al. 2004; Peterson, Wei, and Wong 2009).

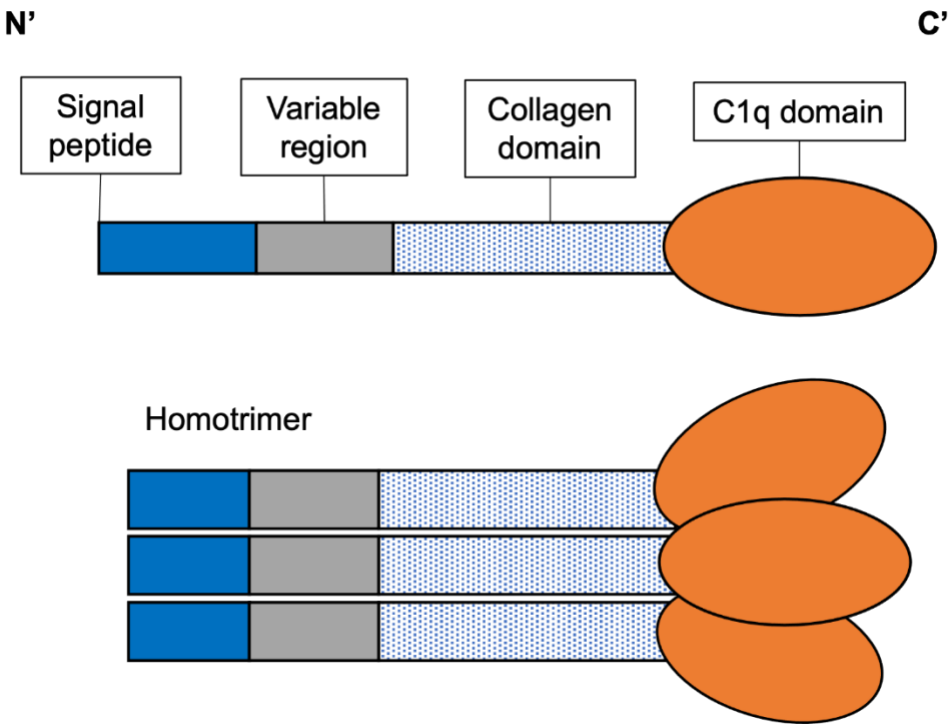

Figure 1.1 Schematic of C1q tumor necrosis factor related protein (CTRP) structure. A monomer is composed of an N-terminus signal peptide, variable region, collagen domain and C-terminal C1q domain. CTRPs are often formed as homotrimers.

Adiponectin is well-characterized as a regulator of inflammation. Likewise, CTRPs have been associated with immune response and metabolic regulation in normal physiology as well as diseases such as diabetes and cancer (Schäffler and Buechler 2012). In particular, CTRP3, CTRP4, CTRP6, and CTRP8 have been linked with regulation of proliferation, migration and tumor-associated inflammation in different cancers (Kong et al. 2021). Elevated CTRP3 expression in human osteosarcoma has been found to promote cell proliferation via extracellular-related kinase (ERK) 1/2 pathway activation (Akiyama et al. 2009). In hepatocellular carcinoma (HCC), elevated expression of CTRP4 secreted by cancer cells was described as a pro-inflammatory cytokine that promotes nuclear factor (NF)-kB and signal transducers and activators of transcription 3 (STAT3)/interleukin 6 (IL6) pathway activation (Li et al., 2011). CTRP6 expression has also been detected in HCC tissues and cell lines. Suppression of CTRP6 in HCC cell lines reduced cell survival and migration, while promoting apoptosis (Wan, Zheng, and Dong 2019). In a xenograft model, CTRP6-expressing HCCs promoted tumor vascularization (Takeuchi, Adachi, and Nagayama 2011). In glioblastoma, CTRP8 was associated with increased tumor invasiveness (Glogowska et al. 2013) and promotion of treatment resistance, mediated through relaxin-family peptide receptor 1 (RXFP1) (Thanasupawat et al. 2018).

There is growing evidence describing the role of the CTRP family in cancer. Most of the studies detailing the impact of CTRP family members in cancer have not identified a specific CTRP-receptor interaction, apart from CTRP8 and RXFP1. Although exciting discoveries about the role of CTRP family members in cancer have emerged, there is still insufficient information regarding the signaling mechanisms employed by this protein family.

1.1.1 CTRP8

First isolated as a cDNA clone from hippocampus cDNA in 2009, CTRP8 is one of the more recently identified and lesser known members of the CTRP family (Peterson, Wei, and Wong 2009). CTRP8 transcripts were detected predominantly in human lung and testis. Similar to other CTRP8 family members, CTRP8 is secreted as a homotrimer and can form heterotrimers with complement-related factor (CRF) (Peterson, Wei, and Wong 2009). Currently, functional analyses of CTRP8 is limited by the lack of a CTRP8 ortholog in mice (Peterson, Wei, and Wong 2009; Schäffler and Buechler 2012) and inadequate availability of CTRP8 detection tools.

1.1.2 CTRP8 in gliomas

In the fatal brain tumor glioblastoma (GBM), CTRP8 has been discovered to impact two key features of GBM: high migratory capacity and treatment resistance (Glogowska et al. 2013; Thanasupawat et al. 2018). CTRP8 was identified as a novel ligand of the G-protein coupled receptor relaxin family peptide 1 (RXFP1) (Glogowska et al. 2013). Human brain cancer cell lines and patient cells expressing RXFP1 displayed increased motility and matrix invasion upon exposure to CTRP8 (Glogowska et al. 2013; 2021). The CTRP8-RXFP1 signaling axis mediates the increase in motility via activation of the phosphoinositide 3-kinase (PI3K) – protein kinase C (PKC) signaling pathway, resulting in elevated cathepsin B production and cell migration through the extracellular matrix component, laminin (Glogowska et al. 2013). CTRP8-RXFP1 interaction also increased levels of active CDC42, a key factor in cytoskeletal remodeling and filopodia formation (Glogowska et al. 2021). CDC42 activation was shown to be dependent on the CTRP8-RXFP1 – Janus Kinase (JAK3) – STAT3 cascade, revealing a new role for CTRP8 in GBM motility regulation (Glogowska et al. 2021).

The CTRP8-RXFP1-STAT3 axis has also demonstrated a role in promoting GBM cell treatment resistance against the standard treatment drug, temozolomide (TMZ) (Thanasupawat et al. 2018). CTRP8 upregulates N-methyl purine DNA (MPG) glycosylase, an initiator of base excision repair (BER) pathway to reduce DNA damage and increase levels of anti-apoptotic Bcl-2 and Bcl-XL proteins, overall contributing to increase cell survival in the presence of TMZ (Thanasupawat et al. 2018). The previous work in our lab has highlighted the role of CTRP8 in impacting GBM, tumor invasiveness into surrounding tissue and resistance to treatment drugs (Figure ***1.2***). Investigating CTRP8 biology can provide valuable insight into the cellular mechanisms that regulate GBM tumorigenicity.

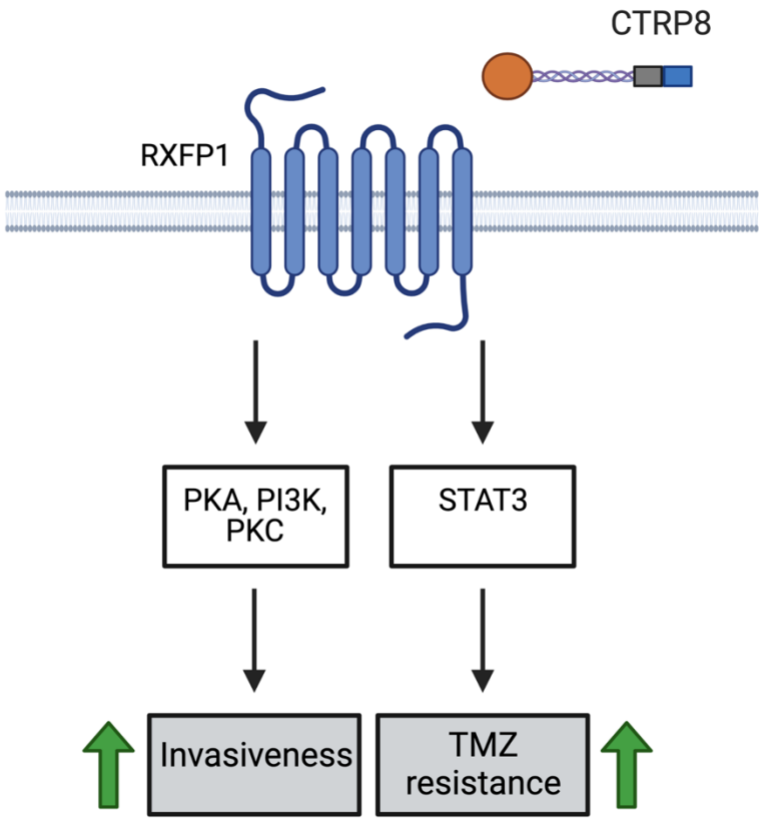

Figure 1.2 Summary of CTRP8-RXFP1 signaling in glioblastoma (GBM). CTRP8 is a novel interaction partner of the G-protein coupled receptor RXFP1. Upregulation of GBM invasiveness

and treatment resistance to temozolomide (TMZ) is mediated through CTRP8-RXFP1 activation of PKA/PI3K/PKC and STAT3 signaling cascades.

1.2 Delta-like homolog 1

Delta-like homolog 1 (DLK1) is an epidermal growth factor (EGF)-like protein, first described in 1987 as a cDNA clone involved in neuroendocrine tissue development (Helman et al. 1987). DLK1, initially termed cDNA *pG2,* was found highly expressed in both normal adrenal cortex and neuroendocrine tumors (Helman et al. 1987). Later, a soluble protein identified as fetal antigen 1 (FA1) was isolated from human amniotic fluid (Fay et al. 1988). In 1993, human Delta-like (dlk) cDNA clone was obtained from adrenal gland cDNA and expression was detected in human small cell lung cancer cell lines and neuroblastoma (Laborda et al. 1993). Also in 1993, pre-adipocyte factor 1 (Pref1) was isolated from a mouse preadipocyte cell line (Smas and Sul 1993). Sequence analyses of *pG2,* FA1, dlk, and Pref1 revealed identical sequence identity of each gene product (Jensen et al. 2001; Bachmann et al. 1996). These previously identified variants *pG2,* FA1, dlk and Pref1 are now more commonly referred to as DLK1.

Human *DLK1* is a maternally imprinted, paternally expressed gene located on chromosome 14q32 and encodes a 383 amino acid protein (Gubina et al. 1999). DLK1 protein structure is composed of an N-terminal signal peptide, six epidermal growth factor (EGF)-like repeats, a juxtamembrane A disintegrin and metalloprotease (ADAM)/Tumor necrosis-alpha converting enzyme (TACE) mediated cleavage site, transmembrane domain and a short C-terminal cytoplasmic domain (Laborda et al. 1993; Smas and Sul 1993) (Figure ***1.3***). Cleavage of DLK1 via ADAM metalloproteases at the juxtamembrane site releases the DLK1 extracellular domain. The soluble DLK1 ectodomain is a functional protein, capable of binding with known DLK1

receptors and interaction partners. DLK1 is a dynamic factor in tissue development and disease, where it acts primarily as a regulator of cell differentiation and proliferation.

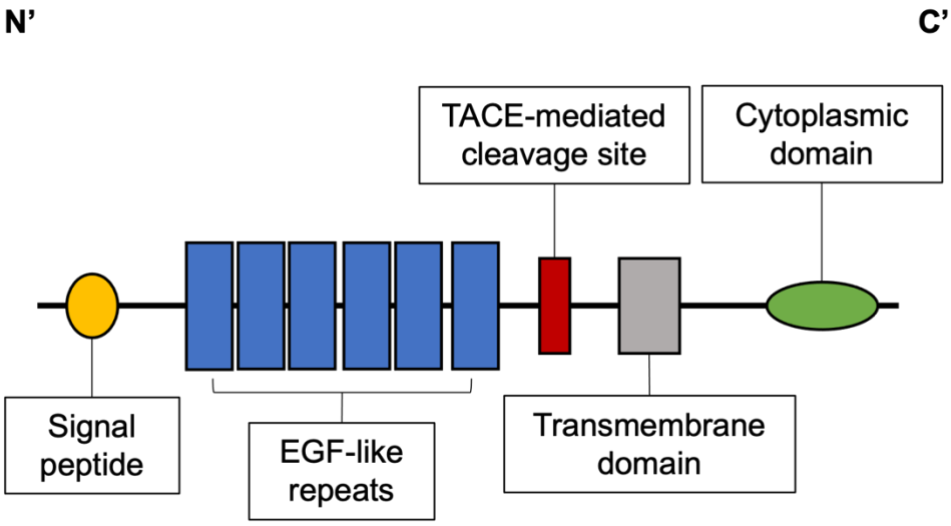

Figure 1.3 Schematic of Delta-like protein homolog 1 (DLK1) protein structure. DLK1 is a membrane bound glycoprotein with an N-terminus signal peptide, six epidermal growth factor (EGF)-like repeats, TACE-mediated cleavage site, transmembrane domain and a short cytoplasmic tail.

1.2.1 DLK1 in development

In human development, expression of DLK1 is present as early as week five of gestation and persists until birth. Extraembryonic tissues express DLK1 in the yolk sac and placenta, as well as a soluble DLK1 form detected in amniotic fluid (Fay et al. 1988; Floridon et al. 2000). Most embryonic tissues are DLK1-positive but as development advances, DLK1 expression becomes more restricted to specific cell types within tissues. In adult tissues, DLK1 expression is generally localized to populations of stem/progenitor cells and (neuro)endocrine cells (Floridon et al. 2000; Appelbe et al. 2013). Among endoderm-derived tissues, DLK1 is expressed in 94% of epithelia during fetal development, then decreases to 11% just months after birth. In adulthood, DLK1

expression is absent in most endoderm-derived structures apart from the pancreas and prostate. In the pancreas islets of Langerhans, DLK1 was localized to only insulin-producing beta cells (Tornehave et al. 1993). In the prostate, DLK1 was expressed in the basal cell layer, and co-expressed with markers identifying cells with a stem-like and neuroendocrine phenotype (Ceder et al. 2008).

The shift of DLK1 expression throughout development from the embryonic stage to adult has been best described in tissues and cells of mesodermal origin. Mesenchymal stem cells (MSC) in fetal adipose tissue displayed an induction in DLK1 expression in the early stages of adipocyte differentiation. Elevated DLK1 expression commits MSCs to the adipogenic lineage as pre-adipocytes and then is reduced during later stages of adipogenesis (Morganstein et al. 2010). In addition to pre-adipocyte cells, DLK1 was localized in CD34-positive cells adjacent to vasculature in white adipose tissue. These cells likely possess adipogenic potential or may also contribute to vascularization (Zwierzina et al. 2015). A similar trend is observed in skeletal muscle where DLK1 is expressed in developing fetal myotubes and satellite cells in adult tissue (Andersen et al. 2009).

Among the ectoderm-derived tissues, DLK1 has been described in subsets of cells in the pituitary gland and brain. In fetal and adult pituitary gland, DLK1 is localized primarily to somatotroph cells (Larsen et al. 1996). In the fetal brain, DLK1 is expressed in pseudostratified and marginal cells of the third ventricle (Floridon et al. 2000). DLK1 is largely absent in the adult brain, and is only expressed in monoaminergic neurons of the pons and mesencephalon (Jensen et al. 2001).

Altogether, the distribution of DLK1 in tissues throughout development point to its role in maintaining cells in an undifferentiated state. This is supported by evidence from transgenic mouse models and *in vitro* studies on cell lines that describe DLK1 as a modulator of cell differentiation

and proliferation. DLK1 null mice were viable, but displayed growth retardation with irregular development of adipose tissue, skeletal muscle and pituitary gland (Moon et al. 2002; Puertas-Avendaño et al. 2011; Appelbe et al. 2013). A conditional DLK1 knockout mouse model was established to delete DLK1 in specific cell types. DLK1 deletion in embryonic pancreatic beta-cells, pituitary somatotrophs and placental endothelial cells did not affect development of these cell types (Appelbe et al. 2013). However, muscle-specific DLK1 knockout decreased total muscle mass and slowed muscle regeneration in a mouse model. (Waddell et al. 2010). The phenotypic outcome of DLK1 knockout mice reveal the important role of DLK1 in development and tissue maturation.

1.2.2 DLK1 in cancer

The early discovery of DLK1 in tumors and subsequent findings about its importance during development made it an attractive target for further study in the context of cancer. In adult tissues, DLK1 expression is mostly restricted to undifferentiated cell types, however it is re-expressed in many malignancies. Initial identification of DLK1 was in neuroendocrine tumors, phaeochromocytoma and neuroblastoma, where it was associated with a less differentiated phenotype (Helman et al. 1987). DLK1 has since been identified in other endocrine tumors such as adrenocortical carcinoma where 100% of cases were DLK1-positive, while surrounding normal adrenal tissue was negative (Turányi et al., 2009; Hadjidemetriou et al., 2019). Localization of elevated DLK1 to the tumor and not normal tissue indicates a potential role for DLK1 in impacting tumor progression. A similar pattern of expression was observed in liver cancers, hepatoblastoma and hepatocellular carcinoma (HCC). DLK1 mRNA and protein were expressed at consistently high levels in 100% of hepatoblastomas compared to negative normal liver tissue (Dezső et al. 2008; Luo et al. 2006). Distribution of DLK1 between tumor and normal tissue was similar in

HCC, although DLK1-positive tissues were only detected in 36%-73% of samples (Dezső et al. 2008; Huang et al. 2007). DLK1-positive HCC and other liver cancers were associated with poor prognosis (Huang et al. 2007; Jin et al. 2008). Elevated DLK1 has been described in many common cancers such as the breast, lung, colon and more which have been previously reviewed (Pittaway et al. 2021). Overall, higher DLK1 expression has been reported in tumors where it is generally associated with poor prognosis.

The importance of DLK1 as a modulator of key developmental processes such as cell differentiation and proliferation has been well reported in various tissue systems. Dysregulation of these processes are hallmarks of cancer initiation and progression (Hanahan and Weinberg 2000). Upregulation of DLK1 in cancer potentially reverts cells to a de-differentiated state seen in early development. Mechanistically, DLK1-mediated regulation of cell differentiation and proliferation is a complex system impacted by the presence of DLK1 protein isoforms and various receptor interactions. In the following sections this will be described further in the context of both tissue development and cancer.

1.2.3 DLK1 isoforms and function

Uncovering DLK1 function and signal transduction is further complicated by the existence of DLK1 isoform-dependent effects. Full-size DLK1 is synthesized as a membrane-bound protein, although soluble DLK1 forms resulting from ADAM-mediated cleavage were discovered in early DLK1 studies. The soluble protein FA1 was determined to have the identical sequence as soluble DLK1 ectodomain, and therefore is considered a product of DLK1 proteolytic cleavage (Fay et al. 1988; Jensen et al. 1994). Mouse DLK1 has four major forms that result from cleavage proximal to the transmembrane domain and at the fourth EGF-like domain to produce smaller soluble forms (Smas, Chen, and Sul 1997). Two human DLK1 isoform have been identified, the cleavable full-

size DLK1 and cleavage-resistant DLK1 (Smas, Green, and Sul 1994; Deiuliis et al. 2006) (Figure ***1.4***). Additional DLK1 soluble isoforms with truncations of the EGF-like domains named Secredeltin, Brevideltin and Brevideltinin were discovered in neuroendocrine tumors (Altenberger et al. 2005). It remains unclear if these soluble forms are products of full-size DLK1 cleavage or if they are simply translated as a soluble protein. The functionality of these particular DLK1 isoforms have yet to be determined.

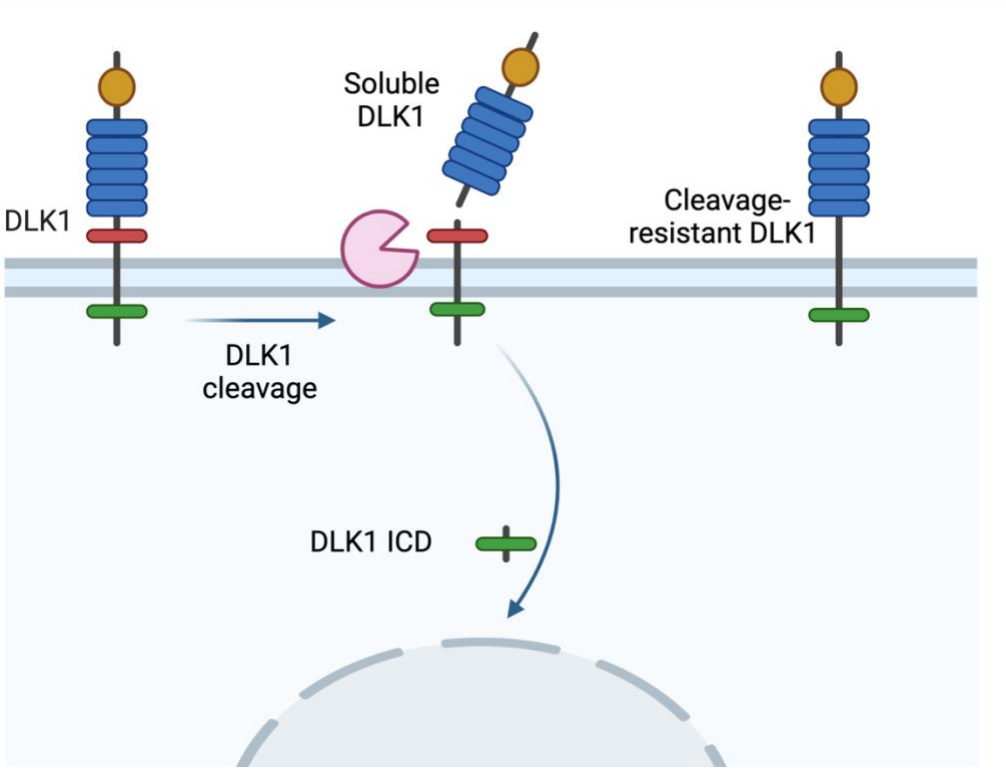

Figure 1.4 Schematic of the human DLK1 isoforms: full-size cleavable DLK1 and cleavage-resistant DLK1. Full-size DLK1 can undergo proteolytic cleavage at the juxtamembrane cleavage site to release both the extracellular EGF-like repeats as a soluble protein and the DLK1 intracellular domain (ICD) from the membrane. Cleavage-resistant DLK1 remains membrane-bound.

Proteolytic cleavage of full-size transmembrane DLK1 releases the extracellular EGF-like domains as a soluble, functional protein. Thus, DLK1 can signal in a dynamic manner through juxtacrine and paracrine signaling to modulate cell differentiation and proliferation (Mei et al. 2002; Mortensen et al. 2012). The molecular mechanisms of DLK1 signaling have been studied most extensively in adipogenesis where DLK1 is generally known to arrest pre-adipocytes in an undifferentiated state (Smas and Sul 1993). It was later demonstrated that there is a more complex role for DLK1 in the modulation of adipogenesis, involving DLK1-isoform specific outcomes (Smas and Sul 1993; Smas, Chen, and Sul 1997; Garcés et al. 1999; Moon et al. 2002). In a mouse pre-adipocyte cell line 3T3L1 transfected with constructs of various mouse DLK1 isoforms, only the full-size cleavable DLK1 and the larger soluble form consisting of the entire DLK1 ectodomain successfully inhibited adipogenesis (Mei et al. 2002). While cleavage-resistant DLK1 was not sufficient to inhibit adipocyte differentiation, it was able to influence tissue size by regulating proliferation. The cleavage-resistant DLK1 isoform inhibited pre-adipocyte proliferation by regulating G1-to-S-phase cell cycle progression (Mortensen et al. 2012). Cleavable and cleavage-resistant forms of DLK1 play different roles but are both essential for regulation of adipogenesis.

Isoform-dependent effects of DLK1 isoforms have also been observed in other models of tissue differentiation. In myogenesis, expression of cleavage-resistant DLK1 in myoblasts increased the thickness of formed myotubes while soluble DLK1 inhibited myotube formation (Shin et al. 2014). Meanwhile DLK1 overexpression promoted differentiation of myoblasts *in vitro*, resulting in muscle hypertrophy (Waddell et al. 2010). Another study demonstrated that DLK1 overexpression had an inhibitory effect on differentiation in a mouse myoblast cell line (Jørgensen et al. 2013). In hepatoblasts, cleavage-resistant DLK1 was shown to promote hepatocyte differentiation, while soluble DLK1 directed hepatoblasts to the cholangiocytic lineage

(Huang et al. 2019). DLK1 may be able to commit undifferentiated cells towards a certain fate dependent on the DLK1 isoform.

It was initially thought that only the soluble DLK1 ectodomain generated from cleavage of transmembrane DLK1 had signaling capabilities. However, recent studies have revealed that the short cytoplasmic tail of DLK1, the DLK1 intracellular domain (ICD), can also be released from the membrane. DLK1 ICD release and nuclear translocation in glioma cell lines U3082MG, U3084MG, U3065MG were upregulated in hypoxic conditions (Grassi, Pantazopoulou, and Pietras 2020). Nuclear localization of the DLK1 ICD was correlated with increased stemness and invasiveness as well as a shift in metabolic pathway preferences. It was proposed that DLK1 ICD can alter p53 and PI3K signaling, however, a detailed signaling mechanism has not yet been elucidated (Grassi, Pantazopoulou, and Pietras 2020). In non-small cell lung carcinoma (NSCLC), DLK1 ICD was identified as a novel interaction partner of nuclear co-repressor 1 (NCOR1) using co-immunoprecipitation and mass spectrometry. Immunohistochemistry of NSCLC tissue samples revealed that DLK1 and NCOR1 nuclear co-localization was associated with cell differentiation and smaller tumors (Tan et al. 2019). The downstream effects of DLK1-NCOR1 have yet to be identified, but it was suggested that this interaction can be involved in cell differentiation and proliferation to impact NSCLC tumor growth. In addition to known functions of full-size and soluble DLK1, these studies reveal exciting prospective roles for DLK1 ICD to participate in nuclear signaling as a transcriptional co-factor.

The mechanisms regulating proteolytic cleavage of DLK1 remain understudied. Evidence from *in vivo* and *in vitro* glioma studies show that the balance of soluble DLK1 versus cleavage-resistant DLK1 can be affected by hypoxia. *In vivo,* DLK1 was concentrated to hypoxic and perivascular regions in brain tumors from a murine glioma model (Grassi, Pantazopoulou, and

Pietras 2020; Grassi et al. 2020). In human glioma and astrocyte cell lines, hypoxic conditions were associated with an upregulation of overall DLK1 expression and increased DLK1 proteolytic cleavage (Grassi, Pantazopoulou, and Pietras 2020; Grassi et al. 2020). As expected, DLK1 protein cleavage was mediated by ADAM17, but was additionally dependent on hypoxia inducible factors (HIFs) (Grassi, Pantazopoulou, and Pietras 2020). Knockdown of HIF1a and/or HIF2a resulted in significant reduction of DLK1 cleavage. Hypoxia may be a physiological stimulus that can modulate DLK1 expression and protein cleavage. Altogether, the cleavage-resistant DLK1, soluble EGF-like domains and DLK1 ICD have all been associated with a biological function, further expanding potential regulatory mechanisms in which DLK1 can be involved.

1.2.4 NOTCH-dependent DLK1 signaling

The NOTCH pathway is highly conserved from invertebrates to mammals, involved in the regulation of critical processes during early development such as cell fate determination and differentiation (Siebel and Lendahl 2017). In mammals, four receptors, NOTCH1-4 are recognized along with five EGF-like canonical ligands in the Delta-Notch-Serrate protein family. The canonical activating ligands in mammals are the Delta-like ligands (DLL1, DLL3, DLL4) and Serrate-like/Jagged ligands (JAG1 and JAG2) (Kopan and Ilagan 2009). The Delta-Notch-Serrate protein family includes DLK1, which bears structural homology to the canonical Delta-like (DLL) and Jagged (JAG) ligands. In contrast to DLL and JAG, DLK1 lacks the conserved Delta-Serrate-LAG2 (DSL) EGF-like domain which is required for canonical ligand interaction with NOTCH receptors (Mei et al. 2002; Baladrón et al. 2005). Despite the lack of a DSL domain, the DLK1 EGF-like domains 5 and 6 interact with the NOTCH1 EGF-like domains 10 and 11, as determined by yeast-two hybrid and co-immunoprecipitation (Baladrón et al. 2005; Bray et al. 2008; Traustadóttir et al. 2016). DLK1 was among the first and most well-characterized non-canonical

NOTCH ligands and a Delta and OSM-11 like (DOS) co-ligand (Kopan and Ilagan 2009; D'Souza, Meloty-Kapella, and Weinmaster 2010).

For an interaction to occur between membrane-bound NOTCH receptors and ligands, the cell membranes on which they are anchored are required to come into close proximity. Binding of a NOTCH receptor to a DLL/JAG ligand on a neighbouring cell is referred to as a *trans* interaction, which then initiates canonical NOTCH signaling activation. Ligand-receptor binding is followed by two proteolytic cleavages of the NOTCH receptor by ADAM-family metalloproteases at the extracellular domain, then gamma-secretase to liberate the NOTCH intracellular domain (NICD) from the membrane (Bray and Bernard 2010). The cleaved NICD is translocated to the nucleus to form a transcriptional complex with CBF1/Su(H)/LAG1 (CSL) DNA-binding protein to promote target gene transcription (Bray and Bernard 2010; D'Souza, Meloty-Kapella, and Weinmaster 2010). Canonical Notch target genes include Hes/Hey family. In mammals, Hes1, Hes5 and Hey1 are the best described downstream Notch target genes (Kageyama and Ohtsuka 1999) (Figure ***1.5***).

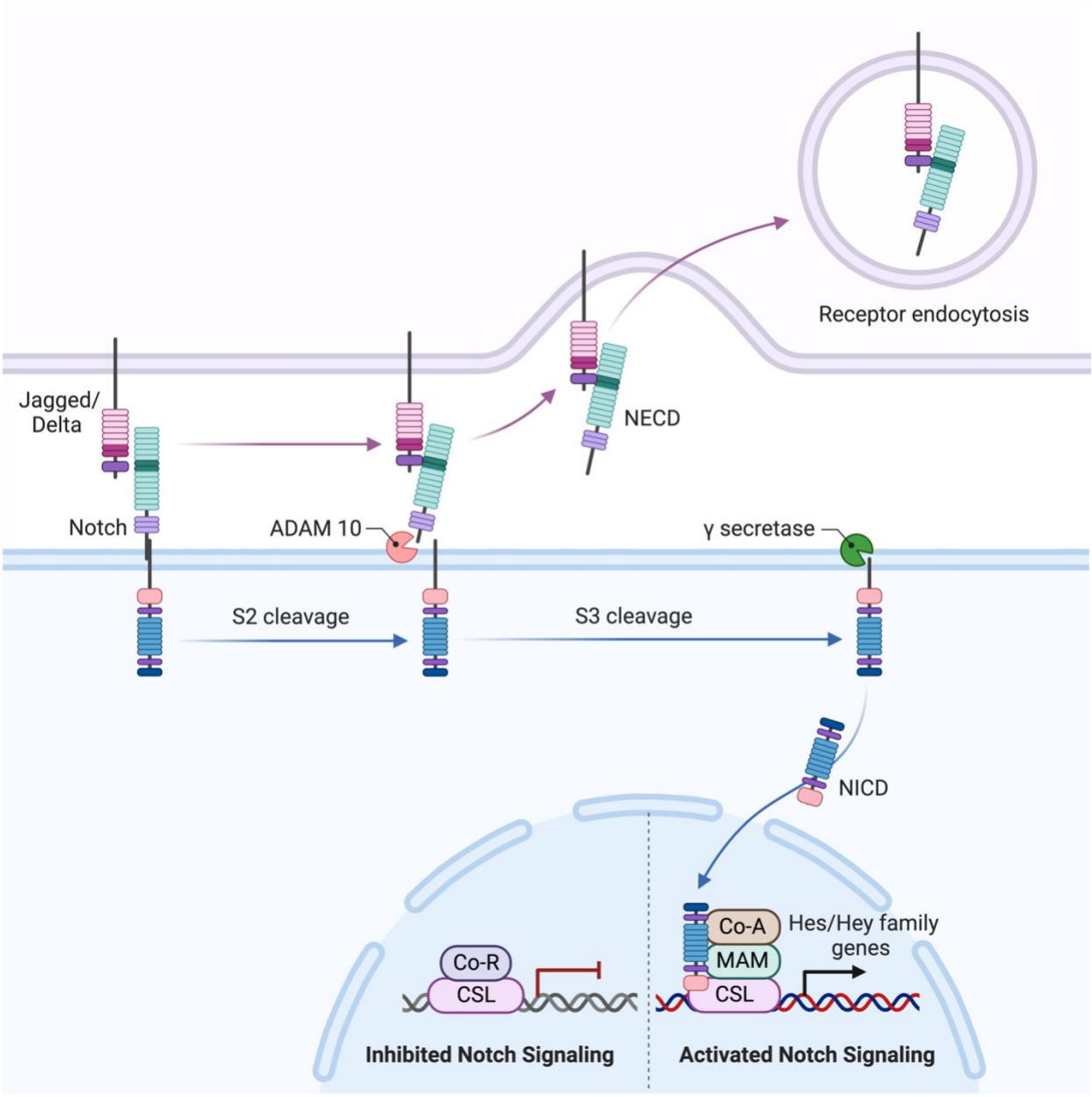

Figure 1.5 Schematic of Canonical Notch signaling activation. Jagged/Delta-like ligand *trans* binding to NOTCH receptors initiates sequential cleavage of the receptor to release the NOTCH intracellular domain (NICD). In the nucleus, NICD forms a transcriptional complex to activate expression of Hes/Hey family genes.

In general, DLK1 is frequently described as an inhibitor of NOTCH activation. Both the cleavage-resistant and soluble DLK1 downregulate canonical NOTCH activation through its interaction with NOTCH1 (Bray et al. 2008; D'Souza, Meloty-Kapella, and Weinmaster 2010; Baladrón et al. 2005; Nueda et al. 2007; Sánchez-Solana et al. 2011). Evidence regarding the molecular mechanism for DLK1-mediated NOTCH inhibition is lacking, although it has been proposed that DLK1 competes with canonical NOTCH ligands for NOTCH receptor binding (Figure ***1.6***). DLK1 binds to NOTCH1 EGF-like domains 10 and 11, while DLL/JAG ligands bind to EGF-like domains 11 and 12 (Traustadóttir et al. 2016; Rebay et al. 1991). The binding sites of DLK1 and DLL/JAG ligands overlap, thus DLK1-binding to NOTCH prevents DLL/JAG from binding, negatively regulating canonical NOTCH activation (Traustadóttir et al. 2016; Baladrón et al. 2005). While DLL/JAG ligands bind to NOTCH1 in *trans*, it has been proposed that DLK1 inhibits NOTCH1 by binding in a *cis* interaction to act as an inhibitor. In *trans* interactions, the membrane-bound receptor and ligand are bound to different cell membranes, while *cis* interactions define a ligand-receptor interaction occurring on the same membrane (D'Souza, Meloty-Kapella, and Weinmaster 2010). Although this may be the case for the membrane-bound DLK1 protein, soluble DLK1 ectodomain can act as a paracrine signaling molecule to inhibit NOTCH signaling (Baladrón et al. 2005).

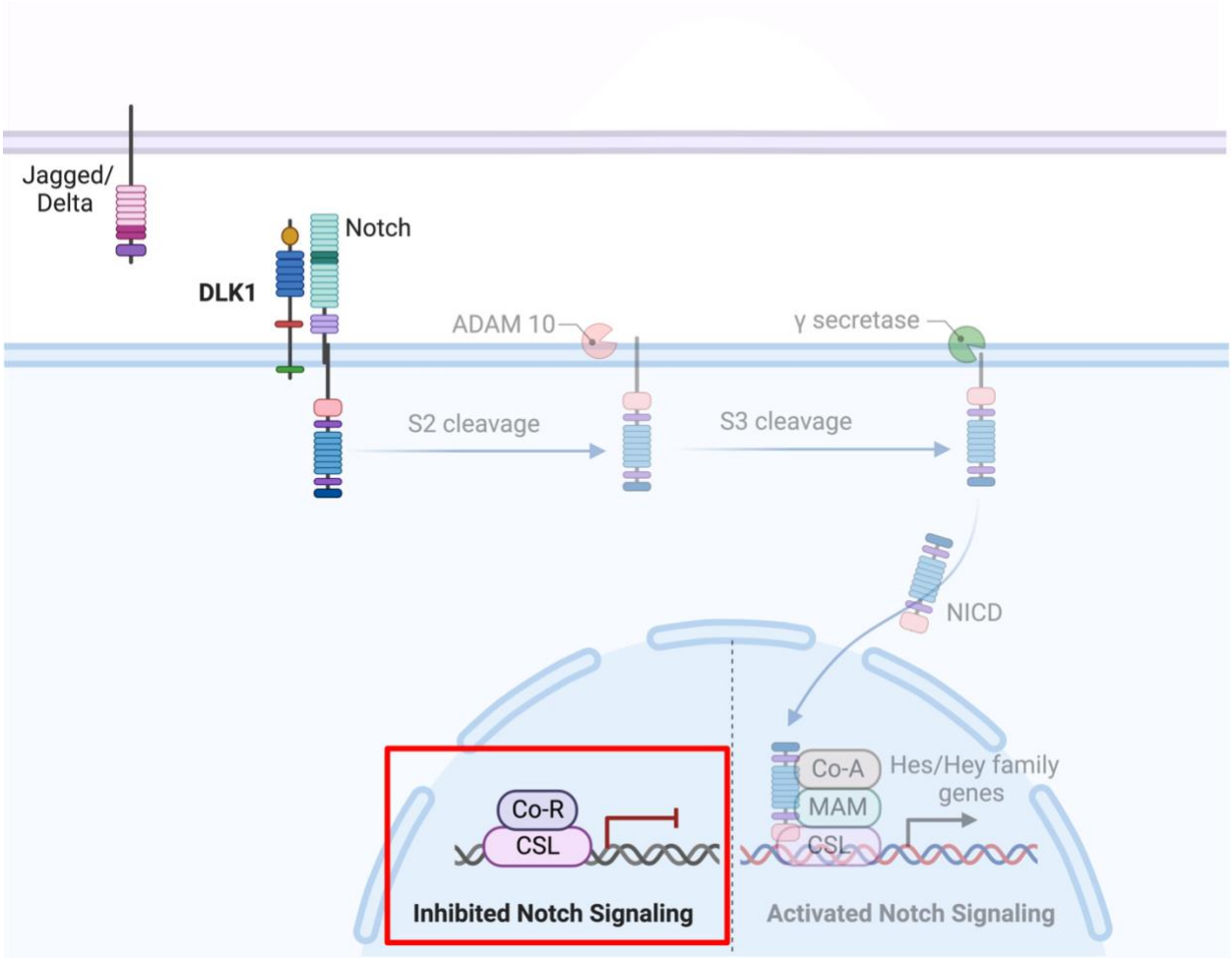

Figure 1.6 Schematic of DLK1 as a NOTCH signaling inhibitor. *Cis* interaction of DLK1 with NOTCH receptor prevents binding of Jagged/Delta-like canonical NOTCH ligands, resulting in inhibition of NOTCH signaling.

In the NOTCH1-expressing fibroblast cell line Balbc/14, ectopic expression of DLK1 reduced NOTCH reporter activity and expression of Hes-1. A similar outcome was observed in Balbc/14 treated with soluble DLK1 EGF-like domains. In 3T3L1 cells, DLK1-mediated reduction of NOTCH1 activity was associated with inhibition of adipogenesis (Baladrón et al. 2005). Interestingly in the embryonic mouse fibroblast cell line C3H10T1/2, NOTCH1 signaling inhibition via DLK1 promoted adipogenesis (Nueda et al. 2007). In this case, DLK1-mediated

NOTCH1 inhibition committed the mesenchymal stem cell-like C3H10T1/2 cells to adipogenic differentiation. Although DLK1 is acting through a common signaling mechanism, the cellular context is also a determining factor for the biological outcome in response to DLK1. The stage of differentiation likely influences the NOTCH-dependent effects of DLK1 in cells.

The impact of DLK1-NOTCH signaling has also been observed in cancer models. Elevated DLK1 expression was previously described in lung cancer tissues. Overexpression of DLK1 in lung cancer cell lines H520 and H1299 increased cell invasion and upregulated MMP9 activity. In this model, DLK1 overexpression was accompanied by the upregulation of NOTCH1 signaling (Li et al. 2014). The regulation of NOTCH1 signaling was described in more detail in melanoma cells. Expression of DLK1 in SK-MEL-2 metastatic melanoma cell line regulated cell proliferation and was inversely correlated with the level of NOTCH1 activity. Increased NOTCH1 inhibition decreased proliferation, while less NOTCH1 inhibition increased proliferation (Nueda et al. 2014). A similar concentration effect was observed in breast cancer. In triple negative breast cancer cells MDA-MB-231, DLK1 inhibited NOTCH1 signaling. Stronger DLK1-mediated inhibition of NOTCH1 activation decreased both MDA-MB-231 invasiveness and proliferation. Meanwhile, less NOTCH1 inhibition enhanced invasiveness and proliferation (Nueda et al. 2017). The effects of DLK1 on NOTCH signaling are perhaps more complex in cancer models. These observations may be impacted by the properties of the cell lines being used as well as the culture conditions.

The inhibitory effect of DLK1 on NOTCH signaling has been best described through its interaction with NOTCH1, although DLK1 has also been shown to reduce NOTCH2, 3 and 4 activity (Nueda et al. 2018). Ectopic expression of DLK1 with NOTCH1-4 in 3T3L1 cells demonstrated an effect on adipogenesis into different types of adipocytes in a NOTCH receptor dependent manner. NOTCH1 overexpression promotes brown-like adipocyte differentiation,

while NOTCH2-4 promote white adipocyte phenotype (Nueda et al. 2018). However, there has yet to be published evidence of a physical interaction between DLK1 and NOTCH2-4. In adipocytes, DLK1 appears to be a universal inhibitor of NOTCH activity with NOTCH receptor-dependent outcomes on adipogenesis. Co-expression of DLK1 with NOTCH2-4 has only been described in certain pediatric malignancies (Falix et al. 2012), although the impact on pathophysiology has not yet been described. It would be valuable to investigate the response to DLK1 in tissues where there NOTCH2, 3 and 4 are more prevalent than NOTCH1.

In addition to the differences in functionality, the stoichiometry of full-size cleavable DLK1 to cleavage-resistant DLK1 isoform is likely a contributing factor to the ability of DLK1 to bind to its receptors and other interaction partners. DLK1 can homodimerize (Baladrón et al. 2001; Traustadóttir et al. 2017), and heterodimerize with Delta-like homolog 2 (DLK2) (Sánchez-Solana et al. 2011). Homodimerization and heterodimerization of DLK1 was associated with increased NOTCH1 activity (Sánchez-Solana et al. 2011). In a scenario where DLK1-DLK1 or DLK1-DLK2 binding is significantly greater than DLK1-NOTCH1 interaction, the inhibitory effect of DLK1 on NOTCH1 signaling would be reduced (Figure ***1.7***).

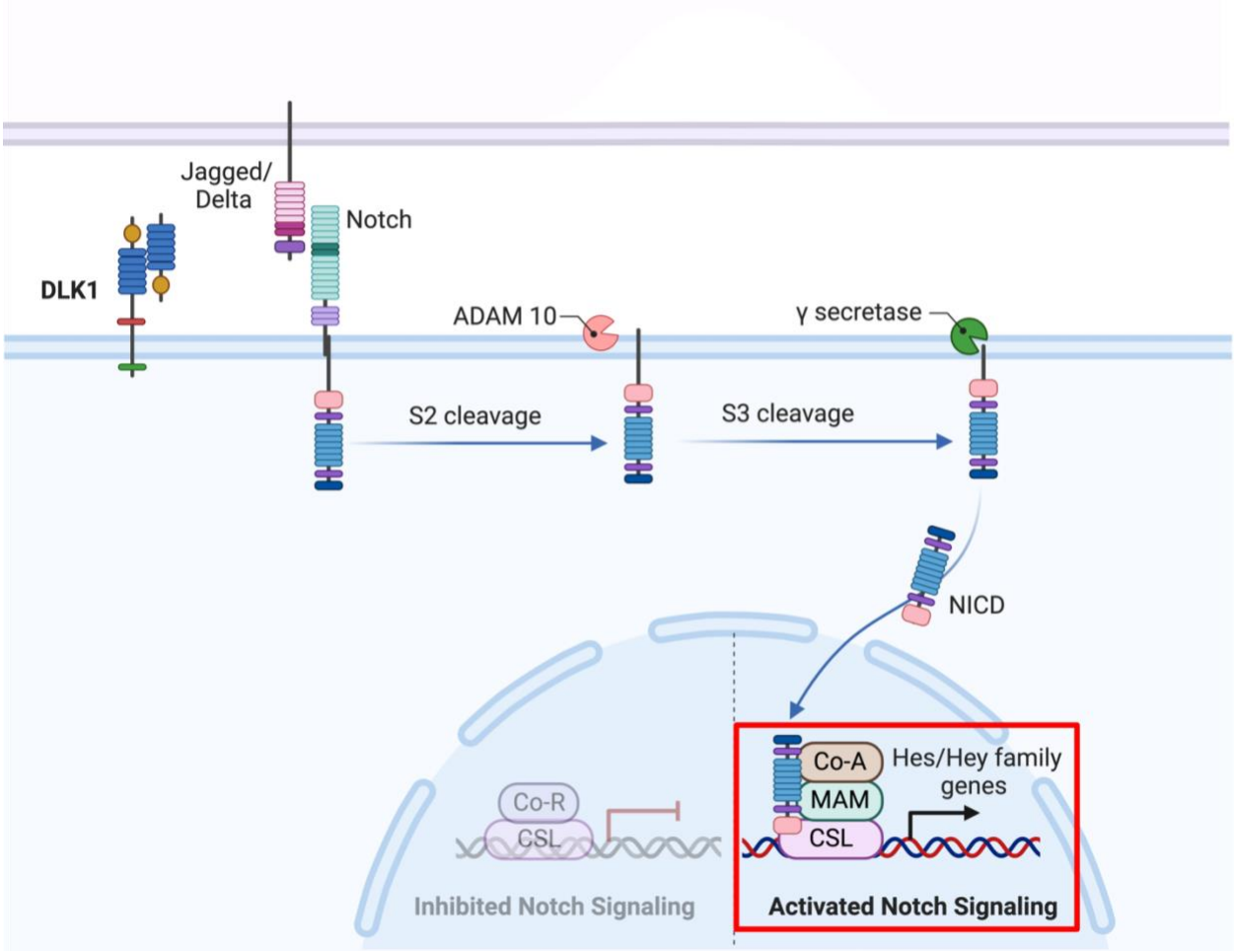

Figure 1.7 Schematic of DLK1-DLK1 interaction blocking NOTCH inhibition. DLK1 can bind to itself to permit canonical Jagged/Delta ligands to bind to NOTCH receptors and activate NOTCH signaling.

Altogether, DLK1 is a widely accepted non-canonical NOTCH ligand with evidence of a interaction between DLK1 and NOTCH1 along with its role in NOTCH signaling inhibition in several cell models. However, regulation of NOTCH signaling is so complex that there remains uncertainty about whether or not NOTCH downregulation is directly caused by DLK1. Additionally, the discovery of DLK1 receptors other than NOTCH1 expands the mechanisms that DLK1 can signal through beyond NOTCH signaling.

1.2.5 NOTCH-independent DLK1 signaling

There is substantial evidence of DLK1 functions involving other major pathways linked to regulation of differentiation. Inhibition of adipogenesis has been associated with DLK1-mediated NOTCH1 downregulation, although there are also NOTCH-independent responses mediated by DLK1 (Wang et al. 2010; Kim et al. 2007; Ruiz-Hidalgo 2002). DLK1 impacts pathways that are responsive to insulin, which promote adipocyte differentiation. DLK1 overexpression in 3T3L1 cells can inhibit insulin or insulin-like growth factor 1 (IGF1)-mediated progression of adipogenesis. Depending on the expression levels of DLK1, changes in the activation and kinetics of mitogen-activated protein kinase (MAPK) pathway activation were observed (Ruiz-Hidalgo 2002). DLK1 null mouse embryonic fibroblasts exhibited increased adipocyte differentiation and reduced mitogen-activated protein kinase kinase (MEK)/extracellular signal-regulated kinase (ERK) phosphorylation. Addition of soluble DLK1 was able to restore MEK/ERK phosphorylation, accompanied with inhibition of adipocyte differentiation (Kim et al. 2007).

The DLK1 juxtamembrane domain interacts with the C-terminus of fibronectin, which can then bind to integrin receptor (Wang et al. 2010; Hudak and Sul 2013). The DLK1-fibronectin-integrin interaction activates focal adhesion kinase (FAK) and small GTPase RAC which mediates induction of ERK/MAPK signaling. The ERK/MAPK activation increases SOX9, resulting in inhibition of translation of adipogenic factors (Wang et al. 2010). DLK1-mediated MEK/ERK activation is necessary for inhibition of adipogenesis. The soluble DLK1 ectodomain was also able to bind fibronectin (Chen et al. 2011; Guasti et al. 2013). In an embryonic mouse chondrogenic cell line, overexpression or treatment with soluble DLK1 reduced expression of mature chondrocyte markers. In this model, DLK1 inhibited insulin-dependent activation of PI3K/Akt signaling but had no effect on MEK/ERK activation. DLK1-fibronectin interaction may mediate

PI3K/Akt inhibition, although the integrin receptor responsible has not been identified (Chen et al. 2011).

Finally, DLK1 can modulate fibroblast growth factor (FGF) signaling through its interaction with cysteine-rich FGF receptor (CFR). By binding to CFR, DLK1 inhibits the ligand-receptor interaction between CFR and FGF18. Phenotypes of CFR-deficient and DLK-transgenic mice were similar with both demonstrating growth retardation. Based on these observations, it was proposed that DLK1-CFR interaction is a novel regulatory mechanism for FGF signaling in mice (Miyaoka et al. 2010).

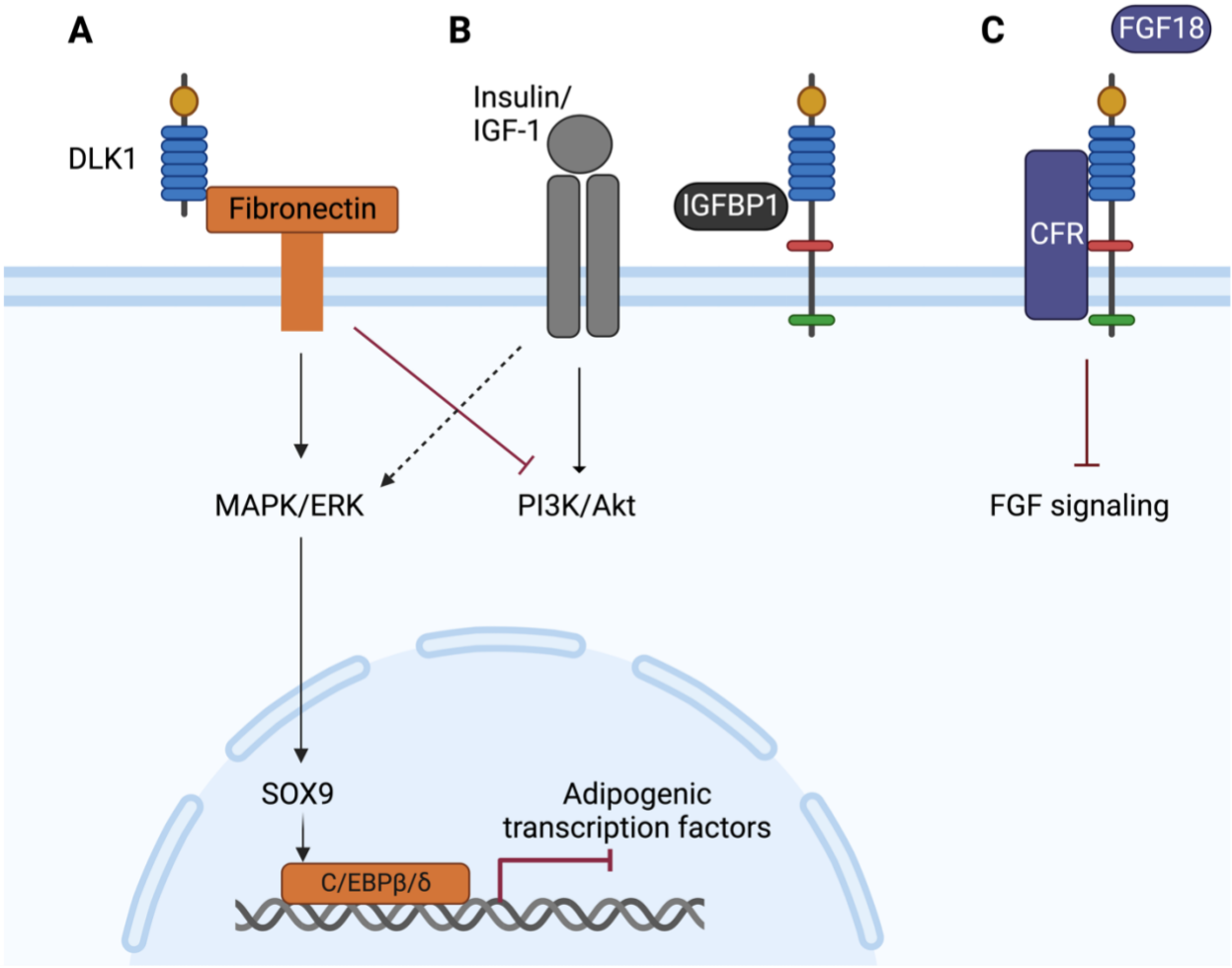

Figure 1.8 Summary of NOTCH-independent DLK1 pathways. A) DLK1 interacts with fibronectin to induce integrin-mediated activation of MAPK/ERK pathways. **B)** DLK1 binds to IGFBP1 to inhibit insulin/IGF-1 mediated effects. **C)** DLK1 inhibits FGF18 binding to CFR, preventing activation of FGF signaling. (Adapted from Traussadóttir et al, 2019).

Evidence regarding NOTCH-independent roles of DLK1 have been gathered largely from non-neoplastic mesoderm-derived tissue and cell models. In cancers, NOTCH-independent roles of DLK1 have not been sufficiently studied. As mentioned earlier, increased DLK1 ICD localization has been observed in glioma cell lines U3082MG, U3084MG, U3065MG cultured in hypoxia. In these cell models, there were no changes in NOTCH reporter activity in response to hypoxia-mediated DLK1 upregulation. However, increased DLK1 ICD release induced by hypoxia was associated with enhanced p53 DNA binding and increased Akt T308 phosphorylation (Grassi, Pantazopoulou, and Pietras 2020). Results were variable between the different cell lines, so there is yet to be robust evidence to support the role of DLK1 ICD in upregulation of p53 and Akt pathway activation. However, the discovery of other DLK1 interaction partners may provide guidance about alternative DLK1 signaling mechanisms if NOTCH-independent DLK1 functions are observed.

1.3 Gliomas and cancer stem cells

Gliomas are the most common primary tumors of the central nervous system, broadly categorized into low grade gliomas and the more malignant grade IV gliomas. Glioblastoma multiforme (GBM) is the most aggressive type, categorized as a grade IV glioma of astrocytic lineage (Louis et al. 2016). Standard GBM treatment involves a combination of surgical resection, radiotherapy and chemotherapy (Stupp et al. 2005; Tamimi and Juweid 2017). However, recurrence often occurs due to the heterogeneity of GBM tumors, which includes a population of

treatment-resistant GBM stem cells (GSCs) that are able to re-establish the tumor (Seymour, Nowak, and Kakulas 2015).

Key functional characteristics of GSCs include the ability for self-renewal, continuous proliferation, and tumor initiation. GSCs in gliomas are analogous to neural stem cells (NSCs) in normal brain (Galli et al. 2004; Singh et al. 2004). Primary brain tumor cells grown in non-adherent, serum-free culture can form tumor spheres and express markers associated with NSCs such as CD133, SOX2, and Nestin. The surface marker CD133 has been used to isolate GSCs from brain tumor samples. When grown in culture, CD133-positive cells were able to differentiate into diverse cell types that capture the heterogeneity of patient tumors (Singh et al. 2004). Increasing glioma malignancy has been positively correlated with higher CD133 expression (Zeppernick et al. 2008; Thon et al. 2010). Regardless of glioma grade, CD133-positive cells isolated from brain tumors were capable of multi-lineage differentiation (Thon et al. 2010). Grade II and grade III primary gliomas with higher CD133 expression were associated with higher incidence of tumor regrowth and progression to grade IV gliomas (Zeppernick et al. 2008).

The GSC population in gliomas appear to be correlated with a more malignant tumor phenotype. These stem-like cells provide a mechanism for brain tumors to survive treatment and re-establish the tumor leading to poor prognosis. Understanding the regulatory mechanisms of GSCs will provide a more complete picture of how to devise treatment strategies to target this cell population.

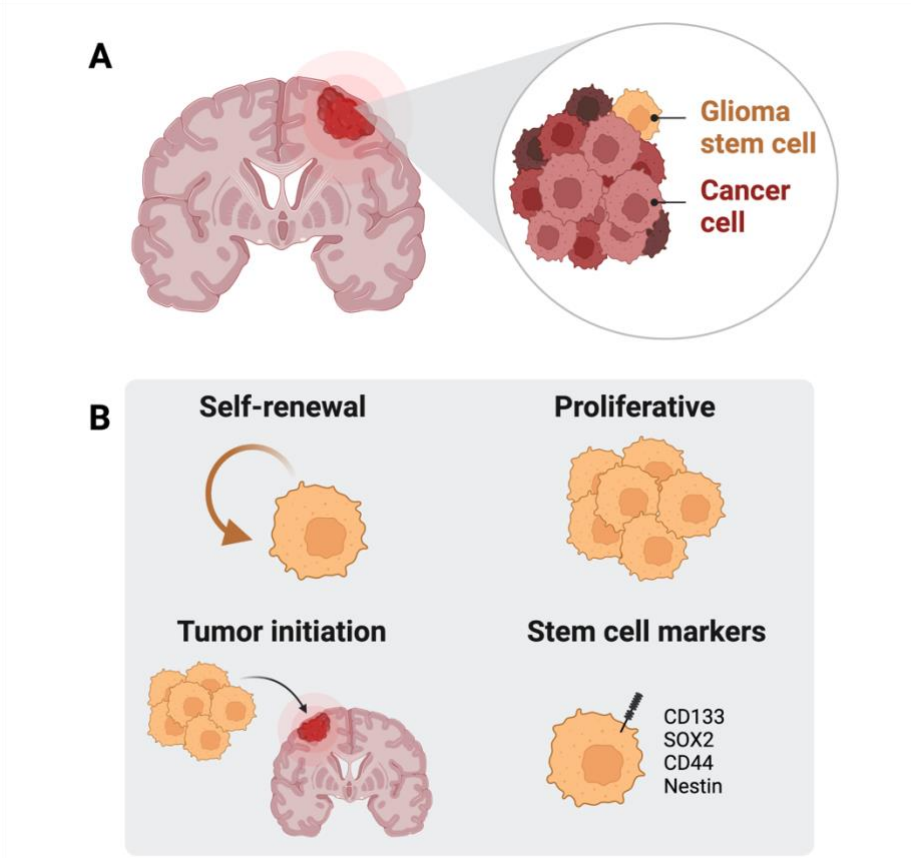

Figure 1.9 Schematic of glioblastoma (GBM) and glioma stem cells (GSC) properties. A) GBM is a heterogeneous brain tumor composed of cancer cells and a population of GSCs that are capable of recapitulating the tumor. **B)** Key characteristics of GSCs are capacity for self-renewal, continuous proliferation, tumor initiation and expression of stem cell markers.

1.3.1 DLK1 in cancer stem cells

As described in a previous section, DLK1 is an important factor for regulating cell differentiation and proliferation. DLK1 expression also increases during regeneration and disease. Genes involved in differentiation and proliferation are often implicated in cancer.

DLK1 was first identified in pediatric neuroendocrine tumors (Helman et al. 1987). In several neuroblastoma cell lines, hypoxia upregulated DLK1 mRNA and protein expression. Neuroblastoma cell line BE(2)C has cancer stem cell characteristics, demonstrated by enhanced

tumor sphere formation and clonogenicity associated with high endogenous DLK1 levels. When DLK1 expression was silenced via siRNA or adenovirus in BE(2)C, cells began to undergo spontaneous differentiation (Kim et al. 2009). This has also been observed *in vivo* with a neuroblastoma xenograft model, emphasizing the inhibitory effect of DLK1 on neuroblastoma differentiation (Begum et al. 2012).

The presence of high DLK1 protein in neuroendocrine tumors garnered interest for the role of DLK1 in brain tumors. In samples of glioblastoma (GBM), astrocytoma and oligodendroglioma, DLK1 expression was elevated compared to normal brain. The difference was significant in GBM, where 32% of samples had at least two-fold greater DLK1 levels than normal brain tissue (Yin et al. 2006). In an analysis of the Cancer Genome Atlas (TCGA) and Chinese Glioma Genome Atlas (CGGA), elevated DLK1 mRNA levels were associated with high-grade gliomas (Grassi, Pantazopoulou, and Pietras 2020). Poor prognosis in gliomas has been linked with the presence of GSCs due to their ability to resist treatments and re-capitulate the tumor. These secondary tumors are often more malignant than the primary tumors, negatively impacting prognosis of GBM patients. Unsurprisingly, DLK1 has been found to play a role in GSC regulation, acting as a promoter of stem cell-like characteristics in GBM.

In a murine glioma model, DLK1 expression was localized to peri-vascular and peri-necrotic regions of hypoxic tumor areas. Hypoxia has a profound effect on DLK1 protein expression and processing in both glioma cells and astrocytes (Grassi et al. 2020; Grassi, Pantazopoulou, and Pietras 2020). Full-size, cleavable DLK1 and cleavage-resistant DLK1 constructs were stably expressed in U3084MG human GBM cells to elucidate the impact of DLK1 on glioma hypoxia response. Hypoxia has been shown to promote stem cell properties of tumor stem cells, and its specific role in GSC biology has been reviewed previously (Boyd et al. 2021).

Indeed, in hypoxic conditions, U3084MG cells expressing full-size DLK1 demonstrated increased colony formation and upregulation of stem cell factors NANOG, OCT4 and SOX2 compared to normoxia. In contrast, promotion of stemness was not observed in U3084MG with cleavage-resistant DLK1 revealing a DLK1 isoform-dependent hypoxia response (Grassi, Pantazopoulou, and Pietras 2020).

Within the tumor microenvironment, astrocytes are a source of DLK1. In peri-necrotic and peri-vascular regions, DLK1 was detected primarily in tumor-associated astrocytes with a smaller population of DLK1-positive tumor cells. Human fetal astrocytes cultured under hypoxic conditions produced significantly greater amounts of soluble DLK1 compared to those cultured under normoxia (Grassi et al. 2020). Conditioned medium containing soluble DLK1 from primary human astrocytes was used for treatment of human GBM cell lines (U3082MG, U3084MG, U3065MG) and primary murine glioma cells (PIGPC). Enhanced colony formation and tumor sphere formation of human and murine glioma cell lines were observed when cultured with DLK1 conditioned medium (Grassi et al. 2020). The soluble ectodomain of DLK1 was sufficient to enhance stem cell properties in glioma cells. The effect of DLK1 on the hypoxia response of glioma cells may be attributed to the stabilization of HIF2a. Glioma cells cultured in hypoxia and treated with soluble DLK1 showed increased HIF2a expression and upregulation of hypoxia response element (HRE) activity via luciferase assay (Grassi et al. 2020).

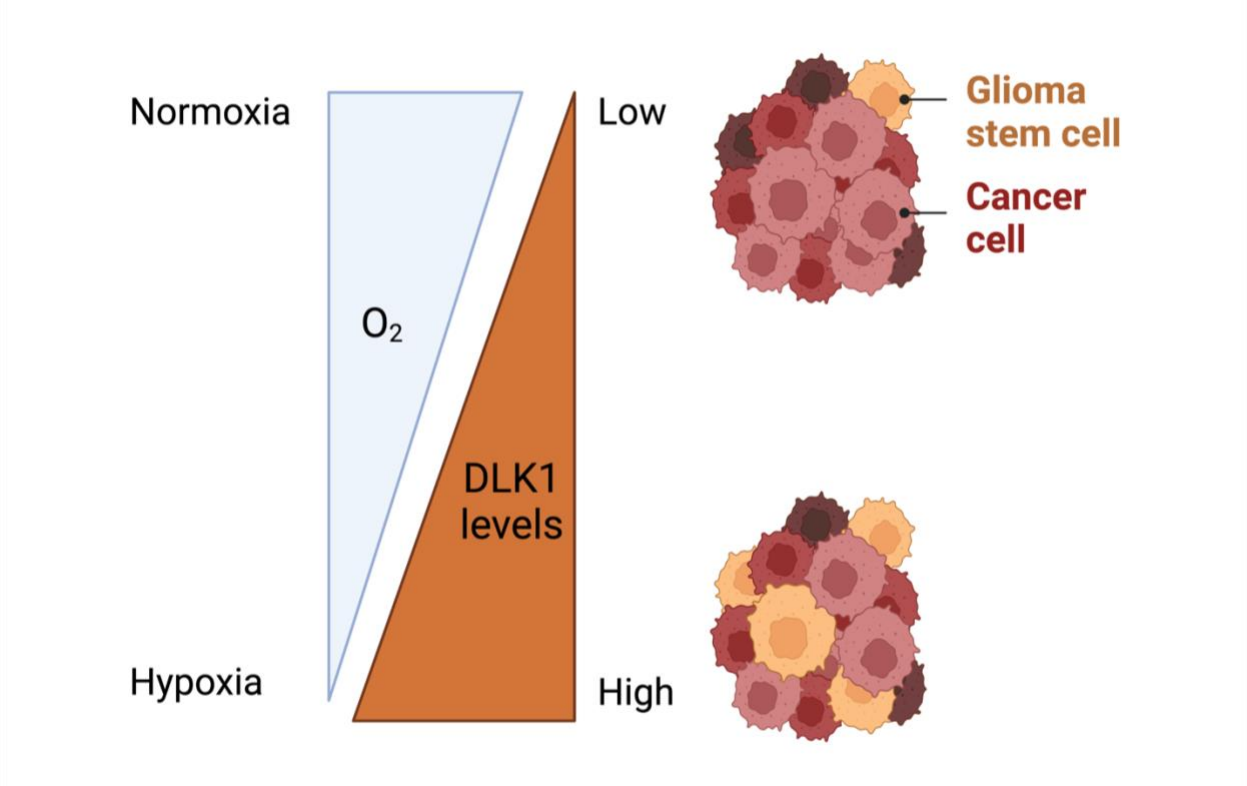

Figure 1.10 Schematic of DLK1 in glioma stem cells. In hypoxic conditions DLK1 expression and proteolytic cleavage increases. This is associated with increased glioma stemness.

Currently, reports of DLK1 in gliomas are limited particularly regarding DLK1 signaling mechanisms. DLK1 regulation is already complex, considering its NOTCH-dependent and NOTCH-independent functions as well as the varying functionalities of DLK1 isoforms. However, it is apparent that DLK1 impacts several factors critical to glioma progression such as stemness, proliferation and migration (Grassi et al. 2020; Grassi, Pantazopoulou, and Pietras 2020; Yin et al. 2006).

1.3.2 Regulatory pathways in glioma stem cells

Regulation of GSCs involve both intrinsic factors such as genetic, epigenetic, and metabolic regulation, as well as extrinsic factors like the niche factors and immune response within the tumor microenvironment. These regulatory mechanisms have been previously reviewed, along

with advances in therapies designed to target each factor (Lathia et al., 2015; Li et al., 2009). This section will specifically describe the regulatory pathways associated with modulation of GSC state, with the potential for DLK1 involvement. Key pathways responsible for neural stem cell fate determination are also activated in GSCs. Among these is the NOTCH pathway, where DLK1 is a known ligand.

Non-canonical NOTCH ligands, such as DLK1, are the least studied in gliomas. As a known antagonist of NOTCH signaling, DLK1 is a promising ligand to investigate in the context of GBM stemness. Generally, GSCs have been correlated with elevated NOTCH activity (Bazzoni and Bentivegna 2019). When NICD was overexpressed in SHG-44 glioma cell line, an increase in sphere formation and Nestin expression was observed (Zhang et al. 2008). Hypoxic conditions promoted GSC expansion through HIF1-a induced activation of NOTCH signaling (Qiang et al. 2012). This is further supporter by a reduction of GSC properties upon inhibition of NOTCH signaling with gamma-secretase inhibitors (Fan et al. 2006; 2010). In gliomas, increased NOTCH activation appears to promote stemness in GSCs. This is contradictory to reports of DLK1 as an inhibitor of NOTCH signaling and as a promoter of cancer stemness both in hypoxia and normoxia (Grassi et al. 2020; Grassi, Pantazopoulou, and Pietras 2020). However, this may be an indication that DLK1 acts through alternative signaling mechanisms to modulate glioma stemness depending on the cellular context.

1.4 Rationale and objectives

There is currently a lack of knowledge about CTRP8 receptors and functionality in cancer. We have previously shown the roles of CTRP8 in promoting GBM invasiveness and treatment resistance mediated through its receptor RXFP1. Apart from RXFP1, there are no other known receptors of CTRP8. However, only a subset of gliomas express RXFP1, and yet CTRP8 appeared

to have significant effects on GBM biology despite the absence of its receptor. This opened the possibility that CTRP8 is capable of binding to other receptors to impact glioma progression.

A yeast-two hybrid screen repeatedly identified the translational products of several human DLK1 gene fragments as putative interaction partners for CTRP8. The role of DLK1 in gliomas and cancer stem cells has been well described and this provides measurable parameters to assess the functionality of CTRP8-DLK1 interaction in GBM.

The objectives of this study are to (1) characterize DLK1 as a novel interaction partner of CTRP8 and (2) identify the impact thereof on glioma stemness and potential signaling mechanisms. We hypothesize that CTRP8 is a novel interaction partner of DLK1. In gliomas and other malignancies, DLK1 is generally accepted as a promoter of stem cell properties in cancer cells. Interaction with CTRP8 may impact DLK1-mediated effects on stemness in gliomas through NOTCH signaling and/or other DLK1 signaling pathways.

2 MATERIALS AND METHODS

2.1 Yeast-two hybrid

ULTImate yeast-two hybrid (Y2H) screening of a human placental cDNA expression library was performed to identify potential interaction partners of human full-size CTRP8, used as bait in the screen (Hybrigenics Services, Evry-Courouronnes, France). When grown in selection medium plus 0.5 mM 3-amino-triazole (3AT) to reduce background, 260 clones encoding 99 different prey proteins were processed out of 31 Million interactions. Of those, 11 prey proteins were classified by a prediction algorithm as "A = Very high" (n=3) and "B = High" (n=8) confidence targets by the company (Formstecher et al. 2005). DLK1 was a category A target and 42 different yeast clones isolated from the human placental library screen grew strongly in selection medium containing plasmid inserts encoding in-frame sequences for human DLK1.

2.2 Cell culture

Human embryonic kidney cell line HEK293, neuroblastoma cell line Kelly and glioma cell line U251 (ATCC, Virginia, USA) were used for transfections and other experiments. HEK293 and U251 were cultured in Dulbecco's Modified Eagle Medium/Nutrient Mixture F12 (DMEM/F12) (Gibco, Massachusetts, USA) supplemented with 10% Fetal Bovine Serum (FBS) (Gibco). Kelly was cultured in Roswell Park Institute (RPMI) (Gibco) with 10% FBS. Cells were kept in a 37°C humidified incubator with 5% CO_2. HEK293 cells were used mainly for co-immunoprecipitation, due to its capability for efficient transfections. Kelly was used as an endogenous expressor of DLK1 in co-immunoprecipitation. U251 cells were used as the glioma model to assess the effects of DLK1 and CTRP8 on glioma biology.

2.3 Expression constructs

Expression constructs used for stable and transient transfection are listed in Table ***2.1***. Unless otherwise indicated, all expression constructs were synthesized and cloned into pcDNA3.1 plasmid by Life Technologies (Massachusetts, USA). Plasmids were transformed into *E. coli* XL Blue cells and DNA prepared with Qiaprep Spin Miniprep Kit (Qiagen, Hilden, Germany). Human DLK1 in pLX304 vector (clone ID: ccsbBroad304_07300) was acquired from DNASU Plasmid Repository (Arizona, USA). DLK1 plasmid was prepared for lentivirus production with the Qiagen Midi Prep kit (Qiagen) and the lentiviral preparation was completed at the University of Manitoba Lentiviral Core Platform.

Table 2.1 Expression constructs for stable and transient transfections

Name	Tag	Antibiotic	Source	Molecular weight (kDa)
CTRP8	FLAG	G418	Life Technologies	28
CTRP8-C1q	FLAG	G418	Life Technologies	15
CTRP8-Cterminus	FLAG	G418	Life Technologies	27
CTRP8-noCollagen(Coll)	FLAG	G418	Life Technologies	27
CTRP8-noVariableRegion (VR)	FLAG	G418	Life Technologies	23
CTRP8-C1qLoop1(L1b)	FLAG	G418	Life Technologies	19
CTRP8-noRXFP1site(mut)	FLAG	G418	Life Technologies	18
DLK1	V5	Blasticidin	DNASU	41

Brevideltinin	MYC	G418	Life Technologies	27
Cleavage-resistant DLK1 (DLK1.CR)	V5	G418	Life Technologies	35

2.4 Stable and transient transfections

For stable and transient transfections, cells were plated and allowed to attach for 24h in DMEM/F12 with 10% FBS. Complexes were prepared for transfection with Effectene Transfection Reagent (Qiagen cat:301425) according to the manufacturer protocol. For transient transfections, cells were collected for protein or RNA extraction 48h after addition of complexes. For stable transfection, begin selection 48h after addition of complexes in cell culture medium with the appropriate mammalian selection antibiotic indicated in Table ***2.1***. Single cell clones were picked and plated in a 24-well plate for expansion.

2.5 Recombinant CTRP8 treatment

Recombinant human FLAG-tagged CTRP8 was produced in *E. coli* as previously described (Thanasupawat et al. 2018). Cells were pre-treated with DMEM/F12 with 1% FBS for 24h prior to treatment with 100ng/mL CTRP8 in DMEM/F12 supplemented with 1% FBS.

2.6 Co-immunoprecipitation

Co-immunoprecipitation (co-IP) was used to assess protein-protein interaction between DLK1 and CTRP8. Cells were plated in 100mm dishes for transient transfection and collected with cold PBS and a cell scraper. Cells were spun for 5min at 1,000 g in 4°C centrifuge, then resuspended in lysis buffer (50mM Tris-HCl, 150mM NaCl, 1mM EDTA, 1mM $MgCl_2$, 0.3% NP-40) with 1:100 protease inhibitor (ThermoFisher, cat:1860932). Protein lysate was homogenized with 22G needle and 1.0mL syringe before centrifuging for 10min at 17,000 g. Supernatant was

collected in a new tube and protein concentration measured with BCA assay kit (ThermoFisher, cat:23225). Readings at 560nm were acquired using Synergy H1 microplate reader (Biotek, Vermont, USA).

For co-IP, 200μg of protein lysate was incubated with 2μg of IgG or specific antibody targeting the protein of interest (Table ***2.2***). Protein samples were placed on a shaker at 4°C overnight. The following day, protein samples were incubated with Protein A/G magnetic beads (ThermoFisher, cat:88803) for 2-4 hours on a shaker at 4°C. With a magnetic separator (GE Life Sciences, Massachusetts, USA), supernatant was collected from the samples, then washed thrice with wash buffer (50mM Tris-HCl, 150mM NaCl, 1mM EDTA, 1mM $MgCl_2$, 0.03% NP-40) with 1:100 protease inhibitor (ThermoFisher). Aliquots of the supernatant and third wash were taken for Western blot. Proteins bound to magnetic beads were eluted with room temperature 3X Laemmli buffer. Co-IP protein samples were separated via SDS-PAGE and detected in Western blot.

Table 2.2 Co-immunoprecipitation antibodies

Antibody	**Host species**	**Source**
Mouse IgG1		Sigma-Aldrich (M5284)
Mouse IgG2a		Cell Signaling Technology (53484)
Rabbit IgG		Cell Signaling Technology (3900)
V5-Tag	Mouse	ThermoFisher (R960-25)
Myc-Tag	Mouse	Abcam (ab32)
DLK1	Mouse	Santa Cruz (sc-376755)

CTRP8 1439	Rabbit	ThermoFisher

2.7 Protein extraction and Western blot

Whole cell protein extracts were prepared by lysing cells with 1X Laemmli loading buffer. Nuclear and cytoplasmic proteins were collected with NE-PER Reagent Kit (ThermoFisher, cat:78835) according to the manufacturer protocol. Protein concentrations were measured with BCA assay (ThermoFisher, cat:23225) using Synergy H1 microplate reader (Biotek). Protein lysates were prepared for Western blot with 5X Laemmli loading buffer, boiled at 95°C for 5min and placed on ice.

Proteins were separated via SDS-PAGE on 10%-12% gel (Bio-Rad, California, USA), then transferred to a nitrocellulose membrane (Cytiva, Massachusetts, USA) using TransBlot Turbo Transfer machine (Bio-Rad). Membranes were incubated in 5% non-fat milk in Tris-buffered saline-0.1% Tween (TBS-T) for 1 hour at RT to block unspecific antibody binding. Primary antibodies were diluted in buffer recommended by manufacturer (Table ***2.3***) and incubated with membranes overnight at 4°C.

Table 2.3 Western blot primary antibodies

Antibody	**Host species**	**Source**	**Blocking buffer**	**Dilution**
Myc-Tag	Rabbit	Cell Signaling Technology (2278)	5% BSA-TBST	1:1000
V5-Tag	Mouse	ThermoFisher (R960-25)	5% milk-TBST	1:2000
CTRP8 1439	Rabbit	ThermoFisher	5% milk-TBST	1:1000

DLK1	Mouse	Santa Cruz (sc-376755)	5% milk-TBST	1:1000
b-actin	Mouse	Santa Cruz (sc-47778)	5% milk-TBST	1:10,000
Lamin A/C	Mouse	Santa Cruz (sc-376248)	5% milk-TBST	1:1000
α-tubulin	Rabbit	Cell Signaling Technology (2144)	5% BSA-TBST	1:1000

The following day, membranes were washed thrice with TBS-T and incubated with horseradish peroxidase (HRP) conjugated secondary antibodies (Table ***2.4***) for 1 hour at RT. For co-IP samples, TrueBlot and CleanBlot secondary antibodies were used to minimize detection of IgG heavy chain and light chain. Membranes were washed thrice with TBS-T before the addition of substrate and image acquisition. Clarity Western ECL Substrate (Bio-Rad, cat. 1705061) were used to visualize protein bands on the ChemiDoc Imaging System (Bio-Rad).

Table 2.4 Western blot secondary antibodies

Antibody	**Host species**	**Source**	**Blocking buffer**	**Dilution**
Mouse TrueBlot Anti-mouse IgG HRP	Rat	Rockland (18-8817-33)	5% milk-TBST	1:1000
CleanBlot IP detection reagent HRP		ThermoFisher (21230)	5% milk-TBST	1:200
Goat anti-mouse HRP	Goat	Cell Signaling Technology (7074s)	5% milk-TBST	1:2000

Goat anti-rabbit HRP	Goat	Cell Signaling Technology (7076s)	5% milk-TBST	1:2000

2.8 Sphere formation assay

To assess the effect of DLK1 on stem cell properties of glioma cells, U251, U251-DLK1 and U251-DLK1/CTRP8 cells were used in a sphere formation assay (Figure ***2.1***). Cells were detached with Trypsin-EDTA to acquire a single cell suspension. Single cells were seeded in ultra-low attachment 6-well plates in brain tumor initiating cell (BTIC) medium containing NeuroCult NS-A Basal and Supplement (STEMCELL Technologies, Vancouver, Canada), 2ug/mL heparin (STEMCELL Technologies), 20ng/mL each of bFGF and EGF (Sigma-Aldrich) for 48 hours for bulk sphere formation. Spheres from bulk formation were dissociated to a single cell suspension with Accumax (Sigma), then seeded one cell per well in 96-well plates in BTIC medium for primary sphere formation. Spheres were allowed to form for 10-12 days prior to quantifying the percentage of wells with successful sphere formation. Wells that contained spheres exceeding 50μm in diameter were included in the count. Primary spheres were dissociated to single cells once again to be re-seeded for secondary sphere formation.

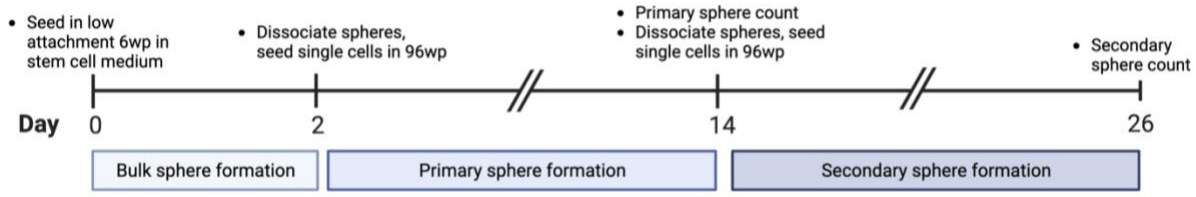

Figure 2.1 Schematic of sphere formation protocol. Single cells were plated in a 6 well-plate (wp) in brain tumor initiating cell medium (BTIC) medium for 48h of bulk sphere formation.

Spheres were dissociated to single cells to seed one cell per well in a 96wp for both primary and secondary sphere formation. Spheres were formed after 10-12 days prior to quantification.

Sphere formation efficiency was determined by calculating the percentage of spheres out of a 96-well plate (Equation ***2.1***). Images of spheres were taken on Zeiss D1 fluorescent microscope (Zeiss, Oberkochen, Germany). Sphere diameters were quantified using Zeiss ZEN Blue software (ver2.3).

$$\%\ of\ wells\ with\ spheres = \frac{Sphere\ count}{96} \times 100$$

Equation 2.1 Sphere formation efficiency calculation

2.9 RNA extraction, cDNA synthesis and polymerase chain reaction (PCR)

RNA was extracted from cells in TRIzol (ThermoFisher) according to the manufacturer protocol. The concentration and purity of RNA samples was assessed by acquiring absorbance readings at 260nm and 280nm on a Synergy H1 microplate reader (Biotek). Quanta qScript cDNA SuperMix (Quantabio, Massachusetts, USA) was used for cDNA synthesis. Reactions were assembled with 1μg of RNA with 4μL cDNA mix plus RNase-DNase free water to a total volume of 20μL. Reaction mixtures were briefly centrifuged to mix and incubated in a thermocycler at the following intervals: 25°C for 5min, 42°C for 30min, 85°C for 5min and holding at 4°C.

For quantitative real-time PCR (qPCR), primers were synthesized by Invitrogen and re-constituted in ddH_2O. All regular qPCR primers have a melting temperature (Tm) of 60°C (Table ***2.5***). High amplicon size primers have a Tm of 63°C (Table ***2.6***).GAPDH was used as the housekeeping gene control. Reactions for qPCR were prepared in MicroAmp Optical 96-well reaction plates (Applied Biosystems, Massachusetts, USA). Each well contains one 20μL reaction

composed of 1X PowerUp SYBR Green Master Mix (Applied Biosystems cat: A25742), 0.2μM each of forward and reverse primer plus 10ng cDNA.

Readings were acquired with QuantaStudio3 real-time PCR system (Applied Biosystems). Relative fold gene expression was determined using the Delta-Delta Ct method. Reaction mixtures pass through three stages: hold, PCR and melt curve. For all primers, the hold stage was 50°C for 2min and 95°C for 10min. The PCR stage for regular qPCR primers listed in Table ***2.5*** consisted of: denaturation at 95°C for 15sec, annealing at 60°C for 1min for 40 cycles. For high amplicon size primers in Table ***2.6*** the PCR stage required denaturation at 95°C, annealing at 63°C for 1min, and extension at 72°C for 1min for 40 cycles. The final melt curve stage is the same for all primers: 95°C for 15sec and finally 60°C for 1min.

Table 2.5 Regular qPCR primers

Name	Forward (F) and reverse (R) primer sequence	Amplicon size (bp)
GAPDH	F – GTCTCCTCTGACTTCAACAGCG R – ACCACCCTGTTGCTGTAGCCAA	120
NOTCH1	F – GGTGAACTGCTCTGAGGAGATC R – GGATTGCAGTCGTCCACGTTGA	150
Hes1	F – GGTGCTGATAACAGCGGAAT R – TGAGCAAGTGCTGAGGGTTT	108
OCT4	F – CCAAACGACCATCTGCCGC R – ATACTGGTTCGCTTTCTCTTTC	170
SOX2	F – CACCCACAGCAAATGACAGC	118

	R – GTCCCCCAAAAAGAAGTCCAG	
ALDH1A3	F – TGCTACAACGCCCTCTATGC	143
	R – CTTCAGGGGTTCTTGTCGCC	

Table 2.6 High amplicon size qPCR primers

Name	Forward (F) and reverse (R) primer sequence	Amplicon size (bp)
CD133*	F – TGGCAACAGCGATCAAGGAGAC	614
	R – ATAGCCGCACACGCCACACAG	
CD44*****	F – TGCCGCTTTGCAGGTGTATTCC	342
	R - TCCATCAAAGGCATTGGGCAGG	

2.10 Notch fluorescent reporter assay

The effect of DLK1 and CTRP8 on Notch activity in U251 cells was assessed with a fluorescent reporter. Notch fluorescent reporter plasmid pMuLE_ENTR_CBF-tdTomato_L3-L2 was a gift from Manfred Ogris (Addgene plasmid #113708; http://n2t.net/addgene:113708; RRID:Addgene_113708) (Maier et al. 2019). A constitutively active pEGFP-C1 construct (Addgene) was used as a control to normalize tdTomato transfection. Plasmids were co-transfected into U251 and U251-DLK1 cells with Effectene reagent (Qiagen, cat:301425) as described in Section 2.4, and fluorescent readings were acquired 48h after transfection by flow cytometry.

Cells were detached with Trypsin-EDTA, washed thrice with PBS and re-suspended in 2mM EDTA in PBS with 1% FBS. DAPI 1:10,000 was used as a viability stain. Fluorophore activity measurements were acquired on CytoFLEX-LX flow cytometer (Beckman-Coulter, California,

USA). Single, live cells with EGFP were detected with SSC-A vs. FITC (525/40nm BP) and tdTomato was selected using SSC-A vs. PE (585/42nm BP). EGFP signal was used to normalize the tdTomato signal prior to calculation of fold change (Equation ***2.2***).

$$Normalized\ NOTCH\ reporter\ signal = \frac{\%\ tdTomato\ cells}{\%EGFP\ cells}$$

$$Fold\ change\ tdTomato = \frac{Test\ normalized\ reporter\ signal}{Reference\ normalized\ reporter\ signal}$$

Equation 2.2 NOTCH activity fold change calculation

2.11 Immunofluorescence

Cells were plated on APTES (Sigma-Aldrich, Missouri, USA) coated coverslips for 24-48h and fixed with 3.7% formaldehyde in PBS for 30 min at RT. Cells were permeabilized with 0.1% Triton-X100 for 10 min at RT. Cells were blocked in 10% Normal Goat Serum (NGS) (Sigma-Aldrich, cat. D9023) in PBS-0.1% Tween (PBS-T) for 1 hour RT. Primary antibodies 1:500 V5-Tag (Thermofisher, cat:R960-35) in 10% NGS-PBS-T were incubated with cells overnight at 4°C. The following day, coverslips were washed thrice with PBS-T, then incubated with 1:1000 Goat anti Mouse Alexa594 in 10% NGS-PBS-T for 1hr at RT. Coverslips washed three times with PBS-T, then stained with 1:60,000 DAPI (Sigma-Aldrich). Coverslips mounted with Fluoromount G (ThermoFisher, cat:00-4958-02). Images were acquired with a Zeiss Z2 fluorescence microscope. Deconvolution and image analysis were performed with Zeiss ZEN Blue software (ver 2.3).

2.12 Statistical analysis

Experiments were completed with at least three biological replicates. Statistical analyses were conducted using GraphPad Prism (ver 9.3). The statistical significance of sphere formation and diameters, fold change of tdTomato+ cells in the reporter assay and relative gene expression

in qPCR were determined with one-way ANOVA. P-values less than 0.05 were considered statistically significant (*P<0.05, **P<0.01, ***P<0.001, ****P<0.0001).

3 RESULTS

3.1 CTRP8 is predicted to interact with DLK1 EGF-like domains

To identify potential interaction partners of CTRP8, human full-size CTRP8 was screened against a human placental cDNA library in a yeast-two hybrid system (Y2H). The screen scored DLK1 as one of three a category A ("very high confidence") interaction partner of full-size CTRP8. CTRP8 bound to fragments corresponding to the N-terminus of DLK1, encompassing the signal peptide to the third EGF-like domain (Figure ***3.1***). The 42 sequenced clones encoding human DLK1 isolated by Y2H identified DLK1 amino acids 3-122 as the predicted CTRP8 interaction domain and region most likely to interact with CTRP8.

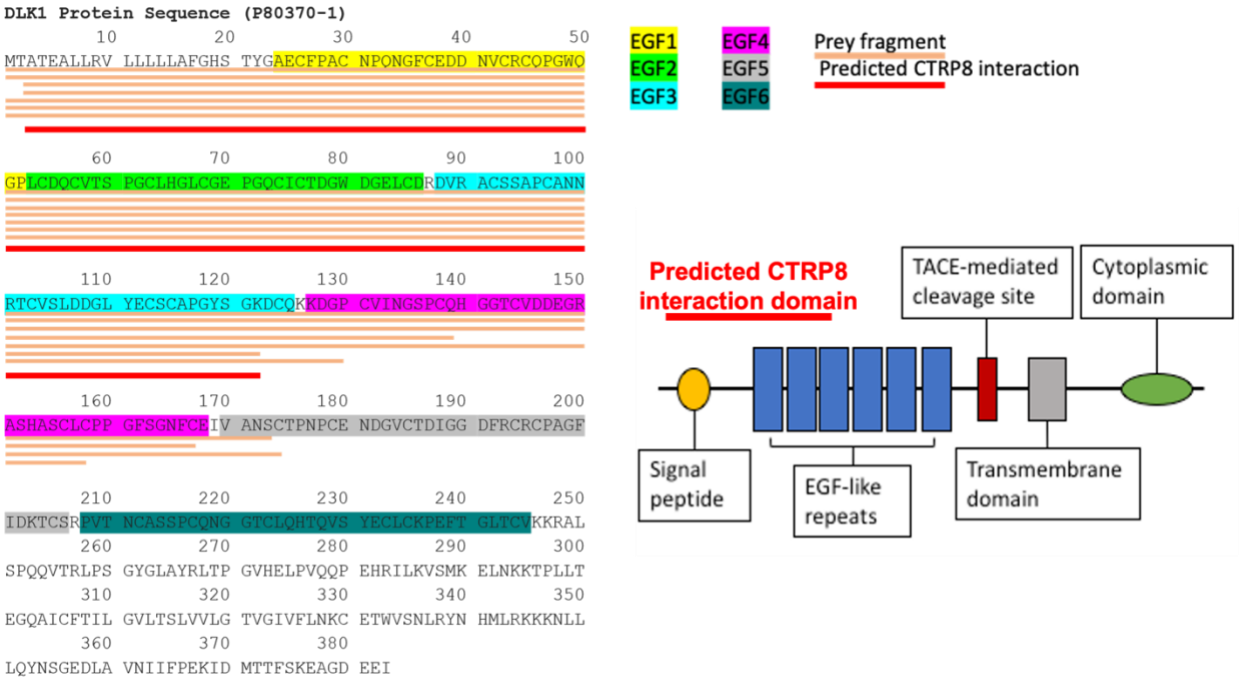

Figure 3.1 Schematic of yeast-two hybrid screen (Y2H) sequence alignments. DLK1 prey fragments (orange) that interact with CTRP8 were identified by Y2H and aligned with DLK1 protein sequence from UniProt (P80730). Y2H identified a predicted CTRP8 interaction domain

on DLK1 (red), corresponding to amino acids 3-122, the signal peptide and three EGF-like repeats of DLK1.

3.2 CTRP8 interacts with full-size DLK1

Co-immunoprecipitation (co-IP) was used to assess the physical interaction between CTRP8 and DLK1. HEK293 cells were stably transduced with full-size DLK1-V5 tagged lentivirus to generate HEK-DLK1 clones (Figure ***3.2***).

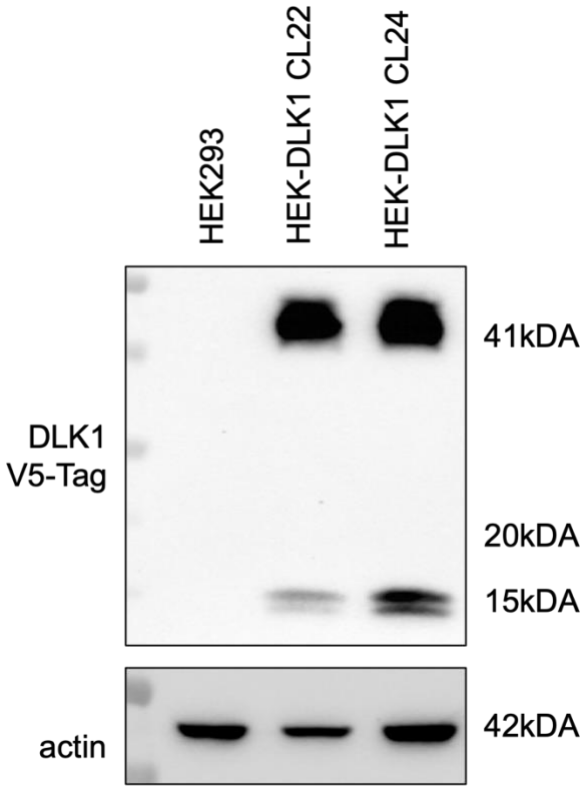

Figure 3.2 Protein expression in HEK293 and HEK-DLK1 clones. Whole cell lysates collected from HEK293 cells and two different HEK-DLK1 clones. DLK1 was detected using the V5-Tag antibody.

A CTRP8-Flag construct was transiently expressed in HEK-DLK1 cells and the proteins collected for co-IP. HEK-DLK1 and HEK-DLK1+CTRP8 protein lysates were incubated with V5-

Tag or mouse IgG2a. The V5-Tag antibody specifically immunoprecipitated full-size DLK1 and co-IPs CTRP8 as detected in Western blot, indicating an interaction between the two proteins. Similarly, in a reverse co-IP, a CTRP8 antiserum was able to immunoprecipitate CTRP8 and co-IP DLK1 (Figure ***3.3***).

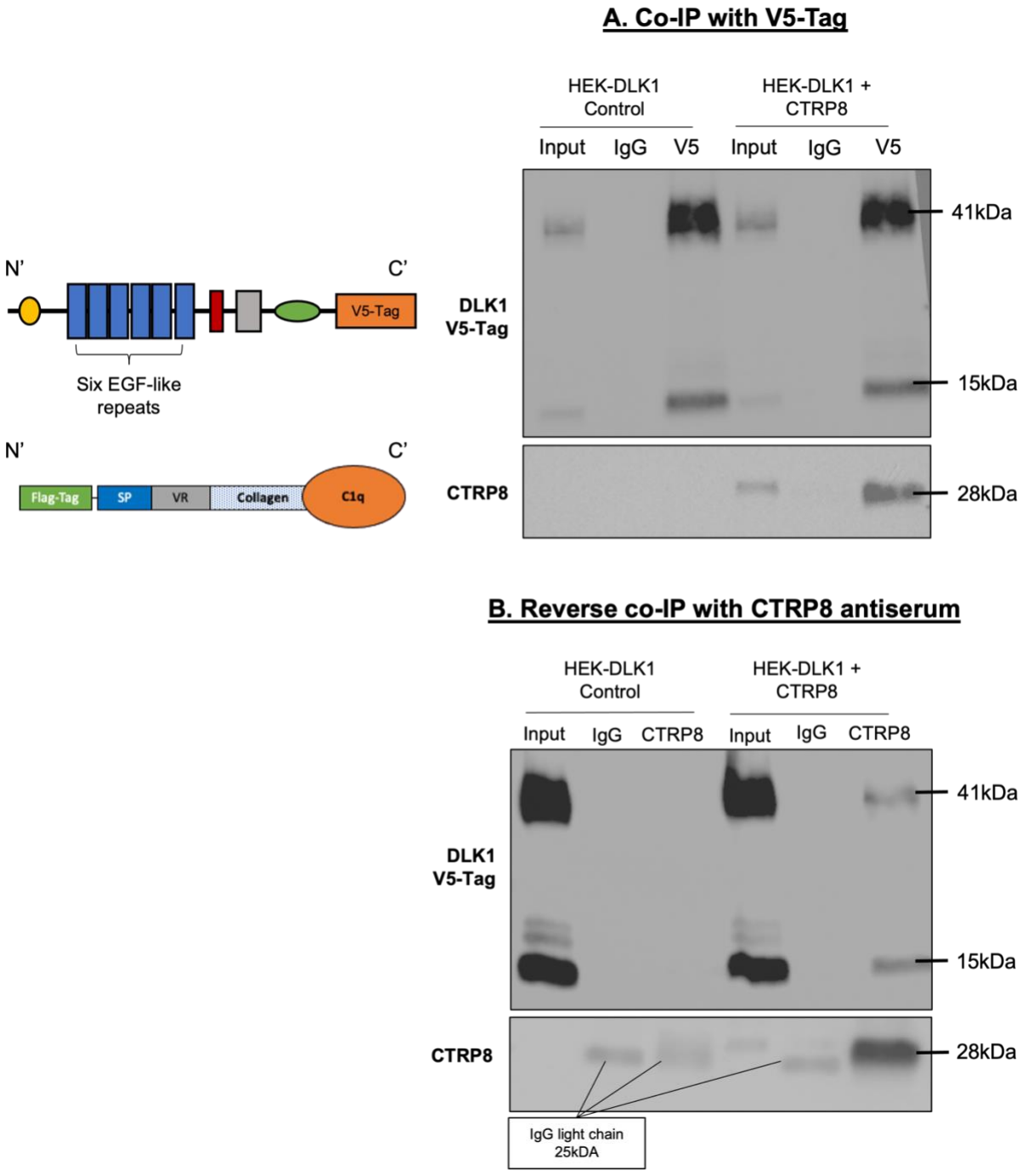

Figure 3.3 Co-IP of full-size DLK1 and CTRP8. HEK293 cells stably expressing DLK1 with V5-Tag were transiently transfected with CTRP8 construct for co-IP. Expression of proteins of interest were confirmed in the "Input" sample (protein lysates prior to incubation with IgG/antibody and magnetic beads). **A)** Protein samples incubated with V5-Tag antibody or mouse IgG2a. **B)** Protein samples were incubated with CTRP8 antiserum or rabbit IgG. Antibody-bound proteins were pulled down with protein A/G magnetic beads. DLK1 and CTRP8 from co-IP reactions were detected using Western blot. Blots are representative of n=3.

We wanted to confirm the CTRP8-DLK1 interaction in a model that endogenously expresses the proteins of interest. The neuroblastoma cell line Kelly was used since it expresses DLK1 endogenously, however does not express CTRP8. Kelly was transiently transfected with CTRP8-FLAG to confirm the CTRP8-DLK1 interaction in a cell model with endogenous DLK1 expression. A DLK1 antibody was able to immunoprecipitate full-size DLK1 and co-IP full-size CTRP8 (Figure ***3.4***). With these results we provide evidence of CTRP8 as a new ligand for DLK1.

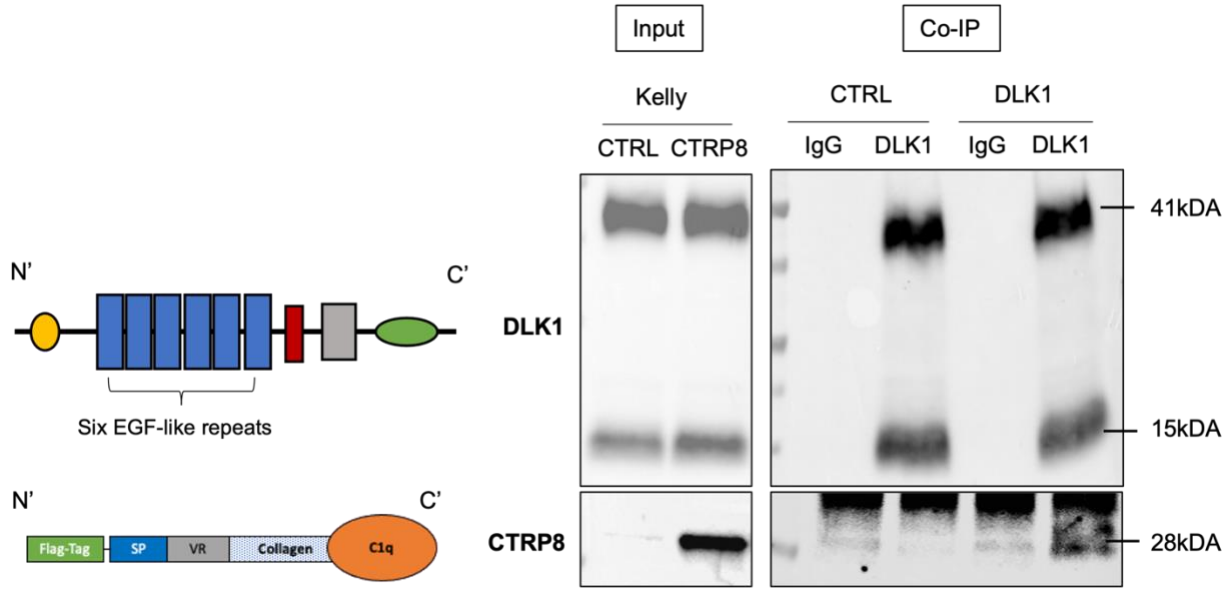

Figure 3.4 Co-IP with full-size DLK1 and CTRP8 in Kelly. Neuroblastoma cell line Kelly was transiently transfected with CTRP8 construct for co-IP. Expression of proteins of interest were

confirmed in the "Input" sample (protein lysates prior to incubation with IgG/antibody and magnetic beads).Protein samples were incubated with DLK1 antibody or mouse IgG1 then pulled down with protein A/G magnetic beads. DLK1 and CTRP8 from co-IP reactions were detected using Western blot. Blots are representative of n=3.

3.3 CTRP8 binds to DLK1 within the first five EGF-like domains

The Y2H results predicted that CTRP8 binds within the first three EGF-like repeats of DLK1. We designed a truncated DLK1 construct, Brevideltinin-Myc, containing DLK1 EGF1-5 to test in a co-IP with full-size CTRP8. Brevideltinin was previously described in neuroendocrine tumors as an endogenously produced soluble DLK1 form (Altenberger et al. 2005). The Myc-tag antibody successfully pulled down Brevideltinin and co-IPed with CTRP8 (Figure ***3.5***). These co-IPs reveal that CTRP8 interacts with DLK1 that contains the first five DLK1 EGF-like domains, in accordance with the interaction domain predicted by the Y2H.

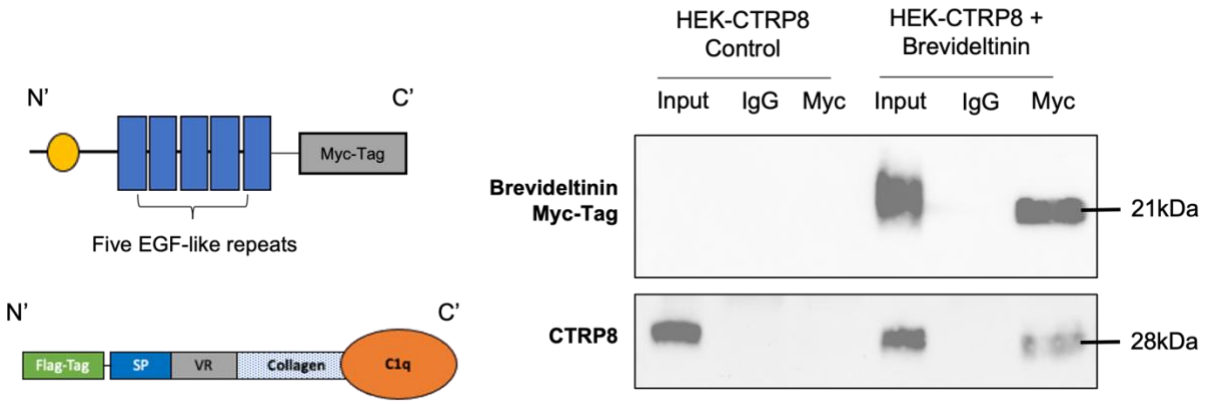

Figure 3.5 Co-IP Brevideltinin and CTRP8. HEK293 cells stably expressing CTRP8 were transiently transfected with Brevideltinin-Myc construct for co-IP. Expression of proteins of interest were confirmed in the "Input" sample (protein lysates prior to incubation with IgG/antibody and magnetic beads).Protein samples were incubated with Myc-Tag antibody or

mouse IgG1 then pulled down with protein A/G magnetic beads. Myc-Tag and CTRP8 from co-IP reactions were detected using Western blot. Blots are representative of n=3.

3.4 CTRP8 with a collagen domain deletion can interact with full-size DLK1

The DLK1-binding site on CTRP8 was not identified in the Y2H and remains unknown. To interrogate which CTRP8 protein regions are involved in DLK1 interaction, we designed constructs expressing modified CTRP8 protein domains for co-IP. The first constructs tested divided the CTRP8 protein into a separate C1q domain (CTRP8 C1q) and the N-terminal variable region (VR), collagen domain and signal peptide (SP) (CTRP8 N-terminus). The CTRP8 C1q was transiently transfected into HEK-DLK1 cells. Using the V5-Tag successfully pulled down full-size DLK1, however CTRP8 C1q did not co-IP (Figure ***3.6***).

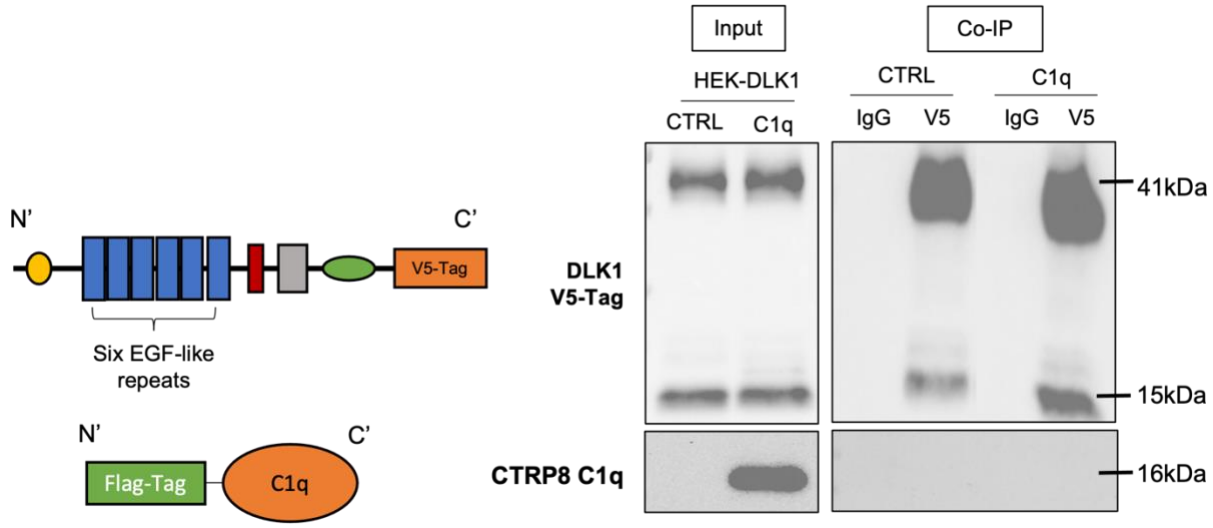

Figure 3.6 Co-IP with full-size DLK1 and CTRP8 C1q. HEK293 cells stably expressing DLK1 with V5-Tag were transiently transfected with CTRP8-C1q construct for co-IP. Expression of proteins of interest were confirmed in the "Input" sample (protein lysates prior to incubation with IgG/antibody and magnetic beads).Protein samples were incubated with V5-Tag antibody or mouse IgG2a for pull down with protein A/G magnetic beads. DLK1 and FLAG-Tag from co-IP reactions were detected using Western blot. Blots are representative of n=2.

Similarly, the CTRP8 N-terminus protein construct was also unable to co-IP with full-size DLK1 (Figure ***3.7***). These initial tests show that peptides encoding the CTRP8 C1q domain or N-terminus alone were not sufficient to bind with DLK1. The next constructs tested were designed with deletions or mutations targeting one domain at a time to uncover the CTRP8 domains necessary for DLK1 interaction.

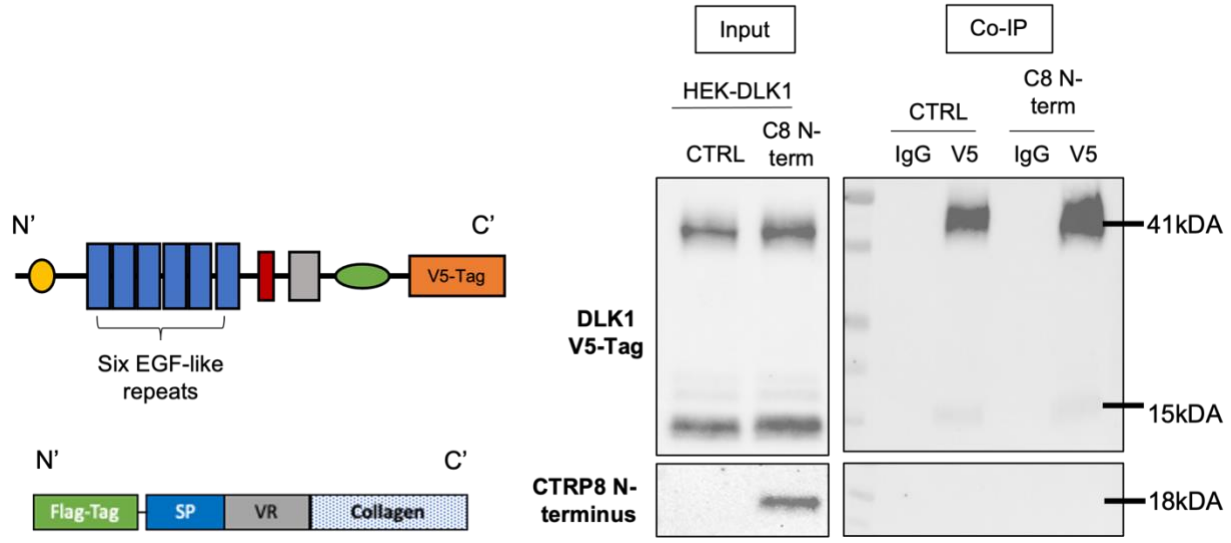

Figure 3.7 Co-IP with full-size DLK1 and CTRP8 N-terminal peptide. HEK293 cells stably expressing DLK1 with V5-Tag were transiently transfected with CTRP8-N-terminal peptide construct for co-IP. Expression of proteins of interest were confirmed in the "Input" sample (protein lysates prior to incubation with IgG/antibody and magnetic beads).Protein samples were incubated with V5-Tag antibody or mouse IgG2a for pull down with protein A/G magnetic beads. DLK1 and CTRP8 from co-IP reactions were detected using Western blot. Blots are representative of n=2.

The barrel-like C1q accounts for more than half of the CTRP8 protein and is made up of nine beta strands to form the highly conserved jelly-roll structure (Klonisch et al. 2017; Ressl et al. 2015). A construct containing only the first loop of C1q (CTRP8- C1qL1b) was co-expressed

with full-size DLK1. The V5-Tag antibody immunoprecipitated DLK1, but did not co-IP CTRP8-C1qL1b. Hence, deletion of a substantial portion of the C1q domain did not permit CTRP8-DLK1 interaction (Figure ***3.8***).

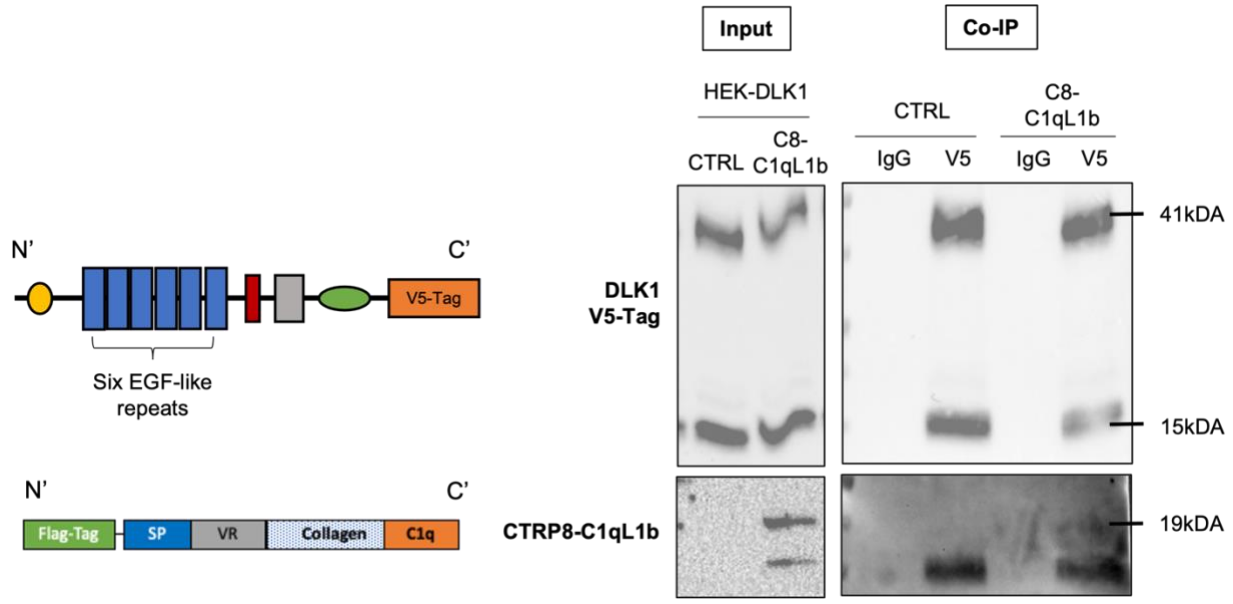

Figure 3.8 Co-IP with full-size DLK1 and CTRP8-C1q loop 1 (L1b). HEK293 cells stably expressing DLK1 with V5-Tag were transiently transfected with CTRP8-C1qL1b construct for co-IP. Expression of proteins of interest were confirmed in the "Input" sample (protein lysates prior to incubation with IgG/antibody and magnetic beads). Protein samples were incubated with V5-Tag antibody or mouse IgG2a for pull down with protein A/G magnetic beads. DLK1 and CTRP8 from co-IP reactions were detected using Western blot. Blots are representative of n=2.

Next, we tested a construct with a deleted CTRP8 VR region (CTRP8-noVR) for co-expression with full-size DLK1. The CTRP8-noVR protein was unable to co-IP with full-size DLK1, indicating no interaction occurred (Figure ***3.9***).

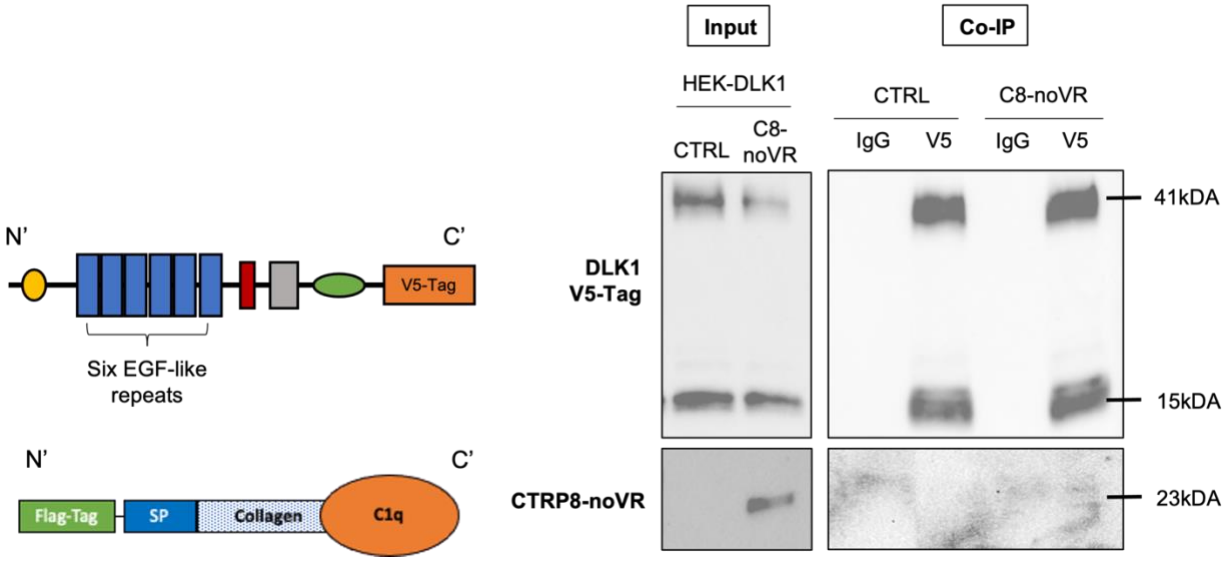

Figure 3.9 Co-IP with full-size DLK1 and CTRP8-noVariableRegion (VR). HEK293 cells stably expressing DLK1 with V5-Tag were transiently transfected with CTRP8-noVR construct for co-IP. Expression of proteins of interest were confirmed in the "Input" sample (protein lysates prior to incubation with IgG/antibody and magnetic beads).Protein samples were incubated with V5-Tag antibody or mouse IgG2a for pull down with protein A/G magnetic beads. DLK1 and FLAG-Tag from co-IP reactions were detected using Western blot. Blots are representative of n=2.

Finally, CTRP8 with a collagen domain deletion (CTRP8-noColl) was co-expressed with full-size DLK1. The V5-Tag antibody successfully co-IPed CTRP8-noColl with full-size DLK1 (Figure ***3.10***). This co-IP result provided information about which CTRP8 domain was required for the interaction with DLK1. These co-IP data suggested that both the C1q domain and variable region of CTRP8 are required for DLK1 binding. The selected deletion of the entire collagen domain still permitted CTRP8-DLK1 interaction to occur.

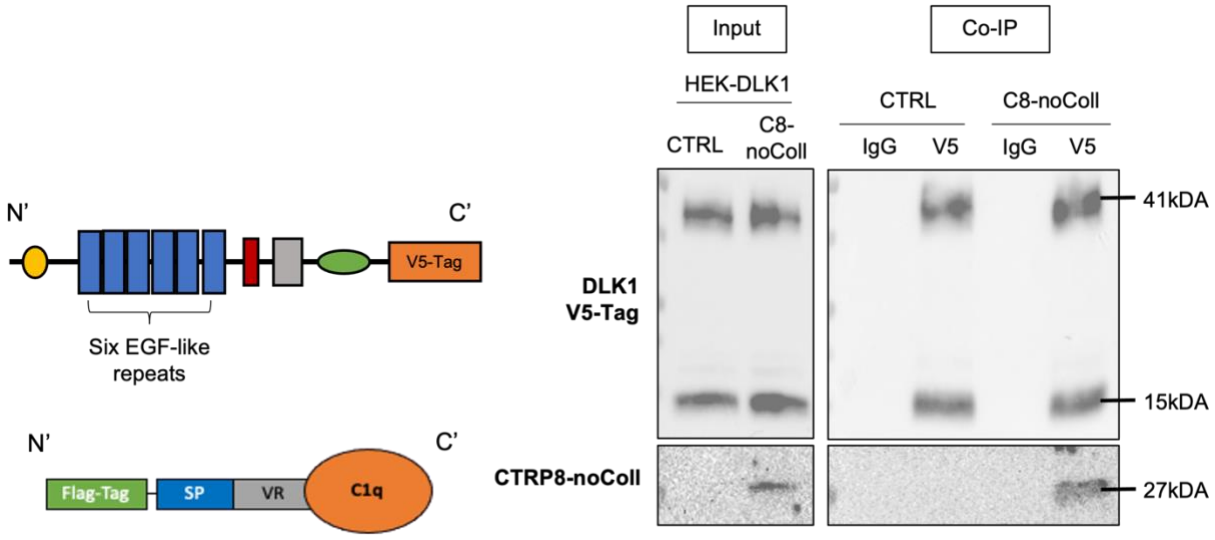

Figure 3.10 Co-IP with full-size DLK1 and CTRP8-VR-noCollagen (noColl). HEK293 cells stably expressing DLK1 with V5-Tag were transiently transfected with CTRP8-noColl construct for co-IP. Expression of proteins of interest were confirmed in the "Input" sample (protein lysates prior to incubation with IgG/antibody and magnetic beads). Protein samples were incubated with V5-Tag antibody or mouse IgG2a for pull down with protein A/G magnetic beads. DLK1 and CTRP8 from co-IP reactions were detected using Western blot. Blots are representative of n=3.

3.5 DLK1 does not interact with the putative RXFP1-binding motif of CTRP8

CTRP8 has been previously identified as a ligand for RXFP1 with a putative RXFP1-binding motif (RAYAAFASVGRREGLHS). A CTRP8 construct with a deletion of the RXFP1-binding domain (CTRP8mut) was designed and co-expressed with DLK1. Using a V5-Tag antibody, CTRP8mut successfully co-IPed fullsize DLK1 (Figure ***3.11***). The previous set of constructs was unable to identify a specific DLK1-binding motif, however positive co-IP of fullsize DLK1 with CTRP8mut suggests that DLK1 may have different requirements than RXFP1 for the interaction with CTRP8.

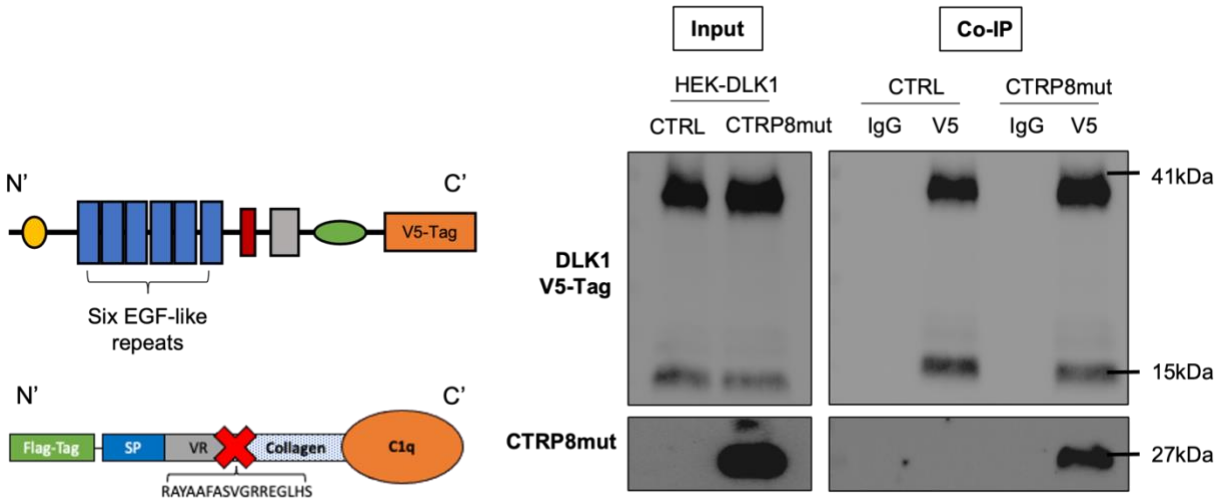

Figure 3.11 Co-IP with full-size DLK1 and CTRP8-noRXFP1site (mut). HEK293 cells stably expressing DLK1 with V5-Tag were transiently transfected with CTRP8mut construct for co-IP. Expression of proteins of interest were confirmed in the "Input" sample (protein lysates prior to incubation with IgG/antibody and magnetic beads). Protein samples were incubated with V5-Tag antibody or mouse IgG2a for pull down with protein A/G magnetic beads. DLK1 and CTRP8 from co-IP reactions were detected using Western blot. Blots are representative of n=3.

In conclusion, we have demonstrated a physical interaction between CTRP8 and DLK1 using co-IP with various protein constructs summarized in Figure ***3.12***. Both full-size DLK1 and Brevideltinin successfully co-IPed with full-size CTRP8. Of the CTRP8 constructs, only CTRP8-noCollagen was able to co-IP with full-size DLK1. Finally, CTRP8mut with a deletion of the RXFP1-binding domain also interacted with full-size DLK1 in co-IP.

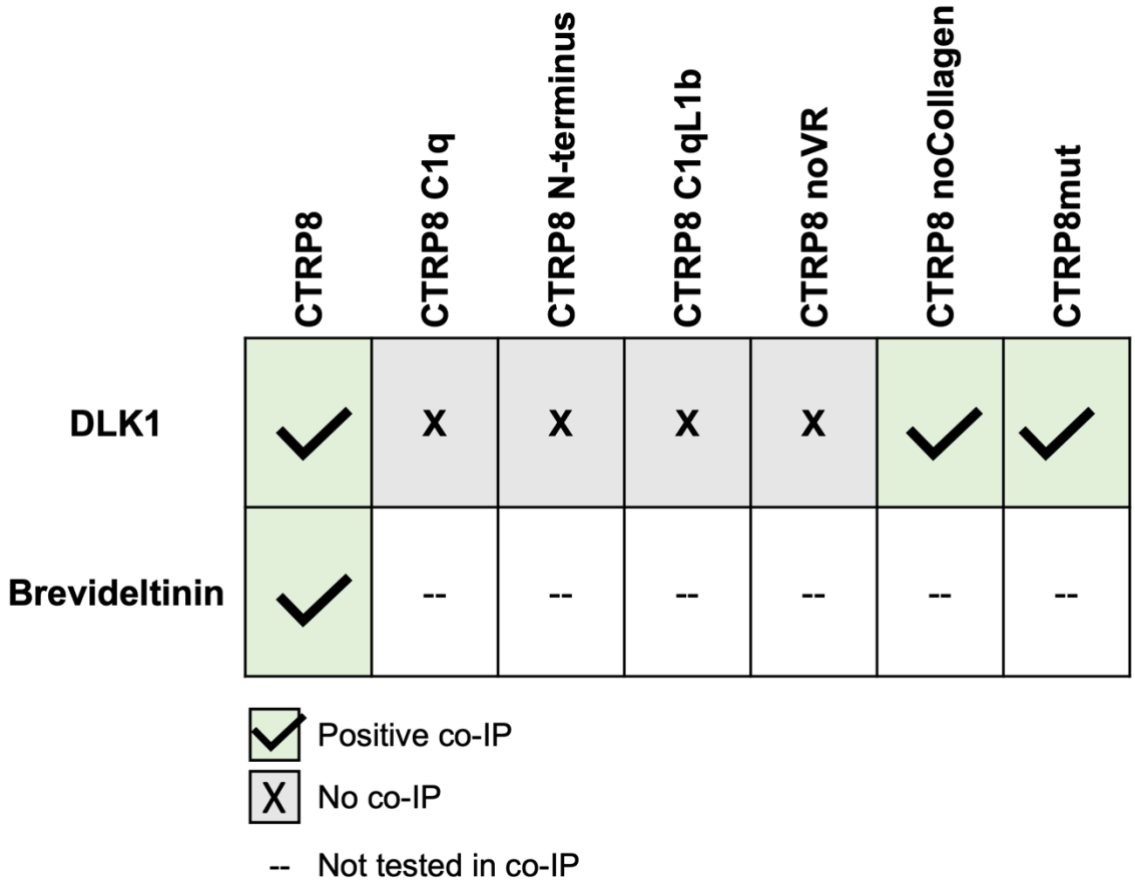

Figure 3.12 Summary of co-IP with DLK1 and CTRP8 constructs. Full-size CTRP8 interacts with both full-size DLK1 and Brevideltinin. Both CTRP8 with a collagen domain deletion and CTRP8 with an RXFP1-binding sequence deletion co-IP with DLK1.

3.6 DLK1 increases sphere formation in U251 human glioma cells

After characterization of the CTRP8-DLK1 interaction, the next objective was to identify the impact of CTRP8-DLK1 interaction on stemness in gliomas. We used the astrocytoma cell line U251 as model system and generated stable transfectants expressing DLK1 (U251-DLK1), DLK1/CTRP8 (U251-DLK1/CTRP8) and cleavage-resistant DLK1 (DLK1.CR) (Figure ***3.13***A). Western blot was used to verify expression of the desired proteins the cell models. DLK1 and

CTRP8 protein expression were observed in U251-DLK1, U251-DLK1/CTRP8 and U251-DLK1.CR, while the parental U251 cells were immunonegative for both proteins (Figure ***3.13***).

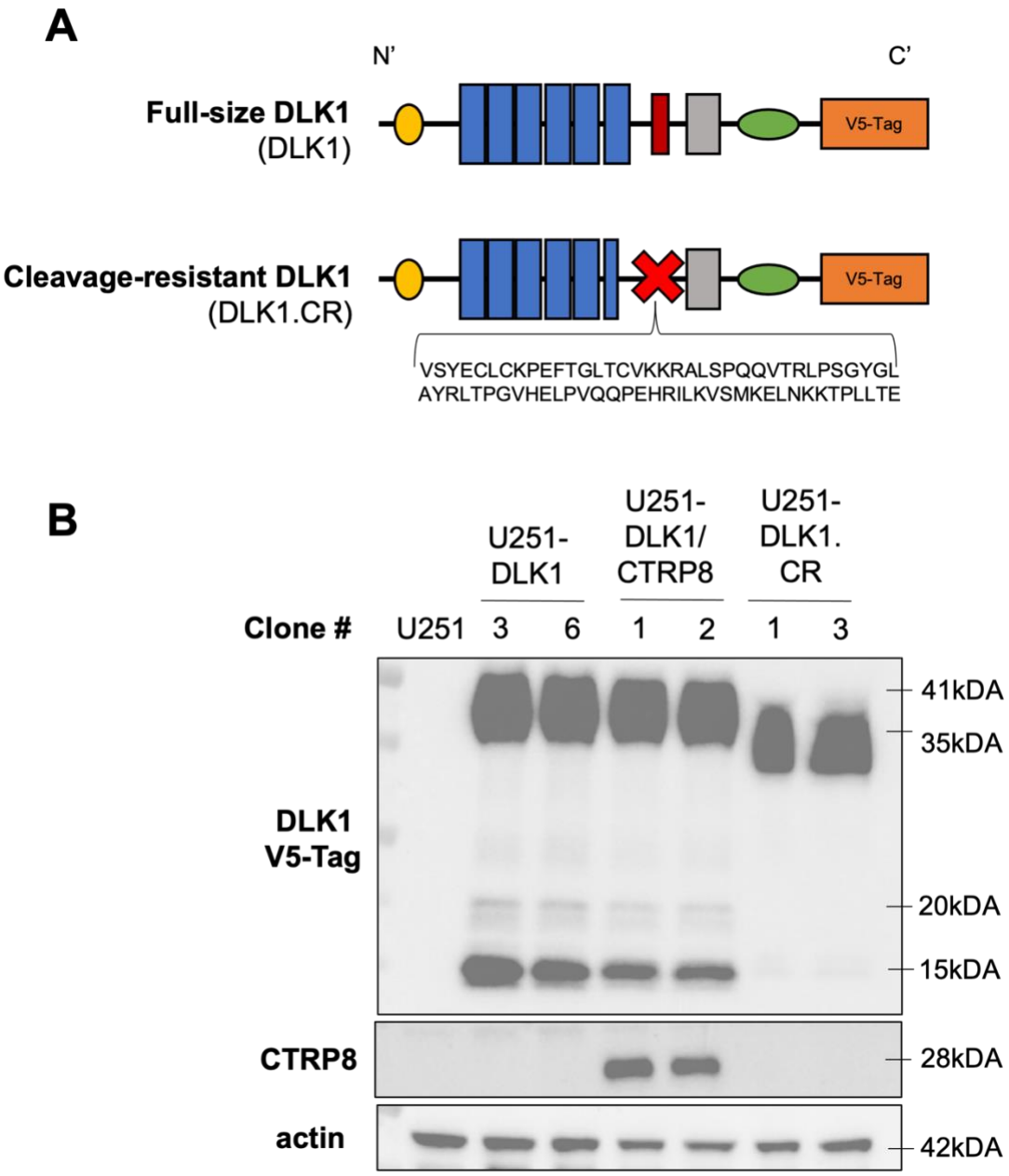

Figure 3.13 DLK1 and CTRP8 protein expression in U251, U251-DLK1, U251-DLK1/ CTRP8 and U251-DLK1 cleavage resistant (DLK1.CR) clones determined by Western blot. **A)** Schematic of full-size and cleavage-resistant DLK1 expression constructs **B)** Whole cell lysates

from U251 and stable transfectants. V5-Tag antibody and CTRP8 antiserum were used for the detection of DLK1 and CTRP8, respectively.

A sphere formation assay was used to assess the stem cell population in U251, U251-DLK1, U251-DLK1/CTRP8 and U251-DLK1.CR transfectants. Primary and secondary sphere formation efficiency in U251 was 21.18% ± 3.70% and 10.42% ± 1.7%, respectively. In U251-DLK1, tumor sphere formation was significantly increased in both primary spheres (51.04% ± 2.21%) and secondary spheres (62.50% ± 3.40%), indicating enhanced sphere formation compared to U251. In U251-DLK1/CTRP8, primary sphere formation (31.60% ± 3.32%) and secondary sphere formation (29.17% ± 6.80%) were significantly reduced in relation to U251-DLK1, but had higher sphere formation capacity when compared to U251 cells. The average diameter of the U251 primary and secondary spheres were 83.82 um ± 12.78 um and 106.45 um ± 15.54 um, respectively. The diameters of U251-DLK1 primary spheres (109.99um ± 25.64um) and secondary spheres (149.46um ± 39.27) were both significantly larger than for U251 spheres. Primary (79.26 um ± 11.11 um) and secondary spheres (128.46um ± 13.12) of U251-DLK1/CTRP8 were similar to those of U251 spheres, and measured significantly lower than U251-DLK1 primary spheres (Figure ***3.14***). Taken together, DLK1 overexpression in U251 increased sphere formation and generated larger tumor sphere sizes. The additional expression of CTRP8 reduced sphere formation and caused more irregularly shaped spheres, which may be an indication of a CTRP8-DLK1 role in regulating the stem cell subpopulation in gliomas.

In U251-DLK1.CR transfectants, primary spheres and secondary spheres formed at 29.51% ± 5.95% and 25% ± 1.70% efficiency, respectively. When compared to U251-DLK1 transfectants, U251-DLK1.CR cells formed significantly fewer primary and secondary spheres. The diameters of U251-DLK1.CR primary spheres (90.73um ± 13.26um) and secondary spheres (98.83um ±

11.854um) were also smaller relative to U251-DLK1 spheres. U251-DLK1.CR spheres were similar to U251 spheres, apart from an increase in secondary sphere formation observed with U251-DLK1.CR transfectants. Lower sphere formation efficiency may be an indication that a full-size cleavable DLK1 is required to sufficiently promote stemness in U251 cells.

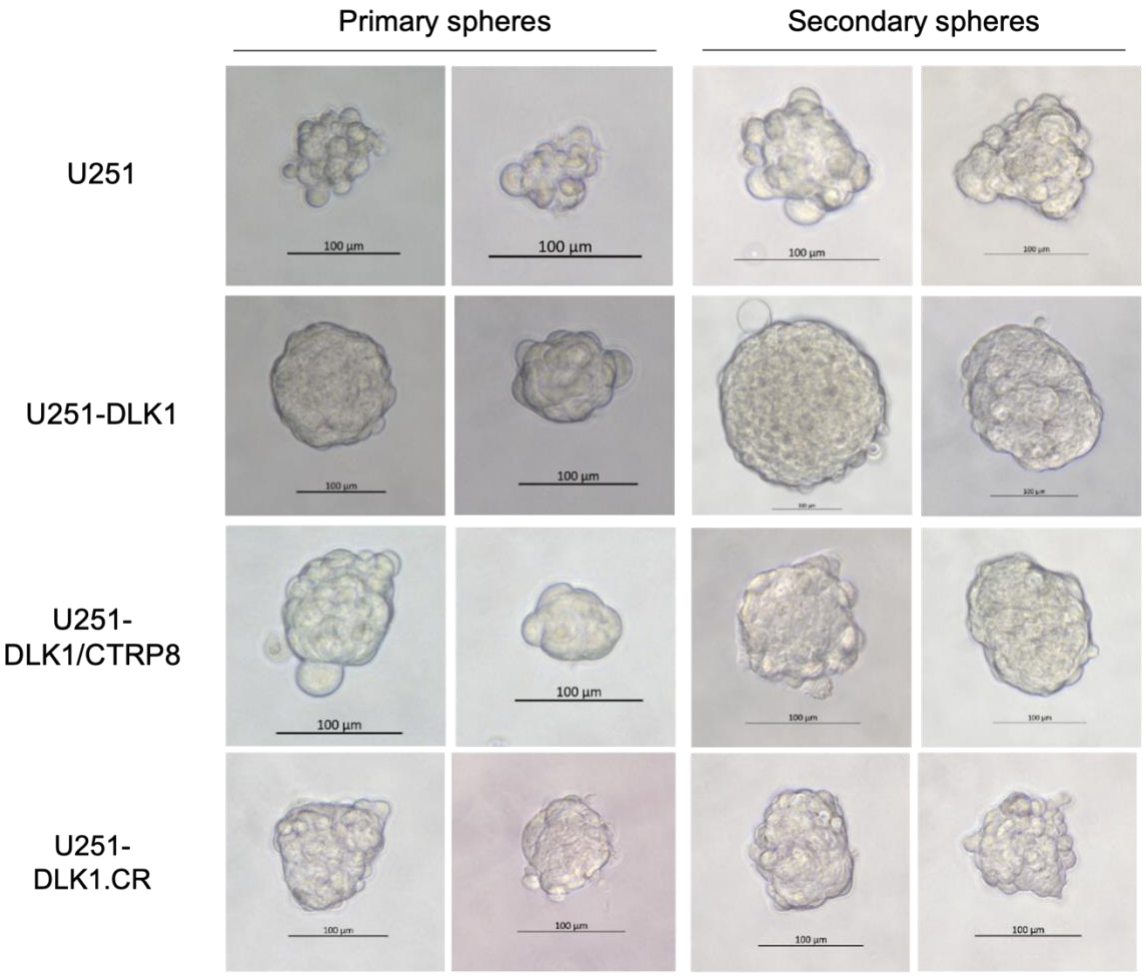

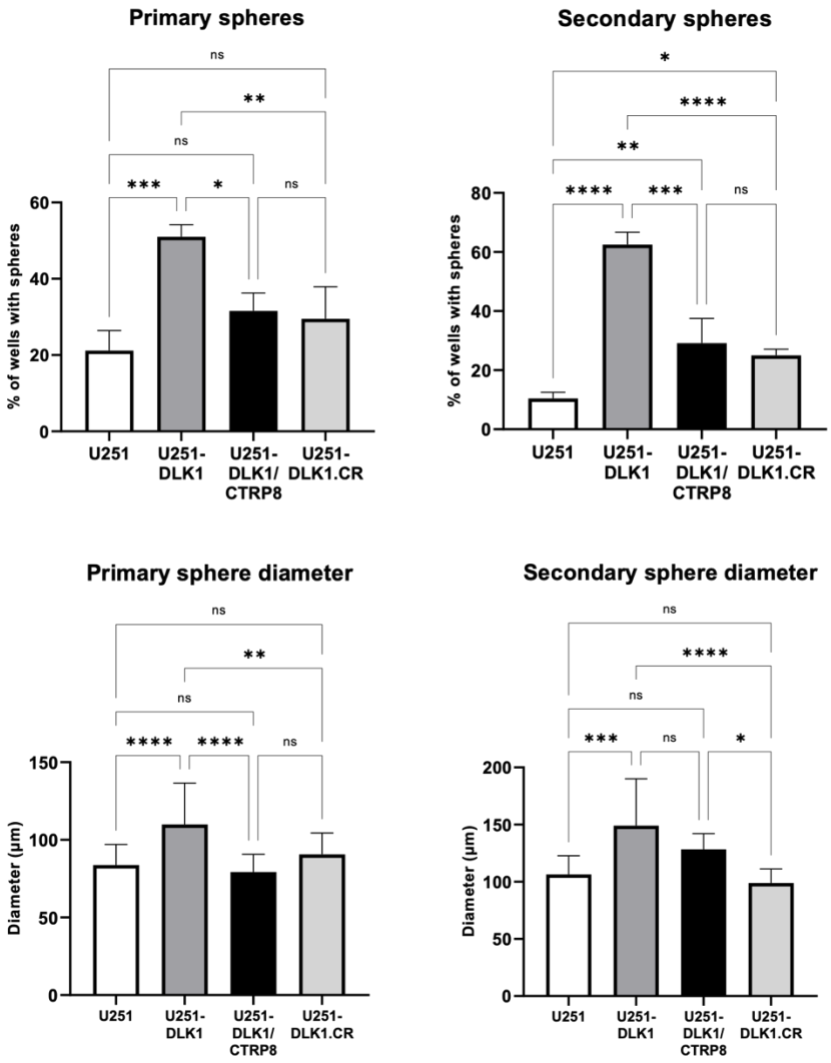

Figure 3.14 Sphere formation assay in U251, U251-DLK1, U251-DLK1/CTRP8 and U251-DLK1 cleavage resistant (DLK1.CR). Cells were plated in brain tumor-initiating cell medium in low attachment plates for 48h of bulk sphere formation. Spheres were dissociated, then seeded as single cells in 96-well plates for primary and secondary sphere formation. Sphere counts and sphere diameters were quantified 12-14 days after single cells were plated. Statistical analysis conducted in Graphpad Prism (*P<0.05, **P<0.01, ***P<0.001, ****P<0.0001, ns=not significant). Representative images of spheres from n=3.

3.7 GSC markers are upregulated in DLK1-expressing U251 glioma cells

In U251-DLK1 transfectants enhanced sphere formation was observed, which was lessened in U251-DLK1/CTRP8 and U251-DLK1.CR. We investigated if a similar trend can be reflected in GSC marker levels of CD133, OCT4, SOX2, CD44 and ALDH1A3 in qPCR. Expression of the commonly used cancer stem cell marker CD133 was significantly upregulated by greater than 3-fold in U251-DLK1 relative to U251. However, CD133 levels in U251-DLK1/CTRP8 were lower compared to U251, with a more dramatic decrease between U251-DLK1/CTRP8 and U251-DLK1 transfectants. Similarly, U251-DLK1 transfectants displayed a 2-fold increase in OCT4 compared to U251 glioma cells. OCT4 showed a slight upregulation in U251-DLK1/CTRP8 relative to U251-DLK1 transfectants, deviating from the expression pattern we observed with CD133. SOX2 also exhibited a significant upregulation by 3-fold in U251-DLK1 transfectants. SOX2 levels in U251-DLK1/CTRP8 transfectants did not show a significant difference from U251 cells, however was downregulated relative to U251-DLK1 transfectants (Figure ***3.15***). Conversely, we observed a 0.5-fold downregulation of CD44 levels in U251-DLK1 transfectants which was reduced even further in U251-DLK1/CTRP8 transfectants relative to U251. Interestingly, ALDH1A3 was ablated in both U251-DLK1 and U251-DLK1/CTRP8 transfectants (Figure ***3.15***).

In U251-DLK1.CR transfectants, we measured levels of GSC markers CD133, CD44, OCT4, SOX2 and ALDH1A3. In accordance with the sphere formation data, we observed a dramatic decrease in CD133 levels in U251-DLK1.CR cells relative to U251-DLK1 transfectants. CD133 expression in U251-DLK1.CR was also lower than that of U251. Similarly, we observed a reduction in OCT4 with U251-DLK1.CR compared to both U251 and U251-DLK1. SOX2 levels in U251-DLK1.CR were similar to those of U251, but significantly less than in U251-DLK1 transfectants. Next, CD44 levels of U251-DLK1.CR were reduced relative to both U251 and

U251-DLK1. Finally, ALDH1A3 was not completely ablated in U251-DLK1.CR, as it was in U251-DLK1 and U251-DLK1/CTRP8, although still significantly reduced in comparison to U251 (Figure ***3.15***). Overall, GSC marker expression in U251-DLK1.CR transfectants pointed to reduced stemness, further supporting the sphere formation results.

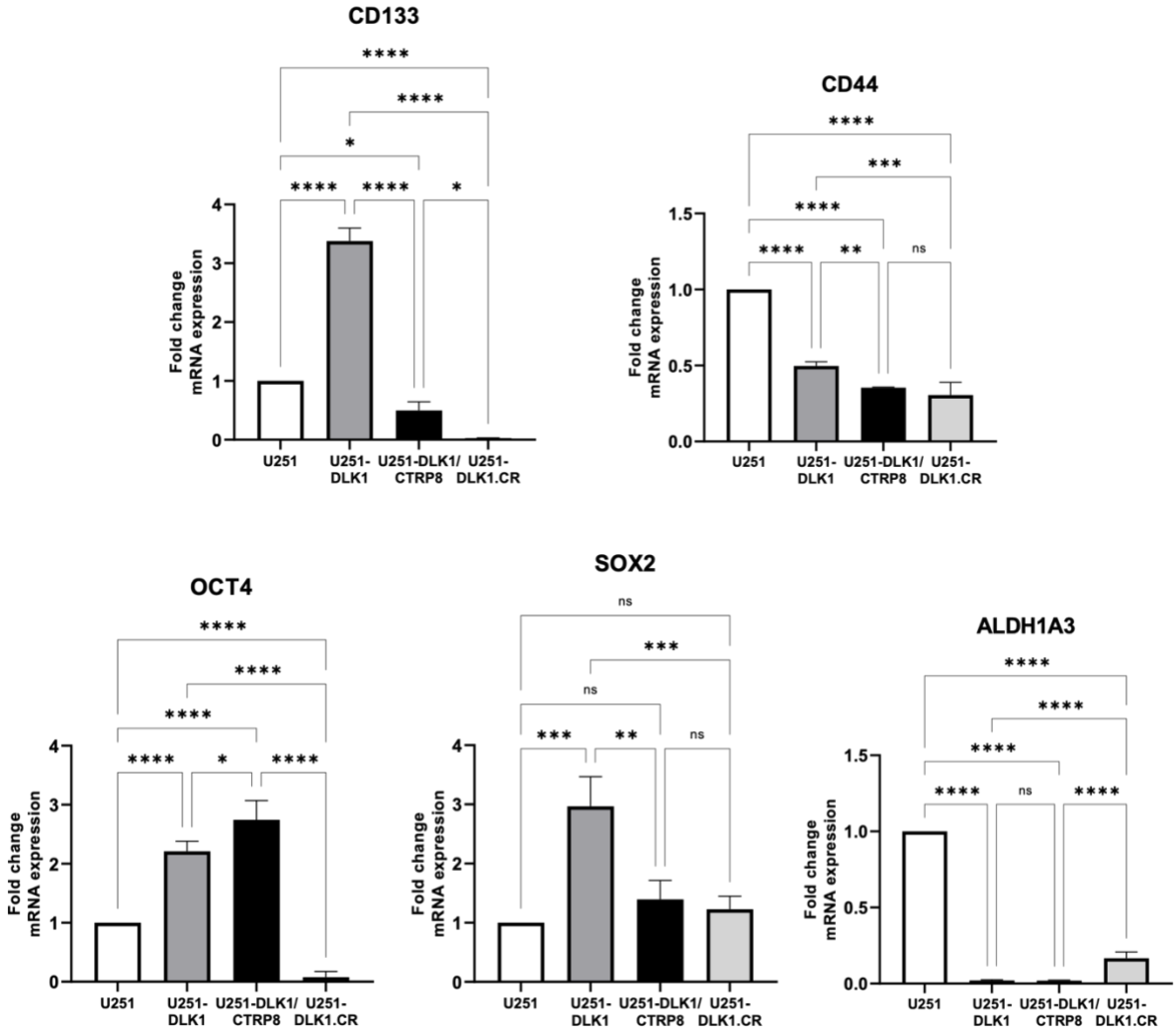

Figure 3.15 GSC cell marker expression in U251, U251-DLK1, U251-DLK1/CTRP8 and U251-DLK1 cleavage resistant (DLK1.CR). Gene expression of CD133, CD44, OCT4, SOX2 and ALDH1A3 quantified via qPCR. Fold change in gene expression was calculated relative to

U251 for n=3. Statistical analyses conducted on Graphpad prism (*P>0.05, **P>0.01, ***P<0.001, ****P<0.005, ns=not significant).

The two GSC subtypes, proneural and mesenchymal, possess distinct expression profiles. In general, CD133, OCT4 and SOX2 are associated to GSC with proneural characteristics, while CD44 and ALDH1A3 a considered mesenchymal GSC markers (Wang et al. 2021; Guerra-Rebollo et al. 2019). We observed an upregulation in CD133, OCT4 and SOX2 in U251-DLK1 transfectants, which was in accordance with the enhanced GSC population demonstrated by the tumor sphere formation assay. The expression profile is not as clear with U251-DLK1/CTRP8 transfectants, where we observed downregulation of CD133 and SOX2, which correlates with the reduced sphere formation in this cell model. But the increase of OCT4 was unexpected, potentially indicating a more selective regulation of stem cell related genes by CTRP8. Finally, CD44 and ALDH1A3 were downregulated in both U251-DLK1 and U251-DLK1/CTRP8 transfectants. Taken together, our results suggest a preference for a proneural GSC differentiation phenotype in DLK1-expressing glioma cells. As exhibited by the reduction of both sphere formation and GSC markers CD133 and SOX2, expression of CTRP8 may promote differentiation with a possible shift towards a mesenchymal GSC type.

Unlike U251-DLK1 and U251-DLK1/CTRP8 transfectants, which exhibited a clearer proneural GSC expression profile, we cannot yet conclude if cleavage-resistant DLK1.CR can preferentially promote a proneural or mesenchymal GSC subtype in U251 glioma. However, U251-DLK1.CR conferred reduced stem cell properties suggesting a critical role of both expression of functional DLK1 and the ability to engage in proteolytic cleavage for the regulation of glioma stemness. Although limited in number, this panel of GSC markers may be revealing

specific roles of CTRP8 and DLK1 in regulating the transition between proneural and mesenchymal GSC subtypes.

3.8 Proneural GSC markers in U251-DLK1 are responsive to soluble rhCTRP8

Co-expression of DLK1 and CTRP8 in U251 cells had a significant effect on the levels of GSC markers. We tested if treatment using recombinant human CTRP8 had a similar impact on GSC marker expression in two different U251-DLK1 clones. As previously observed, CD133 levels were elevated in both U251-DLK1 clone 3 (10-fold increase) and clone 6 (5-fold increase), relative to U251. Treatment with CTRP8 significantly decreased CD133 expression by 2-fold in both U251-DLK1 clones. OCT4 levels were elevated in U251-DLK1 clones 3 and 6 compared to U251, by 9-fold and 11-fold, respectively. A significant 1.5-fold OCT4 increase in response to CTRP8 was observed in U251-DLK1 clone 3 and clone 6. Similarly in SOX2, levels were upregulated by 2-fold in U251-DLK1 clone 3 and 5-fold in U251-DLK1 clone 6. Only U251-DLK1 clone 6 showed a significant SOX2 downregulation by 0.8-fold in response to CTRP8 treatment. CD44 expression decreased in U251-DLK1 clone 3 and clone 6, however CTRP8 treatment did not have a significant effect on CD44 levels. Finally, ALDH1A3 was downregulated in both U251-DLK1 clone 3 and 6. CTRP8 treatment did not affect ALDH1A3 expression in U251-DLK1 transfectants (Figure ***3.16***). Overall, CTRP8 does appear to have an effect on GSC marker expression in U251-DLK1, particularly in the proneural-related genes CD133, OCT4 and SOX2.

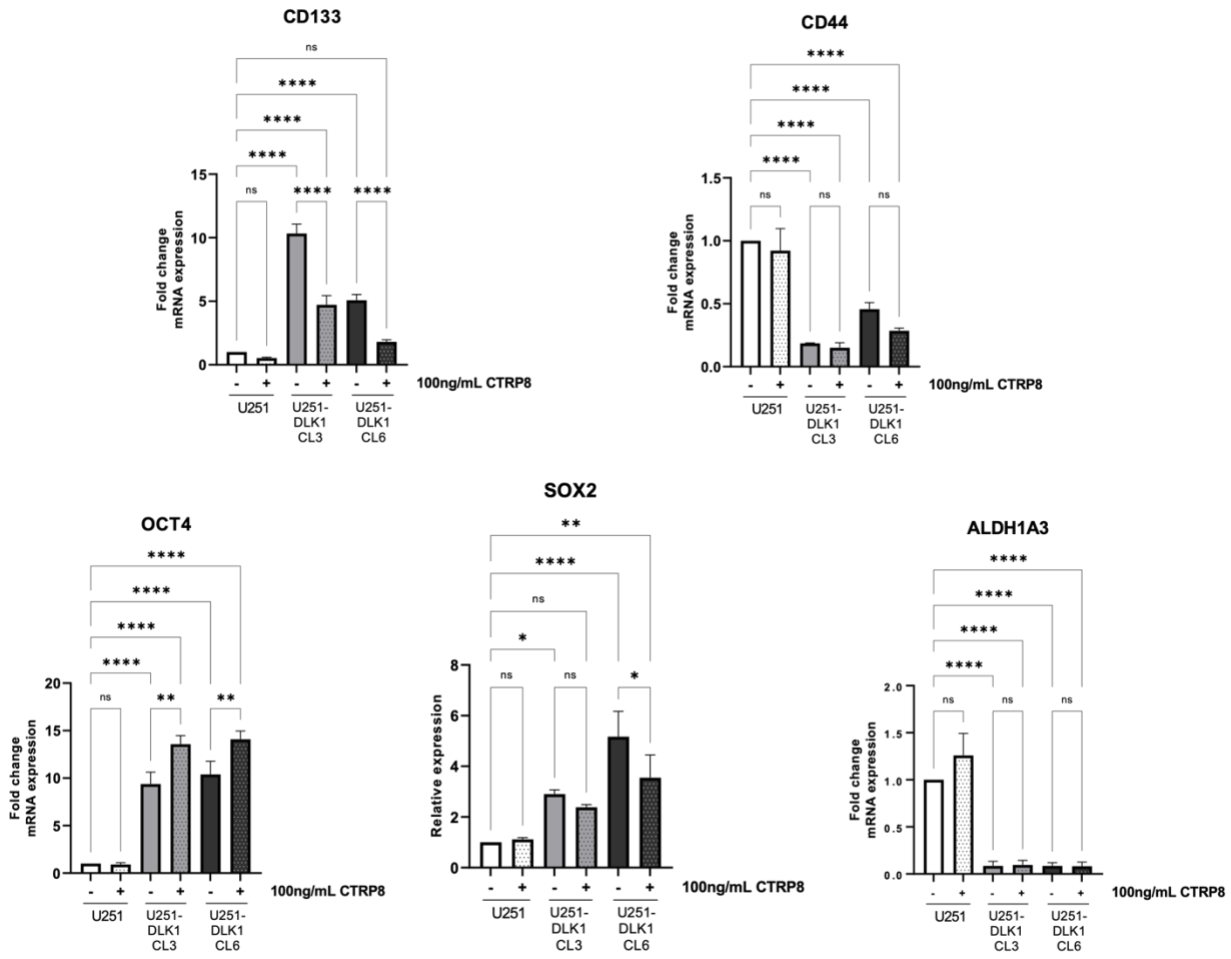

Figure 3.16. GSC marker expression in U251 and U251-DLK1 cells treated with CTRP8. Expression of CD133, CD44, OCT4, SOX2 and CD133 expression measured in qPCR. Fold change in gene expression was calculated relative to U251 for n=3. Statistical analyses conducted in Graphad (*P<0.05, **P<0.01, ****P<0.0001, ns=not significant).

3.9 CTRP8 increases DLK1 ICD release

Our observations in sphere formation and GSC marker expression revealed the importance of DLK1 proteolytic cleavage in regulation of GSC population of U251 cells. Expression of full-size DLK1 was able to promote stemness, while the cleavage-resistant DLK1 form did not cause a significant change in stemness relative to U251. Next, we investigate if CTRP8 has an effect on

protein processing of DLK1. In our U251-DLK1 and U251-cleavage resistant DLK1 (DLK1.CR) model, both constructs have a C-terminal V5-Tag (Figure ***3.17***A). Full-size DLK1 is expected at 41 kDa in Western blot. Using V5-Tag antibody in Western blot, the expected full-size DLK1 band was observed in U251-DLK1 protein samples. Additionally, we detected lower molecular weight DLK1 fragments from 25kDA to 15kDA in nuclear and cytoplasmic protein fractions of U251-DLK1 transfectants. A prominent 15 kDa band detected by the V5-Tag antibody was present at a higher proportion than the full-size 41 kDa band in the nucleus. We suspected this 15 kDa protein to be the C-terminal DLK1 intracellular domain (ICD), since the DLK1 construct expresses a V5-Tag at the C-terminus. U251-DLK1 transfectants treated with recombinant CTRP8 for 24h did not show a significant change in the levels of full-size DLK1 or DLK1 fragments in Western blot (Figure ***3.17***B).

The current proposed mechanism for DLK1-ICD release involves ADAM-mediated cleavage of the extracellular domain, followed by release of the ICD (Grassi, Pantazopoulou, and Pietras 2020). To confirm the identity of a DLK1-ICD fragments, we used the C-terminally V5-tagged cleavage-resistant DLK1 construct (DLK1.CR) with a deletion of the juxtamembrane ADAM/TACE cleavage site. With the lack of an ADAM/TACE cleavage site, it was anticipated that release of DLK1 fragments from the membrane would be prohibited. Using V5-Tag detection in Western blot, the DLK1.CR band was detected at the expected molecular weight of 35 kDa, while the prominent smaller 15 kDa fragment was absent. This confirms that ADAM-mediated cleavage of DLK1 at the juxtamembrane site is required for the release if DLK1-ICD (Figure ***3.17***B). Similar to U251-DLK1 transfectants, the addition of recombinant CTRP8 did not change the expression or subcellular distribution of DLK1.CR.

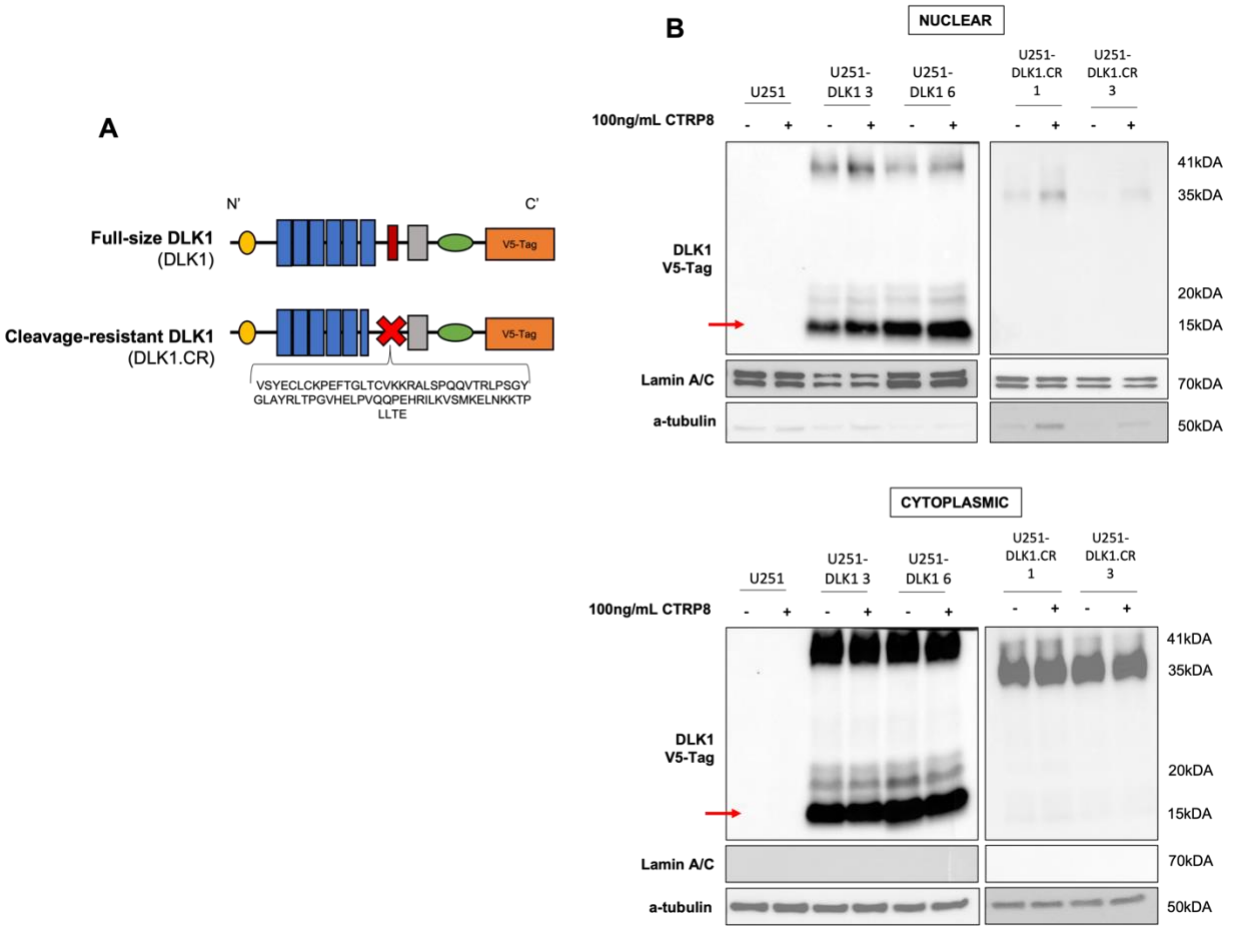

Figure 3.17 V5-Tag expression of U251, U251-DLK1 and U251-cleavage resistant DLK1 (DLK1.CR) treated with CTRP8. A) Schematic of full-size and cleavage-resistant DLK1 expression constructs. Cells were treated with 100ng/mL recombinant human CTRP8 for 24h prior to nuclear and cytoplasmic protein extraction. **B)** V5-Tag detection in Western blot of U251, U251-DLK1 and U251-DLK1.CR protein samples. DLK1 intracellular fragment indicated with red arrow. Blots are representative of n=3.

3.10 CTRP8 increases nuclear localization of DLK1-ICD

In Western blot we observed a 15 kDa DLK1 band in U251-DLK1 cells, which was absent in U251-DLK1.CR. In immunofluorescence (IF), membrane localized DLK1 tagged with V5-tag can be seen in both U251-DLK1 and U251-DLK1.CR transfectants. However, in U251-DLK1

cells, cytoplasmic and nuclear localization of the V5-Tag signal was observed. Punctuate V5-Tag signals in the cytoplasm and nucleus are likely DLK1 fragments that have been liberated from the membrane via proteolytic cleavage. This is further validated in U251-DLK1.CR, where V5-Tag was detected mostly at the membrane (Figure **3.18**). These observations are in support of the Western blot data from nuclear and cytoplasmic protein extracts. To further investigate the subcellular location of this DLK1 fragment in response to CTRP8 treatment, U251-DLK1 and U251-DLK1.CR transfectants were incubated with recombinant CTR8 and labelled with V5-Tag antibody in IF.

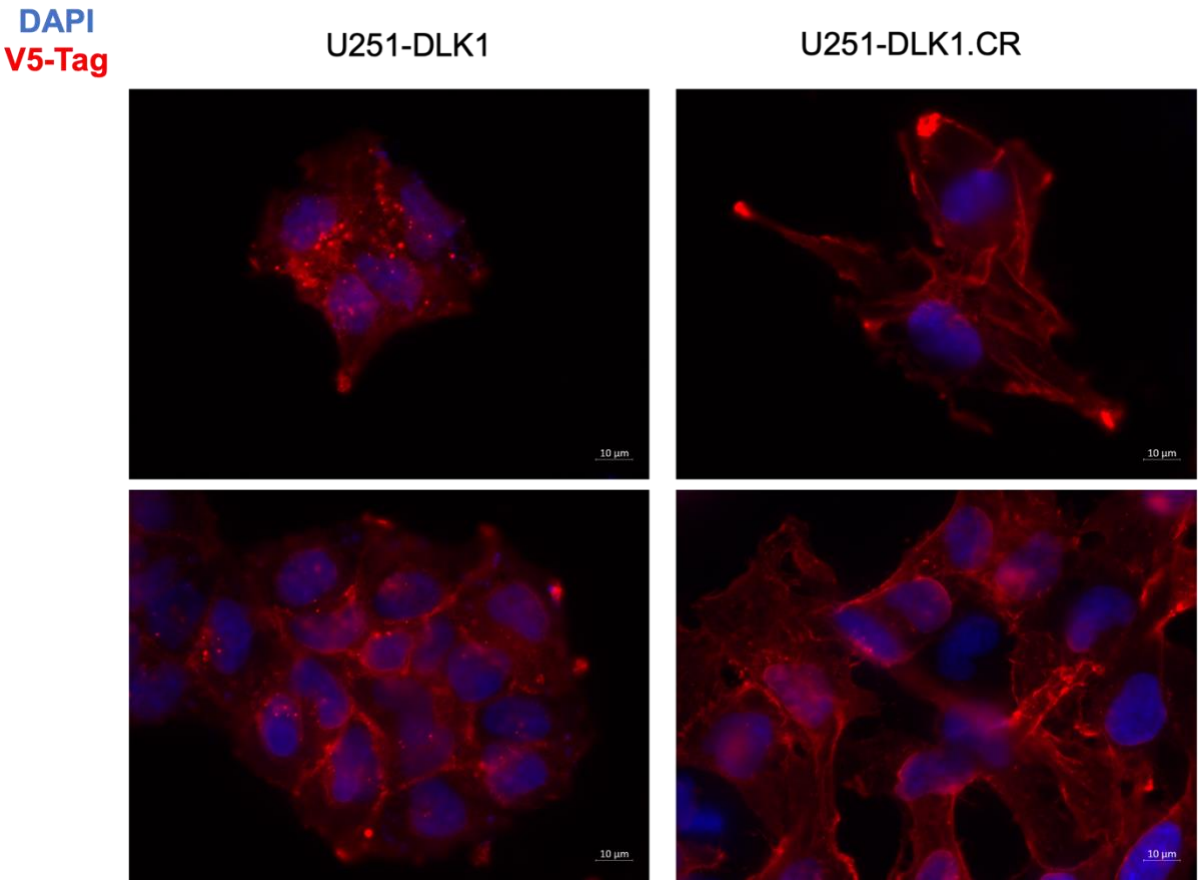

Figure 3.18. U251-DLK1 and U251-DLK1.CR immunofluorescence with V5-Tag. Fixed with 4% formaldehyde and labelled with V5-Tag antibody (red) and DAPI (blue). Images acquired with Zeiss Z2 fluorescent microscope.

In IF nuclear images, punctuated V5-Tag signal was observed in the nucleus and some in the perinuclear compartment. We quantified significantly greater V5-Tag IF signal intensity localized with nuclear DAPI stain in U251-DLK1 cells treated with CTRP8 (11,446.72 ± 2,801.86 units) compared to the control (7,646.52 ± 2,668.27 units). In contrast, the majority of V5-Tag signal in U251-DLK1.CR appeared diffused in the cytoplasm, although some nuclear localization was also detected at a lower mean intensity than in U251-DLK1 transfectants. There was no significant change in V5-Tag signal (both ~3,000 ± 500 units) between control and CTRP8 treated U251-DLK1.CR (Figure **3.19**). The V5-Tag labelling in U251-DLK1.CR was anticipated to be localized only to the cell membrane-localized staining, yet, it was observed in the cytoplasm and weakly detected in the nucleus. We performed a cell permeabilization step in preparation for immunofluorescence, which may have allowed release of cleavage-resistant DLK1 from the membrane. Although permeabilization may affect protein subcellular location, it is required to allow sufficient antibody penetration and binding to the C-terminal V5-Tag on the DLK1 constructs.

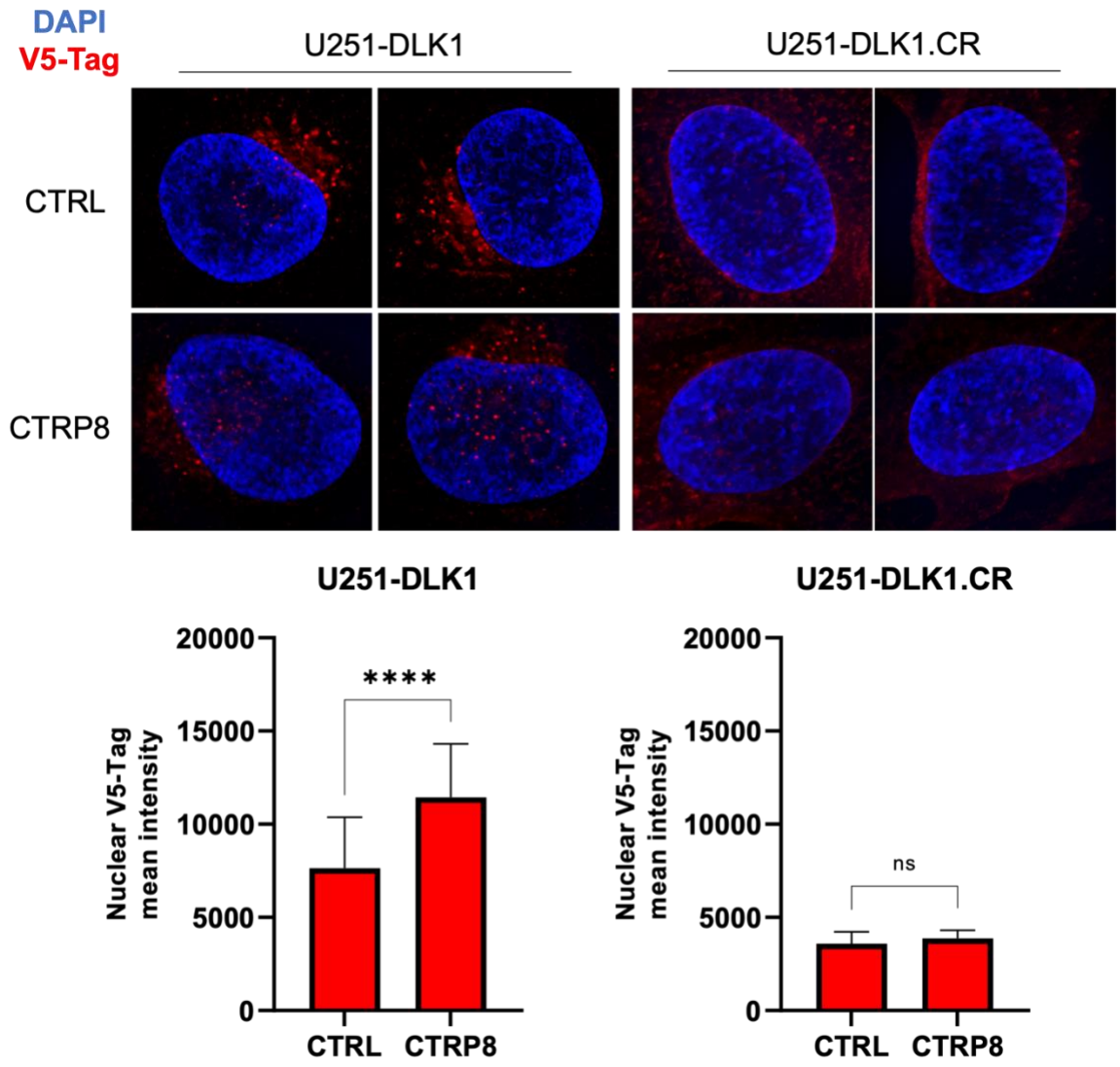

Figure 3.19 Nuclear images of U251-DLK1 and U251-DLK1.CR treated with CTRP8. Cells were plated on coverslips, then treated with 100ng/mL recombinant human CTRP8 for 24h. Fixed with 4% formaldehyde and labelled with V5-Tag antibody (red) and DAPI (blue). Images acquired with Zeiss Z2 fluorescent microscope. V5-Tag signal intensity localized with DAPI from 30 nuclei were quantified in ZEN Blue software for n=3. Statistical analyses conducted in Graphphad (****P<0.0001, ns=not significant).

3.11 CTRP8 does not impact NOTCH1 receptor and Hes1 cellular levels

With the changes in sphere formation and profile of stem cell marker expression between U251-DLK1 and U251-DLK1/CTRP8 transfectants, we wanted to investigate which signaling pathways are responsive to CTRP8-DLK1 interaction. Since DLK1 and NOTCH1 signaling are well-reported regulators of differentiation in development and disease, we tested if CTRP8-DLK1 interaction could affect NOTCH1 activity, since NOTCH1 is the best-known receptor of DLK1 (Baladrón et al. 2005; Traustadóttir et al. 2016). U251 and two different U251-DLK1 clones were treated with recombinant human CTRP8 for 24h, then the transcripts of NOTCH1 and its downstream target Hes1 were measured using qPCR. NOTCH1 transcripts were detected in U251 and both U251-DLK1 clones. Both DLK1 overexpression and CTRP8 treatment did not affect NOTCH1 transcript levels. In U251-DLK1 clone 3 and 6, Hes1 levels were decreased significantly compared to U251 cells (clone 3 by 0.5-fold; clone 6 by 0.2-fold). Based on the expression of Hes1, expression of DLK1 significantly reduced NOTCH1 activation in U251 but CTRP8 treatment had no effect on Hes1 levels in both U251 or the U251-DLK1 transfectants (Figure ***3.20***).

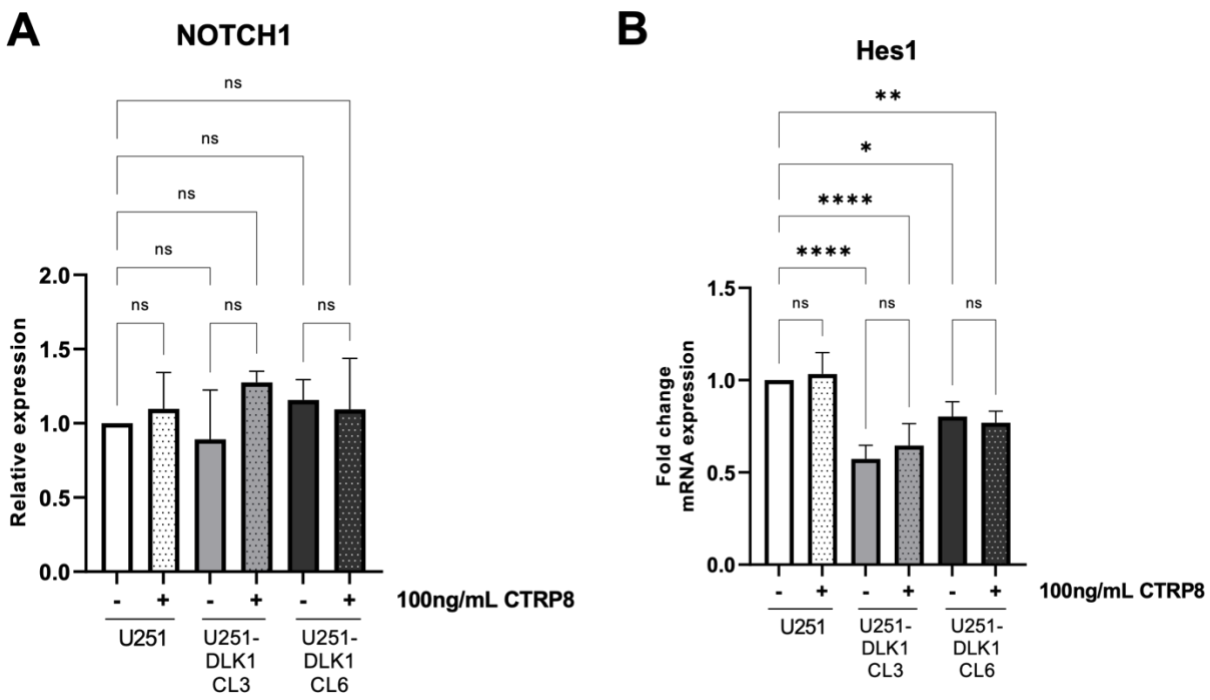

Figure 3.20 NOTCH1 and Hes1 expression in U251, U251-DLK1 clones treated with CTRP8. **A)** NOTCH1 receptor expression and **B)** Hes1 expression measured in qPCR. Fold change was calculated relative to U251 for n=3. Statistical analyses conducted in Graphad (*P<0.05, **P<0.01, ****P<0.0001, ns=not significant).

3.12 DLK1 reduces NOTCH activity independently of CTRP8

To measure NOTCH activity, U251 and U251-DLK1 were transfected with a fluorescent NOTCH reporter plasmid expressing tdTomato under the CBF promoter region (Maier et al. 2019). A constitutively active EGFP was co-expressed with the NOTCH reporter as a reference to account for potential differences in transfection efficiency between cell lines. In fluorescent images, we observed similar EGFP distribution in U251 and U251-DLK1 clones, indicating similar levels of uptake and expression of the plasmid (Figure ***3.21***A). Next, U251 and U251-DLK1 cells were treated with recombinant human CTRP8 for 24h prior to assessing NOTCH reporter activity by flow cytometry. In flow cytometry, all conditions had ~60-70% EGFP-positive cells. The

percentage of EGFP-positive cells was used as a normalizer for tdTomato-positive cells, then fold changes in reporter activity were determined relative to U251. In U251-DLK1 clones 3 and 6, NOTCH activity was reduced by greater than 0.5-fold compared to U251 (Figure ***3.21***B). In both U251 and U251-DLK1 cells, CTRP8 treatment did not cause a significant change in NOTCH reporter activity. The significant decrease in reporter activity indicates reduced NOTCH activation associated with DLK1 expression. However, CTRP8 does not appear to have a significant effect on DLK1-mediated inhibition of NOTCH signaling. This agrees with the qPCR results we observed with Hes1 expression. The NOTCH pathway is a prominent regulator of differentiation and a known target for DLK1 (Falix et al. 2012). In our U251 model DLK1 does act as an inhibitor of NOTCH signaling independently of CTRP8, although we cannot yet conclude if DLK1-mediated NOTCH1 inhibition has an impact on the GSC population. Finally, our data suggest that CTRP8-DLK1 may act through alternative mechanisms to impact stemness.

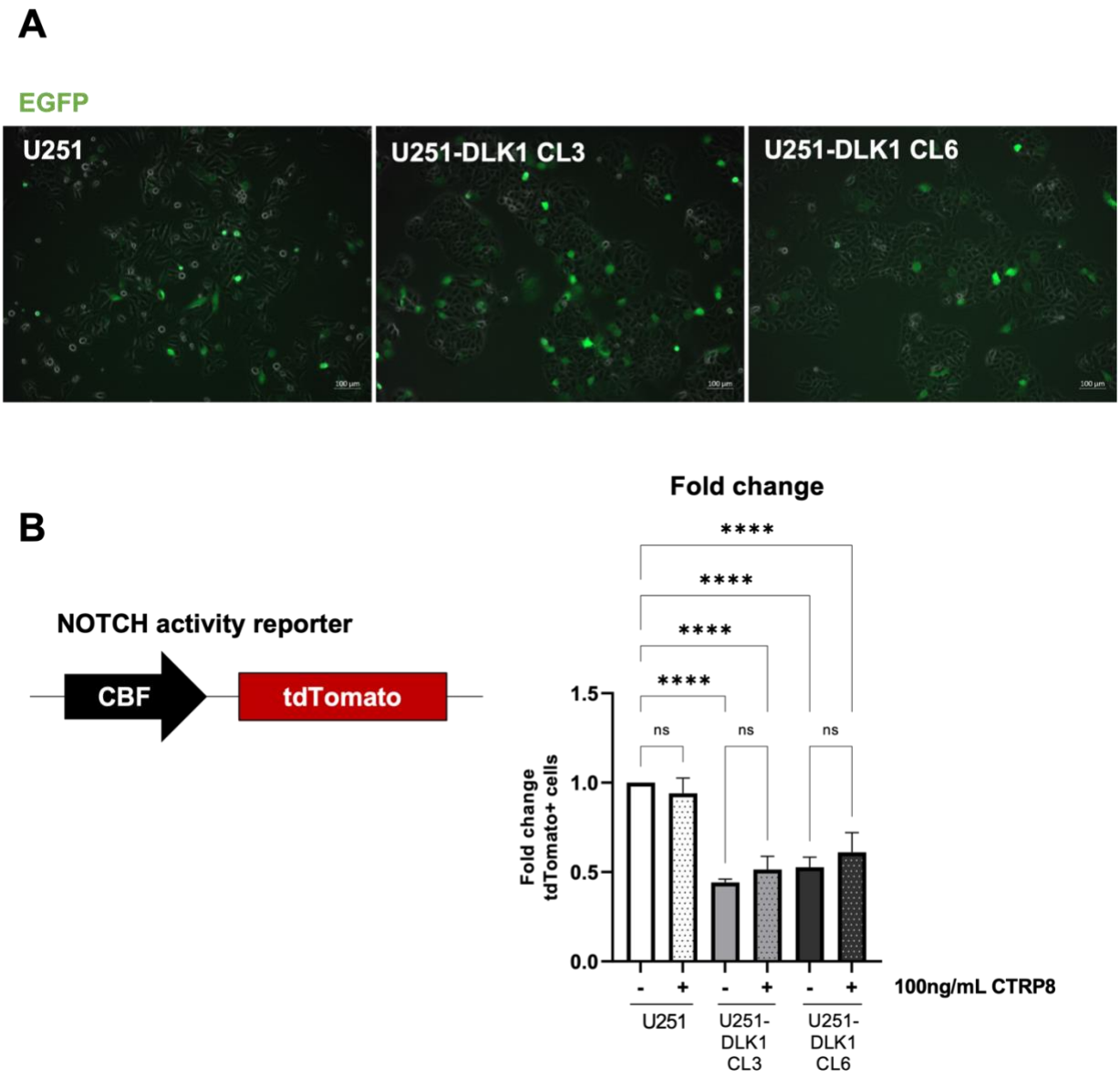

Figure 3.21 NOTCH reporter activity in U251, U251-DLK1 clones treated with CTRP8. A) Distribution of EGFP-positive cells 48h after transfection. Images taken on Zeiss D1 microscope. **B)** NOTCH activity determined by tdTomato-positive cells normalized to EGFP-positive cells. Fold change of NOTCH reporter activity determined relative to U251 for n=3. Statistical analyses conducted in Graphpad (****P<0.0001, ns=not significant).

4 DISCUSSION

4.1 CTRP8-DLK1 interaction

Among the CTRP8 interactions detected in a Y2H screen, DLK1 was scored as a top candidate. The Y2H predicted that CTRP8 binds to amino acids 3-122 of DLK1, which corresponds to the N-terminus up to the third EGF-like domain. We have successfully shown a physical interaction between CTRP8 and full-size DLK1 using co-IP, identifying DLK1 as a novel interaction partner of CTRP8 and a potential new CTRP8 receptor. In agreement with the Y2H predicted interaction domain, CTRP8 interacted within the first five EGF-like domains of DLK1 as demonstrated with co-IP of CTRP8 and Brevideltinin. This CTRP8 interaction with Brevideltinin suggested that CTRP8 can bind soluble isoforms of DLK1 that are known to be endogenously produced in some tumors (Altenberger et al. 2005).

The Y2H screen was not able to identify the CTRP8 domains engaged in the interaction with DLK1. We used a modular approach to determine which CTRP8 domains participate in the CTRP8-DLK1 interaction. Absence of the C1q domain or variable region resulted in no interaction between CTRP8 and DLK1. Only CTRP8 constructs devoid of the collagen domain were still able to successfully co-IP with full-size DLK1. Based on these results, the CTRP8 C1q and variable domains may be facilitating a two-pronged interaction with DLK1 EGF-like domains. We have not yet concluded a specific DLK1-binding motif on CTRP8, although we can suspect that DLK1 likely binds to a different region on CTRP8 than its known receptor, RXFP1. In co-IP, DLK1 successfully interacted with a CTRP8 mutant with its RXFP1-binding domain deleted, indicating that successful CTRP8-DLK1 interaction does not require the RXFP1-binding motif. Furthermore, we consider that the CTRP8-DLK1 interaction may be affected by higher oligomeric organization of CTRP8. Formation of CTRP8 homotrimers is stabilized by the disulfide bonds between cysteine

residues of the variable region and coiling of the collagen domains (Kishore et al. 2004; Wong et al. 2008; Peterson, Wei, and Wong 2009). We can expand on our current approach and generate expression constructs with targeted deletions of residues that are critical for CTRP8 trimer formation, such as the cysteines within the CTRP8 variable region. This will be able to clarify if CTRP8 facilitates interaction with DLK1 as a monomer or trimer.

It is conceivable that DLK1 binding to CTRP8 may not require detection of a specific sequence, but rather involves pattern recognition. CTRP family proteins share structural similarities with pattern recognition molecules (PRMs) of the complement system such as C1q (Kishore et al. 2004; Kirketerp-Møller et al. 2020). The classical complement pathway protein C1q can bind to a broad range of ligands through recognition of molecular patterns, most often discussed in the context of the innate immune response. CTRP6 has been recently identified as a PRM that can interact with components of the classical and lectin complement pathways (Kirketerp-Møller et al. 2020). CTRP8 may use pattern recognition to bind the repetitive EGF-like motifs of DLK1, although this would require more in-depth characterization of the kinetics of CTRP8-DLK1 interaction. Preliminary in silico studies in the Klonisch lab suggest that CTRP8, like CTRP6, can also function as a pattern recognition molecule.

Overall, we have demonstrated a physical interaction between CTRP8 and DLK1 in co-IP and Y2H. Our approach to characterize the CTRP8-DLK1 interaction thus far has relied on modified protein sequences and co-IP. Evidence from co-IP can be supplemented with methods that permit detection of the interaction even when the proteins are not in solution. Techniques such as proximity ligation assay (PLA) and fluorescence resonance energy transfer (FRET) would allow us to observe the interaction in real-time. To resolve more complex aspects such as binding affinities and binding-induced conformational changes, nuclear magnetic resonance spectroscopy

(NMR) methods can be employed. A combination of chemical shift perturbation (CSP) and solvent-paramagnetic relaxation enhancement (PRE) are commonly used in combination. Data extracted from CSP and solvent PRE can be combined with a protein modelling program to generate a three-dimensional model of the CTRP8-DLK1 complex (Purslow et al. 2020). NMR techniques would provide information about the dynamics of CTRP8-DLK1 interaction and how it engages signaling pathways to regulate biological processes. As we investigate the role CTRP8-DLK1 in gliomas, structural biology can be integrated to link protein-protein interaction data to functionality.

4.2 CTRP8-DLK1 in glioma stemness

DLK1 has been shown to enhance stemness in gliomas, as well as other cancers (Grassi and Pietras 2021). In our glioma *in vitro* model, we observed enhanced tumor sphere formation of DLK1-expressing U251 cells, which generated increased sphere numbers of larger sphere size when compared to U251 or U251-DLK1.CR transfectants with non-cleavable DLK1. Co-expression of DLK1 and CTRP8 in U251 resulted in a significant decrease of sphere formation compared to U251-DLK1. Overall, DLK1 over-expression in U251 expanded a GSC population responsible for generating tumor spheres, whereas CTRP8 expression diminished stem cell properties of U251 and may promote a more differentiated cell state. One current limitation of our study is the lack of U251-CTRP8 sphere formation data. This would allow us to conclude if CTRP8 decreases the stem cell population only in the presence of DLK1, or if it can indirectly impact stemness through another receptor present in U251. Preliminary sphere formation experiments with U251-CTPR8 do suggest that there is not a drastic difference between the number and appearance of U251 versus U251-CTRP8 spheres.

More specifically, DLK1 and CTRP8 may regulate the transition between proneural and mesenchymal GSC subtypes, revealed by the profile of GSC markers. Our expression data of GSC markers revealed CD133, OCT4 and SOX2 upregulation in U251-DLK1, resembling a proneural GSC signature. Additionally, downregulation of typical mesenchymal GSC markers CD44 and ALDH1A3 in U251-DLK1 also supported a proneural phenotype (Wang et al. 2021; Mao et al. 2013; Brown et al. 2017). In U251-DLK1/CTRP8 transfectants, all markers apart from OCT4 were reduced which relates to an overall reduction in stemness observed in tumor sphere formation. When U251-DLK1 clones were treated with recombinant human CTRP8, proneural markers CD133, OCT4 and SOX2 were downregulated, showing a similar response to U251-DLK1/CTRP8 clones. Typical mesenchymal GSC markers CD44 and ALDH1A3 did not show significant changes in response to CTRP8 treatment. Results from our panel of GSC markers do not yet reveal if DLK1-CTRP8 interaction can initiate the transition from a proneural to mesenchymal GSC phenotype. Again, here we are limited by the lack of expression data from U251-CTRP8. It would be beneficial to test this panel of GSC markers an compare the expression profile of U251-CTRP8, to see if there is a shift in expression independent of DLK1. Further characterization of these cell models may resolve if there is a CTRP8-DLK1 related shift between GSC subtypes.

In addition to the gene expression signature, proneural and mesenchymal GSCs can be distinguished by metabolic activity, signaling pathways, and localization within the tumor niche (Wang et al. 2021). Our current approach using qPCR and sphere formation may not provide a comprehensive view of GSC-related genes and pathways, thus excluding prospective CTRP8-DLK1 targets. A broader screen of genes and pathways related to GSC regulation using microarrays is warranted and may reveal potential gene targets and signaling pathways that are

responsive to CTRP8-DLK1 interaction. For example, proneural and mesenchymal GSCs can be distinguished by the activity of specific signalling pathways (Wang et al. 2021). Proneural GSCs are associated with NOTCH, Wnt, and PDGFRb signaling (Saito et al. 2014; Rajakulendran et al. 2019; Kim et al. 2012). In contrast, the predominant active pathways in mesenchymal GSCs are NFkB and FOXD1-ALDH1A3 pathways (Kim et al. 2016; Cheng et al. 2016).

Furthermore, features of the GSC niche such as vasculature, hypoxia and immune cell population are associated with proneural or mesenchymal signatures (Wang et al. 2021; Aderetti et al. 2018). In particular, immunocyte infiltration is distinct between proneural and mesenchymal GSCs. High immunocyte infiltration is characteristic of mesenchymal GSCs, mostly of CD8-positive T cells and microglia (Beier et al. 2012). In contrast, proneural GSCs have overall lower immunocyte infiltration and promote an immunosuppressive environment by recruiting M2 macrophages (Beier et al. 2012; Zhou et al. 2015). We can accomplish this using U251-DLK1 and U251-DLK1/CTRP8 cells in a mouse xenograft model established in our lab. By injecting the U251 cells expressing CTRP8 and/or DLK1 into the mouse brain, we can extract data about the tumor formation capabilities of these cells, as well as identify key components of the peri-immune GSC niche. Additionally, it may reveal sources of CTRP8 and DLK1 in the brain. Our current studies have been limited to expression of DLK1 and CTRP8 in tumor cells, which is likely not the case *in vivo*. We have previously identified CTRP8 expression in a population of mast cells and macrophages in prostate and breast cancer (Nivedita-Krishnan et al. 2021), so we can anticipate CTRP8-positive immunocytes within the GSC niche as well.

Analysing the activity of signaling pathways and characterization of infiltrating immune cells within the tumor microenvironment may provide clarity regarding the proneural or mesenchymal signature we observe with CTRP8 and/or DLK1 expression in U251 cells. This will

supplement our findings in sphere formation and GSC marker expression, which suggest a new mechanism regulating GSC population involving CTRP8 and DLK1.

4.3 DLK1 isoform-dependent impact on stemness

Isoform-dependent role of DLK1 in regulation of differentiation and proliferation has primarily been described in development of mesoderm-derived tissues (Smas, Chen, and Sul 1997; Mortensen et al. 2012; Shin et al. 2014; Waddell et al. 2010). More recently, it has been revealed that DLK1 proteolytic cleavage and release of its intracellular domain impacts stemness in gliomas under hypoxic conditions (Grassi, Pantazopoulou, and Pietras 2020). We used a cleavage-resistant DLK1 (DLK1.CR) to assess the impact on GSC properties in U251. In a sphere formation assay, U251-DLK1.CR did not exhibit enhanced sphere formation capability relative to U251. Compared to U251-DLK1, U251-DLK1.CR formed fewer spheres that possessed smaller diameters. In terms of GSC marker expression, CD133 and OCT4 in particular showed dramatic downregulation, demonstrating an overall decrease in stemness in accordance with reduced sphere formation. The re-emergence of ALDH1A3 expression in U251-DLK1.CR may be an indication of a shift towards a mesenchymal GSC signature (Mao et al. 2013; Wang et al. 2021). As mentioned earlier, further characterization of factors such as signaling pathway activity and tumor niche localization would be required to clearly deduce the GSC subtype.

For the first time in gliomas, we described an isoform-dependent DLK1 effect on GSC populations. To expand on the characterization of the U251-DLK1.CR cell model, we can co-express DLK1.CR and CTRP8 in U251 to observe its impact on tumor sphere formation and GSC marker expression as we have done with full-size, cleavable DLK1. In U251 the cleavable form of DLK1 enhanced GSC population, which was lessened by CTRP8. CTRP8 may have an effect on DLK1 protein processing that can drive the reduction in stemness. If this is the case, we would

not expect CTRP8 and DLK1.CR co-expression in U251 to have an impact on GSC population. Overall, in U251 we have shown that upregulation of both DLK1 expression and DLK1 proteolytic cleavage is required to promote glioma stemness along a proneural differentiation program.

The impact of DLK1 cleavage on GSC characteristics may be revealing the role of DLK1 cleavage products in the regulatory mechanism for stemness. DLK1 cleavage products include the soluble ectodomain with well-described functionality, and the lesser known DLK1 intracellular domain. The capability of DLK1 to present both membrane bound and diffusible forms bring forth the possibility for membrane to nuclear signaling to regulate stemness, which we discuss in the context of DLK1-CTRP8 interaction in the following sections.

4.4 CTRP8-DLK1 membrane signaling

In terms of mechanistic regulation of glioma stemness, we consider how the CTRP8-DLK1 interaction may impact signaling with their respective known receptors. By binding to CTRP8, DLK1 may interfere with binding of CTRP8 to its known receptor, RXFP1 (Glogowska et al. 2013; Thanasupawat et al. 2018). Both membrane bound and soluble DLK1 forms have been able to do this with several interaction partners: DLK1-DLK1 blocks NOTCH receptor binding to DLL/JAG ligands (Sánchez-Solana et al. 2011; Traustadóttir et al. 2017), and DLK1-CFR interaction prevents FGF18 binding resulting in FGF signaling inhibition (Miyaoka et al. 2010). However, this is likely not the case because DLK1 and RXFP1 have different CTRP8 binding sites, and DLK1 still interacts with CTRP8 missing an RXFP1-binding motif. Additionally, RXFP1 is not typically associated with cancer stemness, thus the CTRP8-DLK1 effect can likely be attributed to other signaling pathway activity.

Conversely, CTRP8 may interfere with the interaction of DLK1 to its receptors. At present, there are no reports of CTRP8 functioning in this antagonizing capacity. NOTCH1 is a well-

described receptor for DLK1 (Falix et al. 2012; Baladrón et al. 2005; Traustadóttir et al. 2016), and the NOTCH pathway has been associated with context-dependent regulation of glioma stemness (Bazzoni and Bentivegna 2019; Parmigiani, Taylor, and Giachino 2020). We investigated if CTRP8 could interfere with DLK1-NOTCH1 interaction that would result in reduced DLK1-mediated NOTCH signaling inhibition. In U251, DLK1 clearly acted as an inhibitor of NOTCH activation, demonstrated by significant reduction of Hes1 levels and NOTCH reporter activity. However, treatment of U251-DLK1 with recombinant CTRP8 had no effect on NOTCH target gene expression and reporter activity. In this model, CTRP8 was not sufficient to disrupt inhibitory action of DLK1-NOTCH1 interaction. The NOTCH1 binding domain of DLK1 is located at EGF domains 5 and 6 (Traustadóttir et al. 2016; Baladrón et al. 2005). We have shown that CTRP8 interacts with the first five EGF domains of DLK1, suggesting that CTRP8 may not be able to sufficiently block the DLK1-NOTCH1 interaction. In our experimental conditions, CTRP8 treatment occurred with U251 cells overexpressing DLK1. In this DLK1 expressing model, the concentration of CTRP8 may not be sufficient to significantly counteract the inhibitory effect of DLK1 on NOTCH1 activation. In the context of glioma stemness, the NOTCH pathway is one of the key regulatory pathways (Bazzoni and Bentivegna 2019; Parmigiani, Taylor, and Giachino 2020). Further investigation on a possible role of CTRP8 in ameliorating the inhibitory DLK1 effect on NOTCH signaling may require use of cells with endogenous DLK1 expression and/or more moderate levels of DLK1 than observed in our U251-DLK1 clones. By doing so we may more clearly conclude if the CTRP8-DLK1 acts through the NOTCH pathway or alternative mechanisms.

4.5 CTRP8-DLK1 nuclear signaling

Our tumor sphere formation and stem cell marker results revealed contrasting effects of full-size, cleavable DLK1 and DLK1.CR on U251 GSC properties. Increased stemness was only associated with full-size DLK1, which was then reduced upon introduction of CTRP8. Based on these findings we hypothesized that CTRP8 interaction may modulate DLK1 proteolytic cleavage, and the resulting DLK1 cleaved protein products can be involved in the regulatory mechanism of glioma stemness. Upon binding to CTRP8, DLK1 may act as a receptor that undergoes sequential proteolytic cleavages to release its soluble ectodomain and intracellular domain (ICD), in a manner similar to NOTCH receptors upon canonical ligand binding (Bray and Bernard 2010). Using the V5-Tag antibody in Western blot, we detected a lower molecular weight DLK1 fragment around 15 kDA in both nuclear and cytoplasmic protein fractions that we suspected to be the DLK1-ICD. When a cleavage-resistant DLK1 construct was expressed in U251, the 15 kDA band was not detectable in nuclear and cytoplasmic extracts. CTRP8-DLK1 binding may increase DLK1 proteolytic cleavage and thus the release of DLK1-ICD. Indeed, in immunofluorescence we observe increased nuclear localization of DLK1-ICD detected with the V5-Tag antibody in U251-DLK1 cells treated with CTRP8. The current proposed mechanism for DLK1-ICD release involves ADAM-mediated cleavage to release the DLK1 extracellular domain, followed by release of the cytoplasmic domain by an unidentified enzyme (Grassi, Pantazopoulou, and Pietras 2020). It is likely that DLK1-ICD is released by consequent cleavage with a gamma-secretase complex, like other NOTCH receptors and ligands, although this has not yet been described. CTRP8 binding to DLK1 extracellular domains may promote recruitment of ADAMs or gamma-secretases to facilitate the cleavage of DLK1. The involvement of CTRP8 in this capacity needs to be further investigated.

While the mechanism of how CTRP8 may promote DLK1-ICD release and nuclear translocation has yet to be determined, we can speculate on the function of DLK1-ICD in the nucleus. Most DLK1 studies focus on the full-size protein or the soluble form, thus, there is a lack of information about the function of DLK1-ICD. Nuclear localization of the DLK1 cytoplasmic fragment may be anticipated due to a small peptide sequence in the DLK1-ICD N-terminal regions which resembles a nuclear localization signal (NLS). Functionality of DLK1-ICD in gliomas has emerged only recently, where increased DLK1-ICD release was associated with enhanced stemness. However, its exact function in the nucleus has not yet been identified (Grassi, Pantazopoulou, and Pietras 2020). Upon translocation to the nucleus, DLK1-ICD may bind directly to DNA or form a complex with transcriptional factors to regulate gene expression.

DLK1 has been shown to interact with transcription factors: nuclear co-repressor 1 (NCOR1) (Tan et al. 2019) and nuclear factor of activated T-cells (NFATc4) (Subhashini 2016). NCOR1 and NFATc4 are a prospective nuclear interaction partners of DLK1-ICD. In non-small cell lung carcinoma, NCOR1 and DLK1 co-localization was associated with less differentiated tumors, however downstream targets of NCOR1-DLK1 have not yet been identified (Tan et al. 2019). As a known modulator of GBM invasiveness, proliferation and tumor formation capability, NCOR1 is a promising target to investigate in the context of DLK1 and glioma stemness (Heldring et al. 2014). Similarly, specific DLK1-NFATc4 downstream targets have not been resolved, although DLK1 promoted shuttling of NFATc4 to the nucleus (Subhashini 2016). The regulatory role of NFATc4 in neural stem cell function (Moreno et al. 2015) plus studies describing the implications of other NFAT members in gliomas (Tie et al. 2013; Urso et al. 2019), presents NFATc4 as another candidate for a potential DLK1-ICD co-factor. There is currently limited knowledge about both the regulation of DLK1-ICD release and DLK1-ICD function in the nucleus, but our results open

the possibility of CTRP8 acting as a switch to initiate the process of DLK1-ICD nuclear localization.

4.6 Conclusions and outlook

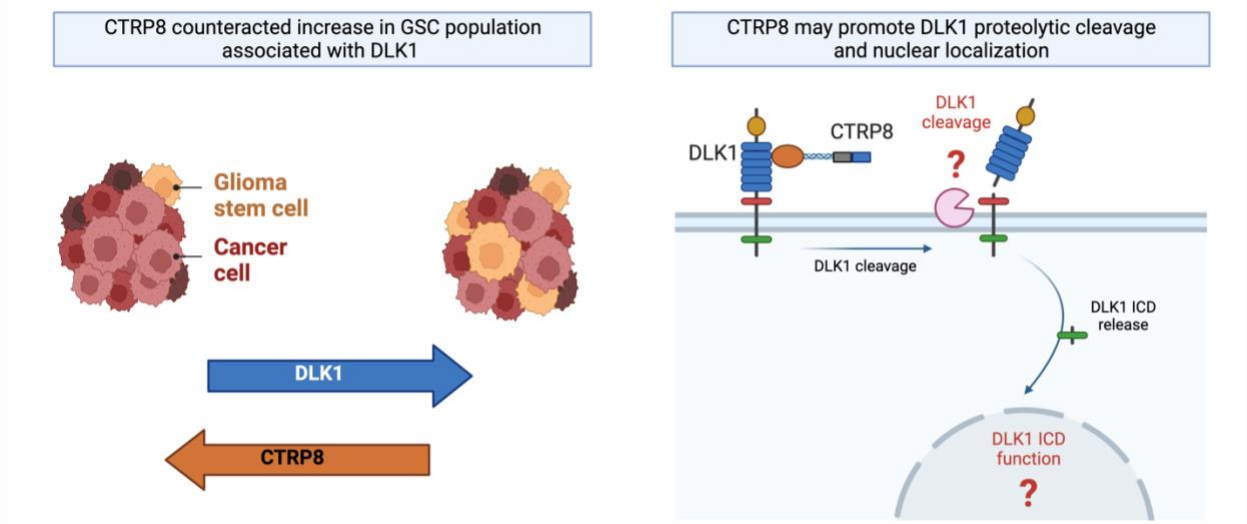

Figure 4.1. Schematic of CTRP8 and DLK1 functionality and potential mechanism in glioma stemness. In U251, DLK1 expression enhanced the glioma stem cell (GSC) population. Co-expression of CTRP8 and DLK1 reduced the GSC properties of U251. In terms of mechanism, CTRP8 may be facilitating increased DLK1 proteolytic cleavage and nuclear localization. Outstanding questions include the mechanism by which CTRP8 promotes DLK1 cleavage, and the role of DLK1 in the nucleus.

In GBM, CTRP8 has been previously described as a promoter of invasiveness and treatment resistance, mediated through its receptor RXFP1 (Glogowska et al. 2013; Thanasupawat et al. 2018; Glogowska et al. 2021). Here we describe a novel CTRP8-DLK1 interaction and revealed its role in the modulation of GSC populations. In particular, DLK1 expression shifts the balance towards a proneural GSC signature, which was counteracted by CTRP8 to decrease the overall stem cell characteristics. Higher GSC population in gliomas correlates to poor prognosis due to their ability to evade drug treatments to then re-capitulate the tumor. Recurrent tumors tend to be

of a higher, more aggressive glioma classification typically of mesenchymal phenotype (Zeppernick et al. 2008; Seymour, Nowak, and Kakulas 2015; Fedele et al. 2019). Regulation of the proneural to mesenchymal GSC homeostasis is complex but has important implications in glioma progression and treatment (Wang et al. 2021; Seymour, Nowak, and Kakulas 2015). For the first time, we report a novel mechanism involving CTRP8 and DLK1 as modulators of glioma stemness. Further investigation into the mechanisms involved would contribute to the understanding of this complex pathway and may be of clinical relevance.

One of the current limitations of this study is the use of overexpressed DLK1 in HEK293 and U251 cell lines. Although it was advantageous for both the co-IP and initial functional studies, it will be important to utilise endogenous expressors of DLK1 in future studies, particularly when inquiring CTRP8-DLK1 biological functions. In glioma cells, this may include induction of DLK1 expression through hypoxia culture conditions (Grassi et al. 2020; Grassi, Pantazopoulou, and Pietras 2020). Hypoxia also potentially connects DLK1 expression and proteolytic cleavage to glioma stemness. In the tumor microenvironment, hypoxia is among the factors that allow GSCs to thrive. A role of hypoxia in the regulation of CTRP8 has not yet been identified but other CTRP family members, CTRP1, CTRP3, CTRP6, and CTRP13, have been associated with ischemic injuries of the heart, brain and renal systems (Jiang et al. 2021; Yuasa et al. 2016; Ding, Wang, and Song 2021; Xiang et al. 2020). In the context of gliomas and other tumors, the role of CTRPs in hypoxic conditions is unidentified. In future CTRP8-DLK1 work, hypoxia should be a physiologically relevant stimulus to incorporate in the analysis of glioma stemness.

In terms of cell models, we have not yet been able to identify glioma cells that are endogenous producers of both CTRP8 and DLK1 under normoxic conditions. To remedy this, we can look to other cell types as a source of CTRP8 or DLK1. Our other work has revealed CTRP8

as a key marker of immune cells in the tumor microenvironments of prostate and breast cancers (Nivedita-Krishnan et al. 2021). In the glioma context, we can use this knowledge to expand the study to include the tumor microenvironment. Soluble CTRP8 from immune cells can be used to treat DLK1-positive glioma cells. Tumor-associated astrocytes have also been reported as a source of DLK1, particularly in hypoxic conditions (Grassi et al. 2020). Another approach to consider is the treatment of CTRP8-positive gliomas with astrocyte cultured medium containing soluble DLK1. These strategies would not only provide endogenously produced CTRP8 and DLK1 but enrich *in vitro* models to more closely represent the complexity of *in vivo* conditions created by the tumor microenvironment.

In conclusion, we have characterized CTRP8 as a novel interaction partner of DLK1. In gliomas, we described DLK1 as a promoter of stemness, meanwhile CTRP8 and DLK1 co-expression reduced stem cell characteristics. Additionally, we demonstrated that GSC population is only enhanced in full-size, cleavable DLK1 which further complicates the signaling and analysis of this dynamic protein. Further investigations are required regarding the mechanism by which CTRP8 promotes DLK1 cleavage and nuclear translocation as well as the function of DLK1-ICD. In future studies it will be exciting to unravel the role of CTRP8 within the complex DLK1 membrane to nuclear signaling network, and the biological outcome of CTRP8-DLK1 interaction in glioma stemness.

5 REFERENCES

Aderetti, Diana A., Vashendriya V.V. Hira, Remco J. Molenaar, and Cornelis J.F. van Noorden. 2018. "The Hypoxic Peri-Arteriolar Glioma Stem Cell Niche, an Integrated Concept of Five Types of Niches in Human Glioblastoma." *Biochimica et Biophysica Acta. Reviews on Cancer* 1869 (2): 346–54. https://doi.org/10.1016/J.BBCAN.2018.04.008.

Akiyama, Hironori, Souhei Furukawa, Satoshi Wakisaka, and Takashi Maeda. 2009. "Elevated Expression of CTRP3/Cartducin Contributes to Promotion of Osteosarcoma Cell Proliferation." *Oncology Reports* 21 (6): 1477–81. https://doi.org/10.3892/OR_00000377.

Altenberger, T, M Bilban, M Auer, E Knosp, S Wolfsberger, W Gartner, I Mineva, C Zielinski, L Wagner, and A Luger. 2005. "Identification of DLK1 Variants in Pituitary-and Neuroendocrine Tumors Q." *Biochemical and Biophysical Research Communications* 340: 995–1005. https://doi.org/10.1016/j.bbrc.2005.12.094.

Andersen, Ditte C., Stine J. Petersson, Louise H. Jørgensen, Peter Bollen, Pernille B. Jensen, Børge Teisner, Henrik D. Schroeder, and Charlotte H. Jensen. 2009. "Characterization of DLK1+ Cells Emerging During Skeletal Muscle Remodeling in Response to Myositis, Myopathies, and Acute Injury." *Stem Cells* 27 (4): 898–908. https://doi.org/10.1634/STEMCELLS.2008-0826.

Appelbe, Oliver K., Aleksey Yevtodiyenko, Hilmarie Muniz-Talavera, and Jennifer V. Schmidt. 2013. "Conditional Deletions Refine the Embryonic Requirement for Dlk1." *Mechanisms of Development* 130 (2–3): 143–59. https://doi.org/10.1016/J.MOD.2012.09.010.

Bachmann, E., T. N. Krogh, P. Højrup, K. Skjødt, and B. Teisner. 1996. "Mouse Fetal Antigen 1 (MFA1), the Circulating Gene Product of Mdlk, Pref-1 and SCP-1: Isolation, Characterization and Biology." *Journal of Reproduction and Fertility* 107 (2): 279–85. https://doi.org/10.1530/JRF.0.1070279.

Baladrón, Victoriano, María José Ruiz-Hidalgo, Elena Gubina, Ezio Bonvini, and Jorge Laborda. 2001. "Specific Regions of the Extracellular Domain of Dlk, an EGF-like Homeotic Protein Involved in Differentiation, Participate in Intramolecular Interactions." *Frontiers in Bioscience : A Journal and Virtual Library* 6 (1): 25–32. https://doi.org/10.2741/BALADRON/PDF.

Baladrón, Victoriano, María José Ruiz-Hidalgo, María-Luisa Nueda, María José M. Díaz-Guerra, José Javier García-Ramírez, Ezio Bonvini, Elena Gubina, and Jorge Laborda. 2005. "Dlk Acts as a Negative Regulator of Notch1 Activation through Interactions with Specific EGF-like Repeats." *Experimental Cell Research* 303 (2): 343–59. https://doi.org/10.1016/J.YEXCR.2004.10.001.

Bazzoni, Riccardo, and Angela Bentivegna. 2019. "Role of Notch Signaling Pathway in Glioblastoma Multiforme Pathogenesis." *Cancers* 11 (3): 292. https://doi.org/10.3390/cancers11030292.

Begum, Asma, Yuri Kim, Qun Lin, and Zhong Yun. 2012. "DLK1, Delta-like 1 Homolog (Drosophila), Regulates Tumor Cell Differentiation in Vivo." *Cancer Letters* 318 (1): 26–33. https://doi.org/10.1016/j.canlet.2011.11.032.

Beier, Christoph P., Praveen Kumar, Katharina Meyer, Petra Leukel, Valentin Bruttel, Ines Aschenbrenner, Markus J. Riemenschneider, et al. 2012. "The Cancer Stem Cell Subtype

Determines Immune Infiltration of Glioblastoma." *Stem Cells and Development* 21 (15): 2753–61. https://doi.org/10.1089/SCD.2011.0660.

Boyd, Nathaniel H., Anh Nhat Tran, Joshua D. Bernstock, Tina Etminan, Amber B. Jones, G. Yancey Gillespie, Gregory K. Friedman, and Anita B. Hjelmeland. 2021. "Glioma Stem Cells and Their Roles within the Hypoxic Tumor Microenvironment." *Theranostics* 11 (2): 665. https://doi.org/10.7150/THNO.41692.

Bray, Sarah, and Fred Bernard. 2010. "Notch Targets and Their Regulation." In *Nature Reviews Molecular Cell Biology 2006 7:9*, 7:253–75. Nature Publishing Group. https://doi.org/10.1016/S0070-2153(10)92008-5.

Bray, Sarah, Shuji Takada, Emma Harrison, Shing Chuan Shen, and Anne C. Ferguson-Smith. 2008. "The Atypical Mammalian Ligand Delta-like Homologue 1 (Dlk1) Can Regulate Notch Signalling in Drosophila." *BMC Developmental Biology* 8 (1): 1–9. https://doi.org/10.1186/1471-213X-8-11/FIGURES/4.

Brown, Daniel V., Gulay Filiz, Paul M. Daniel, Frédéric Hollande, Sebastian Dworkin, Stephanie Amiridis, Nicole Kountouri, Wayne Ng, Andrew P. Morokoff, and Theo Mantamadiotis. 2017. "Expression of CD133 and CD44 in Glioblastoma Stem Cells Correlates with Cell Proliferation, Phenotype Stability and Intra-Tumor Heterogeneity." *PLOS ONE* 12 (2): e0172791. https://doi.org/10.1371/JOURNAL.PONE.0172791.

Ceder, Jens A., Linda Jansson, Leszek Helczynski, and Per Anders Abrahamsson. 2008. "Delta-Like 1 (Dlk-1), a Novel Marker of Prostate Basal and Candidate Epithelial Stem Cells, Is Downregulated by Notch Signalling in Intermediate/Transit Amplifying Cells of the Human Prostate." *European Urology* 54 (6): 1344–53. https://doi.org/10.1016/J.EURURO.2008.03.006.

Chen, Li, Diyako Qanie, Abbas Jafari, Hanna Taipaleenmaki, Charlotte H. Jensen, Anna Marja Saamanen, Maria Luisa Nueda Sanz, Jorge Laborda, Basem M. Abdallah, and Moustapha Kassem. 2011. "Delta-like 1/Fetal Antigen-1 (Dlk1/FA1) Is a Novel Regulator of Chondrogenic Cell Differentiation via Inhibition of the Akt Kinase-Dependent Pathway." *Journal of Biological Chemistry* 286 (37): 32140–49. https://doi.org/10.1074/jbc.M111.230110.

Cheng, Peng, Jia Wang, Indrayani Waghmare, Stefania Sartini, Vito Coviello, Zhuo Zhang, Sung Hak Kim, et al. 2016. "FOXD1-ALDH1A3 Signaling Is a Determinant for the Self-Renewal and Tumorigenicity of Mesenchymal Glioma Stem Cells." *Cancer Research* 76 (24): 7219. https://doi.org/10.1158/0008-5472.CAN-15-2860.

D'Souza, Brendan, Laurence Meloty-Kapella, and Gerry Weinmaster. 2010. "Canonical and Non-Canonical Notch Ligands." *Current Topics in Developmental Biology* 92 (C): 73. https://doi.org/10.1016/S0070-2153(10)92003-6.

Deiuliis, Jeffrey A., Bing Li, Pasha A. Lyvers-Peffer, Steven J. Moeller, and Kichoon Lee. 2006. "Alternative Splicing of Delta-like 1 Homolog (DLK1) in the Pig and Human." *Comparative Biochemistry and Physiology. Part B, Biochemistry & Molecular Biology* 145 (1): 50–59. https://doi.org/10.1016/J.CBPB.2006.06.003.

Dezső, Katalin, Judit Halász, Hanne Cathrine Bisgaard, Sándor Paku, Eszter Turányi, Zsuzsa Schaff, and Peter Nagy. 2008. "Delta-like Protein (DLK) Is a Novel Immunohistochemical Marker for Human Hepatoblastomas." *Virchows Archiv : An International Journal of*

Pathology 452 (4): 443–48. https://doi.org/10.1007/S00428-007-0571-8.

Ding, H., Z. Wang, and W. Song. 2021. "CTRP3 Protects Hippocampal Neurons from Oxygen-Glucose Deprivation-Induced Injury through the AMPK/Nrf2/ARE Pathway." *Human & Experimental Toxicology* 40 (7): 1153–62. https://doi.org/10.1177/0960327121989412.

Falix, Farah A., Daniël C. Aronson, Wouter H. Lamers, and Ingrid C. Gaemers. 2012. "Possible Roles of DLK1 in the Notch Pathway during Development and Disease." *Biochimica et Biophysica Acta - Molecular Basis of Disease*. Elsevier. https://doi.org/10.1016/j.bbadis.2012.02.003.

Fan, Xing, Leila Khaki, Thant S. Zhu, Mary E. Soules, Caroline E. Talsma, Naheed Gul, Cheryl Koh, et al. 2010. "NOTCH Pathway Blockade Depletes CD133-Positive Glioblastoma Cells and Inhibits Growth of Tumor Neurospheres and Xenografts." *Stem Cells* 28 (1): 5–16. https://doi.org/10.1002/STEM.254.

Fan, Xing, William Matsui, Leila Khaki, Duncan Stearns, Jiong Chun, Yue Ming Li, and Charles G. Eberhart. 2006. "Notch Pathway Inhibition Depletes Stem-like Cells and Blocks Engraftment in Embryonal Brain Tumors." *Cancer Research* 66 (15): 7445–52. https://doi.org/10.1158/0008-5472.CAN-06-0858.

Fay, Toby N, Ian Jacobs, Borge Teisner, Otto Poulsen, Michael G Chapman, Isabel Stabile, Hans Bohn, Jes G Westergaard, and Jurgis G Grudzinskas. 1988. "Two Fetal Antigens (FA-1 and FA-2) and Endometrial Proteins (PP12 and PP14) Isolated from Amniotic Fluid; Preliminary Observations in Fetal and Maternal Tissues." *European Journal of Obstetrics & Gynecology and Reproductive Biology* 29: 73–85.

Fedele, Monica, Laura Cerchia, Silvia Pegoraro, Riccardo Sgarra, and Guidalberto Manfioletti. 2019. "Proneural-Mesenchymal Transition: Phenotypic Plasticity to Acquire Multitherapy Resistance in Glioblastoma." *International Journal of Molecular Sciences* 20 (11): 2746. https://doi.org/10.3390/IJMS20112746.

Floridon, Charlotte, Charlotte Harken Jensen, Poul Thorsen, Ole Nielsen, Lone Sunde, Jes Grabow Westergaard, Sten Grove Thomsen, and Boerge Teisner. 2000. "Does Fetal Antigen 1 (FA1) Identify Cells with Regenerative, Endocrine and Neuroendocrine Potentials? A Study of FA1 in Embryonic, Fetal, and Placental Tissue and in Maternal Circulation." *Differentiation* 66 (1): 49–59. https://doi.org/10.1046/J.1432-0436.2000.066001049.X.

Formstecher, Etienne, Sandra Aresta, Vincent Collura, Alexandre Hamburger, Alain Meil, Alexandra Trehin, Céline Reverdy, et al. 2005. "Protein Interaction Mapping: A Drosophila Case Study." *Genome Research* 15 (3): 376. https://doi.org/10.1101/GR.2659105.

Galli, Rossella, Elena Binda, Ugo Orfanelli, Barbara Cipelletti, Angela Gritti, Simona De Vitis, Roberta Fiocco, Chiara Foroni, Francesco Dimeco, and Angelo Vescovi. 2004. "Isolation and Characterization of Tumorigenic, Stem-like Neural Precursors from Human Glioblastoma." *Cancer Research* 64 (19): 7011–21. https://doi.org/10.1158/0008-5472.CAN-04-1364.

Garcés, Carmen, María José Ruiz-Hidalgo, Ezio Bonvini, Julia Goldstein, and Jorge Laborda. 1999. "Adipocyte Differentiation Is Modulated by Secreted Delta-like (Dlk) Variants and Requires the Expression of Membrane-Associated Dlk." *Differentiation* 64 (2): 103–14. https://doi.org/10.1046/J.1432-0436.1999.6420103.X.

Glogowska, Aleksandra, Usakorn Kunanuvat, Jörg Stetefeld, Trushar R Patel, Thatchawan Thanasupawat, Jerry Krcek, Ekkehard Weber, et al. 2013. “C1q-Tumour Necrosis Factor-Related Protein 8 (CTRP8) Is a Novel Interaction Partner of Relaxin Receptor RXFP1 in Human Brain Cancer Cells.” *The Journal of Pathology* 231 (4): 466–79. https://doi.org/10.1002/path.4257.

Glogowska, Aleksandra, Thatchawan Thanasupawat, Jason Beiko, Marshall Pitz, Sabine Hombach-Klonisch, and Thomas Klonisch. 2021. “Novel CTRP8-RXFP1-JAK3-STAT3 Axis Promotes Cdc42-Dependent Actin Remodeling for Enhanced Filopodia Formation and Motility in Human Glioblastoma Cells.” *Molecular Oncology*. https://onlinelibrary-wiley-com.uml.idm.oclc.org/doi/full/10.1002/1878-0261.12981.

Grassi, Elisa Stellaria, Pauline Jeannot, Vasiliki Pantazopoulou, Tracy J. Berg, and Alexander Pietras. 2020. “Niche-Derived Soluble DLK1 Promotes Glioma Growth.” *Neoplasia (United States)* 22 (12): 689–701. https://doi.org/10.1016/j.neo.2020.10.005.

Grassi, Elisa Stellaria, Vasiliki Pantazopoulou, and Alexander Pietras. 2020. “Hypoxia-Induced Release, Nuclear Translocation, and Signaling Activity of a DLK1 Intracellular Fragment in Glioma.” *Oncogene* 39 (20): 4028–44. https://doi.org/10.1038/s41388-020-1273-9.

Grassi, Elisa Stellaria, and Alexander Pietras. 2021. “Emerging Roles of DLK1 in the Stem Cell Niche and Cancer Stemness.” *The Journal of Histochemistry and Cytochemistry : Official Journal of the Histochemistry Society*. https://doi.org/10.1369/00221554211048951.

Guasti, Leonardo, Dominic Cavlan, Kathryn Cogger, Zahida Banu, Amreen Shakur, Salima Latif, and Peter J. King. 2013. “Dlk1 Up-Regulates Gli1 Expression in Male Rat Adrenal Capsule Cells Through the Activation of B1 Integrin and ERK1/2.” *Endocrinology* 154 (12): 4675–84. https://doi.org/10.1210/en.2013-1211.

Gubina, E., M.J. Ruiz-Hidalgo, V. Baladrón, and J. Laborda. 1999. “Assignment1 of DLK1 to Human Chromosome Band 14q32 by in Situ Hybridization.” *Cytogenetic and Genome Research* 84 (3–4): 206–7. https://doi.org/10.1159/000015259.

Guerra-Rebollo, Marta, Cristina Garrido, Lourdes Sánchez-Cid, Carolina Soler-Botija, Oscar Meca-Cortés, Nuria Rubio, and Jerónimo Blanco. 2019. “Targeting of Replicating CD133 and OCT4/SOX2 Expressing Glioma Stem Cells Selects a Cell Population That Reinitiates Tumors upon Release of Therapeutic Pressure.” *Scientific Reports* 9 (1). https://doi.org/10.1038/S41598-019-46014-0.

Hadjidemetriou, Irene, Katia Mariniello, Gerard Ruiz-Babot, James Pittaway, Alessandra Mancini, Demetris Mariannis, Celso E. Gomez-Sanchez, et al. 2019. “DLK1/PREF1 Marks a Novel Cell Population in the Human Adrenal Cortex.” *The Journal of Steroid Biochemistry and Molecular Biology* 193 (October): 105422. https://doi.org/10.1016/J.JSBMB.2019.105422.

Hanahan, Douglas, and Robert A. Weinberg. 2000. “The Hallmarks of Cancer.” *Cell* 100 (1): 57–70. https://doi.org/10.1016/S0092-8674(00)81683-9.

Heldring, Nina, Ulrika Nyman, Peter Lönnerberg, Sofie Önnestam, Anna Herland, Johan Holmberg, and Ola Hermanson. 2014. “NCoR Controls Glioblastoma Tumor Cell Characteristics.” *Neuro-Oncology* 16 (2): 241–49. https://doi.org/10.1093/neuonc/not214.

Helman, L J, C J Thiele, W M Linehan, B D Nelkin, S B Baylin, and M A Israel. 1987.

"Molecular Markers of Neuroendocrine Development and Evidence of Environmental Regulation." *Proceedings of the National Academy of Sciences* 84 (8): 2336–39. https://doi.org/10.1073/PNAS.84.8.2336.

Huang, Jiefang, Xiaonan Zhao, Jian Wang, Yiji Cheng, Qiong Wu, Bei Wang, Fang Zhao, et al. 2019. "Distinct Roles of Dlk1 Isoforms in Bi-Potential Differentiation of Hepatic Stem Cells." *Stem Cell Research and Therapy* 10 (1): 1–13. https://doi.org/10.1186/s13287-019-1131-2.

Huang, Xin Zhang, Min Zhang, Jing De Zhu, Yun Li Zhang, Yun Lin, Ke Sheng Wang, et al. 2007. "Up-Regulation of DLK1 as an Imprinted Gene Could Contribute to Human Hepatocellular Carcinoma." *Carcinogenesis* 28 (5): 1094–1103. https://doi.org/10.1093/CARCIN/BGL215.

Hudak, Carolyn S., and Hei Sook Sul. 2013. "Pref-1, a Gatekeeper of Adipogenesis." *Frontiers in Endocrinology* 4 (JUL): 79. https://doi.org/10.3389/fendo.2013.00079.

Jensen, C. Harken, Thomas N. Krogh, Peter Højrup, Per P. Clausen, Karsten Skjødt, Lars-Inge -I Larsson, Jan J. Enghild, and Børge Teisner. 1994. "Protein Structure of Fetal Antigen 1 (FA1): A Novel Circulating Human Epidermal-Growth-Factor-Like Protein Expressed in Neuroendocrine Tumors and Its Relation to the Gene Products of Dlk and PG2." *European Journal of Biochemistry* 225 (1): 83–92. https://doi.org/10.1111/J.1432-1033.1994.00083.X.

Jensen, Morten Meyer, Henrik Daa Schroder, Anette Kliem, Jens Zimmer, and Børge Teisner. 2001. "Neurons in the Monoaminergic Nuclei of the Rat and Human Central Nervous System Express FA1/Dlk." *Neuroreport* 12 (18): 3959–63. https://doi.org/10.1097/00001756-200112210-00021.

Jiang, Weifeng, Jungang Song, Suitao Zhang, Yanyan Ye, Jun Wang, and Yilin Zhang. 2021. "CTRP13 Protects H9c2 Cells Against Hypoxia/Reoxygenation (H/R)-Induced Injury Via Regulating the AMPK/Nrf2/ARE Signaling Pathway." *Cell Transplantation* 30. https://doi.org/10.1177/09636897211033275.

Jin, Zhong Hui, Ren Jie Yang, Bin Dong, and Bao Cai Xing. 2008. "Progenitor Gene DLK1 Might Be an Independent Prognostic Factor of Liver Cancer." *Http://Dx.Doi.Org.Uml.Idm.Oclc.Org/10.1517/14712598.8.4.371* 8 (4): 371–77. https://doi.org/10.1517/14712598.8.4.371.

Jørgensen, Louise H., Jeeva Sellathurai, Erica E. Davis, Tania Thedchanamoorthy, Rua W.A. Al-Bader, Charlotte H. Jensen, and Henrik D. Schrøder. 2013. "Delta-like 1 Homolog (Dlk1): A Marker for Rhabdomyosarcomas Implicated in Skeletal Muscle Regeneration." *PloS One* 8 (4). https://doi.org/10.1371/JOURNAL.PONE.0060692.

Kageyama, Ryoichiro, and Toshiyuki Ohtsuka. 1999. "The Notch-Hes Pathway in Mammalian Neural Development." *Cell Research* 9 (3): 179–88. https://doi.org/10.1038/SJ.CR.7290016.

Kim, Ravesanker Ezhilarasan, Emma Phillips, Daniel Gallego-Perez, Amanda Sparks, David Taylor, Katherine Ladner, et al. 2016. "Serine/Threonine Kinase MLK4 Determines Mesenchymal Identity in Glioma Stem Cells in an NF-KB-Dependent Manner." *Cancer Cell* 29 (2): 201–13. https://doi.org/10.1016/J.CCELL.2016.01.005.

Kim, Eunhee Kim, Qiulian Wu, Olga Guryanova, Masahiro Hitomi, Justin D. Lathia, David

Serwanski, et al. 2012. “Platelet-Derived Growth Factor Receptors Differentially Inform Intertumoral and Intratumoral Heterogeneity.” *Genes & Development* 26 (11): 1247–62. https://doi.org/10.1101/GAD.193565.112.

Kim, Jung Hyun Kim, Yuhui Wang, and Hei Sook Sul. 2007. “Pref-1 (Preadipocyte Factor 1) Activates the MEK/Extracellular Signal-Regulated Kinase Pathway To Inhibit Adipocyte Differentiation.” *Molecular and Cellular Biology* 27 (6): 2294–2308. https://doi.org/10.1128/MCB.02207-06/ASSET/DAAF5421-0C8D-4920-8E91-EFBA90EFCB11/ASSETS/GRAPHIC/ZMB0060766180007.JPEG.

Kim, Yuri, Qun Lin, Daniel Zelterman, and Zhong Yun. 2009. “Hypoxia-Regulated Delta-like 1 Homologue Enhances Cancer Cell Stemness and Tumorigenicity.” *Cancer Research* 69 (24): 9271–80. https://doi.org/10.1158/0008-5472.CAN-09-1605.

Kirketerp-Møller, Nikolaj, Rafael Bayarri-Olmos, Karen Angeliki Krogfelt, and Peter Garred. 2020. “C1q/TNF-Related Protein 6 Is a Pattern Recognition Molecule That Recruits Collectin-11 from the Complement System to Ligands.” *Journal of Immunology (Baltimore, Md. : 1950)* 204 (6): 1598–1606. https://doi.org/10.4049/JIMMUNOL.1901316.

Kishore, Uday, Christine Gaboriaud, Patrick Waters, Annette K Shrive, Trevor J Greenhough, Kenneth B.M. Reid, Robert B Sim, and Gerard J Arlaud. 2004. “C1q and Tumor Necrosis Factor Superfamily: Modularity and Versatility.” *Trends in Immunology*. https://doi.org/10.1016/j.it.2004.08.006.

Klonisch, Thomas, Aleksandra Glogowska, Thatchawan Thanasupawat, Maxwell Burg, Jerry Krcek, Marshall Pitz, Appalaraju Jaggupilli, Prashen Chelikani, G William Wong, and Sabine Hombach-Klonisch. 2017. “Structural Commonality of C1q TNF-Related Proteins and Their Potential to Activate Relaxin/Insulin-like Family Peptide Receptor 1 Signalling Pathways in Cancer Cells.” *British Journal of Pharmacology* 174 (10): 1025–33. https://doi.org/10.1111/bph.13559.

Kong, Mowei, Yu Gao, Xiang Guo, Yuyu Xie, and Yamei Yu. 2021. “Role of the CTRP Family in Tumor Development and Progression.” *Oncology Letters* 22 (4). https://doi.org/10.3892/OL.2021.12984.

Kopan, Raphael, and Ma. Xenia G. Ilagan. 2009. “The Canonical Notch Signaling Pathway: Unfolding the Activation Mechanism.” *Cell* 137 (2): 216. https://doi.org/10.1016/J.CELL.2009.03.045.

Laborda, Jorge, E. A. Sausville, T. Hoffman, and V. Notario. 1993. “Dlk, A Putative Mammalian Homeotic Gene Differentially Expressed in Small Cell Lung Carcinoma and Neuroendocrine Tumor Cell Line.” *Journal of Biological Chemistry* 268 (6): 3817–20. https://doi.org/10.1016/s0021-9258(18)53544-4.

Larsen, J. B., C. H. Jensen, H. D. Schroder, B. Teisner, P. Bjerre, and C. Hagen. 1996. “Fetal Antigen 1 and Growth Hormone in Pituitary Somatotroph Cells.” *Lancet (London, England)* 347 (8995): 191. https://doi.org/10.1016/S0140-6736(96)90374-8.

Lathia, Justin D., Stephen C. Mack, Erin E. Mulkearns-Hubert, Claudia L.L. Valentim, and Jeremy N. Rich. 2015. “Cancer Stem Cells in Glioblastoma.” *Genes & Development* 29 (12): 1203. https://doi.org/10.1101/GAD.261982.115.

Li., Zhizhong, Hui Wang, Christine E. Eyler, Anita B. Hjelmeland, and Jeremy N. Rich. 2009.

"Turning Cancer Stem Cells inside out: An Exploration of Glioma Stem Cells Signalling Pathways." *Journal of Biological Chemistry* 284 (25): 16705–9. https://doi.org/10.1074/jbc.R900013200.

Li, Qi, Lanlan Wang, Weifeng Tan, Zhi Peng, Yang Luo, Yingmei Zhang, Guoying Zhang, et al. 2011. "Identification of C1qTNF-Related Protein 4 as a Potential Cytokine That Stimulates the STAT3 and NF-KB Pathways and Promotes Cell Survival in Human Cancer Cells." *Cancer Letters* 308 (2): 203–14. https://doi.org/10.1016/J.CANLET.2011.05.005.

Li, Jinjing Tan, Ying Zhang, Naijun Han, Xuebing Di, Ting Xiao, Shujun Cheng, Yanning Gao, and Yu Liu. 2014. "DLK1 Promotes Lung Cancer Cell Invasion through Upregulation of MMP9 Expression Depending on Notch Signaling." Edited by Yunli Zhou. *PLoS ONE* 9 (3): e91509. https://doi.org/10.1371/journal.pone.0091509.

Louis, David N., Arie Perry, Guido Reifenberger, Andreas von Deimling, Dominique Figarella-Branger, Webster K. Cavenee, Hiroko Ohgaki, Otmar D. Wiestler, Paul Kleihues, and David W. Ellison. 2016. "The 2016 World Health Organization Classification of Tumors of the Central Nervous System: A Summary." *Acta Neuropathologica* 131 (6): 803–20. https://doi.org/10.1007/S00401-016-1545-1.

Luo, Jian Hua, Baoguo Ren, Sergei Keryanov, George C. Tseng, Uma N.M. Rao, Satdarshan P. Monga, Steven Strom, et al. 2006. "Transcriptomic and Genomic Analysis of Human Hepatocellular Carcinomas and Hepatoblastomas." *Hepatology* 44 (4): 1012–24. https://doi.org/10.1002/HEP.21328.

Maier, Julia, Salma Elmenofi, Alexander Taschauer, Martina Anton, Haider Sami, and Manfred Ogris. 2019. "Luminescent and Fluorescent Triple Reporter Plasmid Constructs for Wnt, Hedgehog and Notch Pathway." *PLOS ONE* 14 (12): e0226570. https://doi.org/10.1371/JOURNAL.PONE.0226570.

Mao, Ping, Kaushal Joshi, Jianfeng Li, Sung Hak Kim, Peipei Li, Lucas Santana-Santos, Soumya Luthra, et al. 2013. "Mesenchymal Glioma Stem Cells Are Maintained by Activated Glycolytic Metabolism Involving Aldehyde Dehydrogenase 1A3." *Proceedings of the National Academy of Sciences of the United States of America* 110 (21): 8644–49. https://doi.org/10.1073/PNAS.1221478110/-/DCSUPPLEMENTAL.

Mei, Baisong, Ling Zhao, Li Chen, and Hei Sook Sul. 2002. "Only the Large Soluble Form of Preadipocyte Factor-1 (Pref-1), but Not the Small Soluble and Membrane Forms, Inhibits Adipocyte Differentiation: Role of Alternative Splicing." *Biochemical Journal* 364 (1): 137–44. https://doi.org/10.1042/bj3640137.

Miyaoka, Yuichiro, Minoru Tanaka, Toru Imamura, Shinji Takada, and Atsushi Miyajima. 2010. "A Novel Regulatory Mechanism for Fgf18 Signaling Involving Cysteine-Rich FGF Receptor (Cfr) and Delta-like Protein (Dlk)." *Development* 137 (1): 159–67. https://doi.org/10.1242/DEV.041574.

Moon, Cynthia M. Smas, Kichoon Lee, Josep A. Villena, Kee-Hong Kim, Eun Jun Yun, and Hei Sook Sul. 2002. "Mice Lacking Paternally Expressed Pref-1/Dlk1 Display Growth Retardation and Accelerated Adiposity." *Molecular and Cellular Biology* 22 (15): 5585–92. https://doi.org/10.1128/MCB.22.15.5585-5592.2002/ASSET/A62FAB2D-E831-44D3-BBC5-76153D6D56E0/ASSETS/GRAPHIC/MB1521760006.JPEG.

Moreno, Marta, Virginia Fernández, Josep M. Monllau, Víctor Borrell, Carles Lerin, and Núria

De La Iglesia. 2015. “Transcriptional Profiling of Hypoxic Neural Stem Cells Identifies Calcineurin-NFATc4 Signaling as a Major Regulator of Neural Stem Cell Biology.” *Stem Cell Reports* 5 (2): 157–65. https://doi.org/10.1016/J.STEMCR.2015.06.008.

Morganstein, Daniel L., Pensee Wu, Meritxell R. Mane, Nick M. Fisk, Roger White, and Malcolm G. Parker. 2010. “Human Fetal Mesenchymal Stem Cells Differentiate into Brown and White Adipocytes, and Reveal a Role for ERRα in Human UCP1 Expression.” *Cell Research* 20 (4): 434. https://doi.org/10.1038/CR.2010.11.

Mortensen, Sussi B., Charlotte H. Jensen, Mikael Schneider, Mads Thomassen, Torben A. Kruse, Jorge Laborda, Søren P. Sheikh, and Ditte C. Andersen. 2012. “Membrane-Tethered Delta-like 1 Homolog (DLK1) Restricts Adipose Tissue Size by Inhibiting Preadipocyte Proliferation.” *Diabetes* 61 (11): 2814–22. https://doi.org/10.2337/db12-0176.

Nivedita-Krishnan, Sai, Thatchawan Thanasupawat, Leanne Arreza, G. William Wong, Karen Sfanos, Bruce Trock, Marc Bazin, M. Girish Shah, Sabine Hombach-Klonisch, and Thomas Klonisch. 2021. “C1q Tumor Necrosis Factor-Related Peptide 8 (CTRP8) Is a Novel Factor in Human Mast Cells.” Poster presented at: Canadian Cancer Resesarch Conference.

Nueda, Victoriano Baladrón, Beatriz Sánchez-Solana, María-Ángeles Ballesteros, and Jorge Laborda. 2007. “The EGF-like Protein Dlk1 Inhibits Notch Signaling and Potentiates Adipogenesis of Mesenchymal Cells.” *Journal of Molecular Biology* 367 (5): 1281–93. https://doi.org/10.1016/j.jmb.2006.10.043.

Nueda, María Luisa, María Julia González-Gómez, María Milagros Rodríguez-Cano, Eva María Monsalve, María José M. Díaz-Guerra, Beatriz Sánchez-Solana, Jorge Laborda, and Victoriano Baladrón. 2018. “DLK Proteins Modulate NOTCH Signaling to Influence a Brown or White 3T3-L1 Adipocyte Fate.” *Scientific Reports* 8 (1). https://doi.org/10.1038/S41598-018-35252-3.

Nueda, Ana-Isabel Naranjo, Victoriano Baladrón, and Jorge Laborda. 2017. “Different Expression Levels of DLK1 Inversely Modulate the Oncogenic Potential of Human MDA-MB-231 Breast Cancer Cells through Inhibition of NOTCH1 Signaling.” *The FASEB Journal* 31 (8): 3484–96. https://doi.org/10.1096/fj.201601341RRR.

Nueda, Ana Isabel Naranjo, Victoriano Baladrón, and Jorge Laborda. 2014. “The Proteins DLK1 and DLK2 Modulate NOTCH1-Dependent Proliferation and Oncogenic Potential of Human SK-MEL-2 Melanoma Cells.” *Biochimica et Biophysica Acta - Molecular Cell Research* 1843 (11): 2674–84. https://doi.org/10.1016/j.bbamcr.2014.07.015.

Parmigiani, Elena, Verdon Taylor, and Claudio Giachino. 2020. “Oncogenic and Tumor-Suppressive Functions of NOTCH Signaling in Glioma.” *Cells* 9 (10): 2304. https://doi.org/10.3390/cells9102304.

Peterson, Jonathan M, Zhikui Wei, and G William Wong. 2009. “CTRP8 and CTRP9B Are Novel Proteins That Hetero-Oligomerize with C1q/TNF Family Members.” https://doi.org/10.1016/j.bbrc.2009.08.014.

Pittaway, James F H, Constantinos Lipsos, Katia Mariniello, and Leonardo Guasti. 2021. “The Role of Delta-like Non-Canonical Notch Ligand 1 (DLK1) in Cancer.” *Endocrine-Related Cancer* 28 (12): R271–87. https://doi.org/10.1530/ERC-21-0208.

Puertas-Avendaño, R. A., M. J. González-Gómez, M. D. Ruvira, M. J. Ruiz-Hidalgo, N.

Morales-Delgado, J. Laborda, C. Díaz, and A. R. Bello. 2011. “Role of the Non-Canonical Notch Ligand Delta-Like Protein 1 in Hormone-Producing Cells of the Adult Male Mouse Pituitary.” *Journal of Neuroendocrinology* 23 (9): 849–59. https://doi.org/10.1111/J.1365-2826.2011.02189.X.

Purslow, Jeffrey A., Balabhadra Khatiwada, Marvin J. Bayro, and Vincenzo Venditti. 2020. “NMR Methods for Structural Characterization of Protein-Protein Complexes.” *Frontiers in Molecular Biosciences* 7 (January): 9. https://doi.org/10.3389/FMOLB.2020.00009/BIBTEX.

Qiang, L., T. Wu, H. W. Zhang, N. Lu, R. Hu, Y. J. Wang, L. Zhao, et al. 2012. “HIF-1α Is Critical for Hypoxia-Mediated Maintenance of Glioblastoma Stem Cells by Activating Notch Signaling Pathway.” *Cell Death and Differentiation* 19 (2): 284. https://doi.org/10.1038/CDD.2011.95.

Rajakulendran, Nishani, Katherine J. Rowland, Hayden J. Selvadurai, Moloud Ahmadi, Nicole I. Park, Sergey Naumenko, Sonam Dolma, et al. 2019. “Wnt and Notch Signaling Govern Self-Renewal and Differentiation in a Subset of Human Glioblastoma Stem Cells.” *Genes & Development* 33 (9–10): 498–510. https://doi.org/10.1101/GAD.321968.118.

Rebay, Ilaria, Robert J. Fleming, Richard G. Fehon, Lucy Cherbas, Peter Cherbas, and Spyros Artavanis-Tsakonas. 1991. “Specific EGF Repeats of Notch Mediate Interactions with Delta and Serrate: Implications for Notch as a Multifunctional Receptor.” *Cell* 67 (4): 687–99. https://doi.org/10.1016/0092-8674(91)90064-6.

Ressl, Susanne, Brandon K. Vu, Sandro Vivona, David C. Martinelli, Thomas C. Südhof, and Axel T. Brunger. 2015. “Structures of C1q-like Proteins Reveal Unique Features among the C1q/TNF Superfamily.” *Structure (London, England : 1993)* 23 (4): 688–99. https://doi.org/10.1016/J.STR.2015.01.019.

Ruiz-Hidalgo, M. 2002. “Dlk Modulates Mitogen-Activated Protein Kinase Signaling to Allow or Prevent Differentiation.” *Experimental Cell Research* 274 (2): 178–88. https://doi.org/10.1006/excr.2001.5464.

Saito, Norihiko, Jun Fu, Siyuan Zheng, Jun Yao, Shuzhen Wang, Diane D. Liu, Ying Yuan, et al. 2014. “A High Notch Pathway Activation Predicts Response to γ Secretase Inhibitors in Proneural Subtype of Glioma Tumor-Initiating Cells.” *Stem Cells (Dayton, Ohio)* 32 (1): 301–12. https://doi.org/10.1002/STEM.1528.

Sánchez-Solana, Beatriz, María Luisa Nueda, María Desamparados Ruvira, María José Ruiz-Hidalgo, Eva María Monsalve, Samuel Rivero, José Javier García-Ramírez, María José M. Díaz-Guerra, Victoriano Baladrón, and Jorge Laborda. 2011. “The EGF-like Proteins DLK1 and DLK2 Function as Inhibitory Non-Canonical Ligands of NOTCH1 Receptor That Modulate Each Other’s Activities.” *Biochimica et Biophysica Acta - Molecular Cell Research* 1813 (6): 1153–64. https://doi.org/10.1016/j.bbamcr.2011.03.004.

Schäffler, Andreas, and Christa Buechler. 2012. “CTRP Family: Linking Immunity to Metabolism.” *Trends in Endocrinology & Metabolism* 23 (4): 194–204. https://doi.org/10.1016/j.tem.2011.12.003.

Seymour, Tracy, Anna Nowak, and Foteini Kakulas. 2015. “Targeting Aggressive Cancer Stem Cells in Glioblastoma.” *Frontiers in Oncology* 5 (JUL): 159. https://doi.org/10.3389/FONC.2015.00159/BIBTEX.

Shin, Sangsu, Yeunsu Suh, Henry N. Zerby, and Kichoon Lee. 2014. "Membrane-Bound Delta-like 1 Homolog (Dlk1) Promotes While Soluble Dlk1 Inhibits Myogenesis in C2C12 Cells." *FEBS Letters* 588 (7): 1100–1108. https://doi.org/10.1016/j.febslet.2014.02.027.

Siebel, C, and U Lendahl. 2017. "Notch Signaling in Development, Tissue Homeostasis, and Disease." *Physiol Rev* 97: 1235–94. https://doi.org/10.1152/physrev.00005.2017.-Notch.

Singh, Sheila K., Ian D. Clarke, Takuichiro Hide, and Peter B. Dirks. 2004. "Cancer Stem Cells in Nervous System Tumors." *Oncogene* 23 (43 REV. ISS. 6): 7267–73. https://doi.org/10.1038/sj.onc.1207946.

Smas, Cynthia M., Li Chen, and Hei Sook Sul. 1997. "Cleavage of Membrane-Associated Pref-1 Generates a Soluble Inhibitor of Adipocyte Differentiation." *Molecular and Cellular Biology* 17 (2): 977–88. https://doi.org/10.1128/mcb.17.2.977.

Smas, Cynthia M., Daniel Green, and Hei Sook Sul. 1994. "Structural Characterization and Alternate Splicing of the Gene Encoding the Preadipocyte EGF-like Protein Pref-1." *Biochemistry* 33 (31): 9257–65. https://doi.org/10.1021/BI00197A029.

Smas, Cynthia M., and Hei Sook Sul. 1993. "Pref-1, a Protein Containing EGF-like Repeats, Inhibits Adipocyte Differentiation." *Cell* 73 (4): 725–34. https://doi.org/10.1016/0092-8674(93)90252-L.

Stupp, Roger, Warren P. Mason, Martin J. van den Bent, Michael Weller, Barbara Fisher, Martin J.B. Taphoorn, Karl Belanger, et al. 2005. "Radiotherapy plus Concomitant and Adjuvant Temozolomide for Glioblastoma." *New England Journal of Medicine* 352 (10): 987–96. https://doi.org/10.1056/NEJMOA043330/SUPPL_FILE/987SA1.PDF.

Subhashini, Nidhi. 2016. "Dlk1 Membrane-to-Nuclear Signalling during Motor Neuron Functional Diversification." *Unpublished Doctoral Dissertation*. Georg August University Göttingen.

Takeuchi, Tamotsu, Yoshihiro Adachi, and Tomoko Nagayama. 2011. "Expression of a Secretory Protein C1qTNF6, a C1qTNF Family Member, in Hepatocellular Carcinoma." *Analytical Cellular Pathology* 34 (3): 113–21. https://doi.org/10.3233/ACP-2011-009.

Tamimi, Ahmad Faleh, and Malik Juweid. 2017. "Epidemiology and Outcome of Glioblastoma." In *Glioblastoma*, 143–53. Codon Publications. https://doi.org/10.15586/codon.glioblastoma.2017.ch8.

Tan, Jinjing, Susu Zhang, Lin Li, Jing Mu, Ziyu Wang, Lina Zhang, Mei Jiang, et al. 2019. "Abnormally Localized DLK1 Interacts with NCOR1 in Non-Small Cell Lung Cancer Cell Nuclear." *Bioscience Reports* 39 (12): 20192362. https://doi.org/10.1042/BSR20192362.

Thanasupawat, Thatchawan, Aleksandra Glogowska, Maxwell Burg, Jerry Krcek, Jason Beiko, Marshall Pitz, Guo-Jun Zhang, Sabine Hombach-Klonisch, and Thomas Klonisch. 2018. "C1q/TNF-related Peptide 8 (CTRP8) Promotes Temozolomide Resistance in Human Glioblastoma." *Molecular Oncology* 12 (9): 1464–79. https://doi.org/10.1002/1878-0261.12349.

Thon, Niklas, Karin Damianoff, Jemima Hegermann, Stefan Grau, Bjarne Krebs, Oliver Schnell, Jörg Christian Tonn, and Roland Goldbrunner. 2010. "Presence of Pluripotent CD133+ Cells Correlates with Malignancy of Gliomas." *Molecular and Cellular Neuroscience* 43 (1): 51–59. https://doi.org/10.1016/J.MCN.2008.07.022.

Tie, Xinxin, Sheng Han, Lingxuan Meng, Yunjie Wang, and Anhua Wu. 2013. “NFAT1 Is Highly Expressed in, and Regulates the Invasion of, Glioblastoma Multiforme Cells.” *PloS One* 8 (6). https://doi.org/10.1371/JOURNAL.PONE.0066008.

Tornehave, Ditte, Pernille Jansen, Børge Teisner, Hanne Boje Rasmussen, John Chemnitz, and Gonzalo Moscoso. 1993. “Fetal Antigen 1 (FA1) in the Human Pancreas: Cell Type Expression, Topological and Quantitative Variations during Development.” *Anatomy and Embryology* 187 (4): 335–41. https://doi.org/10.1007/BF00185891.

Traustadóttir, Gunnhildur Ásta, Charlotte H. Jensen, Mads Thomassen, Hans Christian Beck, Sussi B. Mortensen, Jorge Laborda, Victoriano Baladrón, Søren P. Sheikh, and Ditte C. Andersen. 2016. “Evidence of Non-Canonical NOTCH Signaling: Delta-like 1 Homolog (DLK1) Directly Interacts with the NOTCH1 Receptor in Mammals.” *Cellular Signalling* 28 (4): 246–54. https://doi.org/10.1016/j.cellsig.2016.01.003.

Traustadóttir, Gunnhildur Ásta, Charlotte Harken Jensen, Jose Javier Garcia Ramirez, Hans Christian Beck, Søren Paludan Sheikh, and Ditte Caroline Andersen. 2017. “The Non-Canonical NOTCH1 Ligand Delta-like 1 Homolog (DLK1) Self Interacts in Mammals.” *International Journal of Biological Macromolecules* 97 (April): 460–67. https://doi.org/10.1016/j.ijbiomac.2017.01.067.

Turányi, Eszter, Katalin Dezső, Sándor Paku, and Peter Nagy. 2009. “DLK Is a Novel Immunohistochemical Marker for Adrenal Gland Tumors.” *Virchows Archiv : An International Journal of Pathology* 455 (3): 295–99. https://doi.org/10.1007/S00428-009-0819-6.

Urso, Katia, Andrés Fernández, Patricia Velasco, Javier Cotrina, Belén de Andrés, Pilar Sánchez-Gómez, Aurelio Hernández-Laín, Sonsoles Hortelano, Juan Miguel Redondo, and Eva Cano. 2019. “NFATc3 Controls Tumour Growth by Regulating Proliferation and Migration of Human Astroglioma Cells.” *Scientific Reports* 9 (1). https://doi.org/10.1038/S41598-019-45731-W.

Waddell, Jolena N., Peijing Zhang, Yefei Wen, Sanjay K. Gupta, Aleksey Yevtodiyenko, Jennifer V. Schmidt, Christopher A. Bidwell, Ashok Kumar, and Shihuan Kuang. 2010. “Dlk1 Is Necessary for Proper Skeletal Muscle Development and Regeneration.” *PloS One* 5 (11). https://doi.org/10.1371/JOURNAL.PONE.0015055.

Wan, Xiaolong, Caixia Zheng, and Lei Dong. 2019. “Inhibition of CTRP6 Prevented Survival and Migration in Hepatocellular Carcinoma through Inactivating the AKT Signaling Pathway.” *Journal of Cellular Biochemistry* 120 (10): 17059–66. https://doi.org/10.1002/JCB.28967.

Wang, Yuhui, Ling Zhao, Cynthia Smas, and Hei Sook Sul. 2010. “Pref-1 Interacts with Fibronectin To Inhibit Adipocyte Differentiation.” *Molecular and Cellular Biology* 30 (14): 3480–92. https://doi.org/10.1128/mcb.00057-10.

Wang, Hao Zhang, Shengchao Xu, Zhixiong Liu, and Quan Cheng. 2021. “The Adaptive Transition of Glioblastoma Stem Cells and Its Implications on Treatments.” *Signal Transduction and Targeted Therapy* 6 (1): 1–13. https://doi.org/10.1038/s41392-021-00491-w.

Wong, G William, Sarah A. Krawczyk, Claire Kitidis-Mitrokostas, Tracy Revett, Ruth Gimeno, and Harvey F. Lodish. 2008. “Molecular, Biochemical and Functional Characterizations of

C1q/TNF Family Members: Adipose-Tissue-Selective Expression Patterns, Regulation by PPAR-γ Agonist, Cysteine-Mediated Oligomerizations, Combinatorial Associations and Metabolic Functions." *Biochemical Journal* 416 (2): 161–77. https://doi.org/10.1042/BJ20081240.

Wong, G William, Jin Wang, Christopher Hug, Tsu Shuen Tsao, and Harvey F. Lodish. 2004. "A Family of Acrp30/Adiponectin Structural and Functional Paralogs." *Proceedings of the National Academy of Sciences of the United States of America* 101 (28): 10302–7. https://doi.org/10.1073/pnas.0403760101.

Xiang, Heli, Wujun Xue, Yang Li, Jin Zheng, Chenguang Ding, Meng Dou, and Xiaoyan Wu. 2020. "C1q/TNF-Related Protein 6 (CTRP6) Attenuates Renal Ischaemia-Reperfusion Injury through the Activation of PI3K/Akt Signalling Pathway." *Clinical and Experimental Pharmacology & Physiology* 47 (6): 1030–40. https://doi.org/10.1111/1440-1681.13274.

Yin, D., D. Xie, S. Sakajiri, C. W. Miller, H. Zhu, M. L. Popoviciu, J. W. Said, K. L. Black, and H. P. Koeffler. 2006. "DLK1: Increased Expression in Gliomas and Associated with Oncogenic Activities." *Oncogene* 25 (13): 1852–61. https://doi.org/10.1038/sj.onc.1209219.

Yuasa, Daisuke, Koji Ohashi, Rei Shibata, Naoki Mizutani, Yoshiyuki Kataoka, Takahiro Kambara, Yusuke Uemura, et al. 2016. "C1q/TNF-Related Protein-1 Functions to Protect against Acute Ischemic Injury in the Heart." *FASEB Journal : Official Publication of the Federation of American Societies for Experimental Biology* 30 (3): 1065–75. https://doi.org/10.1096/FJ.15-279885.

Zeppernick, Felix, Rezvan Ahmadi, Benito Campos, Christine Dictus, Burkhard M. Helmke, Natalia Becker, Peter Lichter, Andreas Unterberg, Bernhard Radlwimmer, and Christel C. Herold-Mende. 2008. "Stem Cell Marker CD133 Affects Clinical Outcome in Glioma Patients." *Clinical Cancer Research* 14 (1): 123–29. https://doi.org/10.1158/1078-0432.CCR-07-0932.

Zhang, Xue Ping, Gang Zheng, Lian Zou, Hui Ling Liu, Li Hong Hou, Peng Zhou, Dan Dan Yin, et al. 2008. "Notch Activation Promotes Cell Proliferation and the Formation of Neural Stem Cell-like Colonies in Human Glioma Cells." *Molecular and Cellular Biochemistry* 307 (1–2): 101–8. https://doi.org/10.1007/S11010-007-9589-0/FIGURES/4.

Zhou, Susan Q. Ke, Zhi Huang, William Flavahan, Xiaoguang Fang, Jeremy Paul, Ling Wu, et al. 2015. "Periostin Secreted by Glioblastoma Stem Cells Recruits M2 Tumour-Associated Macrophages and Promotes Malignant Growth." *Nature Cell Biology* 17 (2): 170–82. https://doi.org/10.1038/NCB3090.

Zwierzina, Marit E., Asim Ejaz, Mario Bitsche, Michael J.F. Blumer, Maria C. Mitterberger, Monika Mattesich, Arno Amann, et al. 2015. "Characterization of DLK1(PREF1)+/CD34+ Cells in Vascular Stroma of Human White Adipose Tissue." *Stem Cell Research* 15 (2): 403–18. https://doi.org/10.1016/J.SCR.2015.08.004.